2014-01-01

Experimental Evaluation Of Flame Stability And Pollutant Emissions From A Multi-Tube Fuel Injector

Sarzina Hossain
University of Texas at El Paso, shossain@miners.utep.edu

EXPERIMENTAL EVALUATION OF FLAME STABILITY AND POLLUTANT EMISSIONS FROM A MULTI-TUBE FUEL INJECTOR

SARZINA HOSSAIN

Department of Mechanical Engineering

APPROVED:

Norman Love Jr., Ph.D., Chair

Ahsan R Choudhuri, Ph.D.

Paras Mandal, Ph.D.

Charles Ambler, Ph.D.
Dean of the Graduate School

Dedication

To my Parents

EXPERIMENTAL EVALUATION OF FLAME STABILITY AND POLLUTANT EMISSIONS FROM A MULTI-TUBE FUEL INJECTOR

by

SARZINA HOSSAIN, B.SC.Engg. (Mech)

THESIS

Presented to the Faculty of the Graduate School of

The University of Texas at El Paso

in Partial Fulfillment

of the Requirements

for the Degree of

MASTER OF SCIENCE

Department of Mechanical Engineering

THE UNIVERSITY OF TEXAS AT EL PASO

August 2014

Acknowledgements

I would like to acknowledge my advisor and mentor Dr. Norman Love and Dr. Ahsan Choudhuri for providing me with the opportunity and encouragement to follow my academic pursuits. Dr. Norman Love always worked closely with me to enhance my technical expertise. I also earned valuable knowledge during work with him. I would also like to thank my supervisors to give me financial support towards earning my MS degree. I would like to thank to other committee member Dr. Paras Mandal. for giving me his valuable suggestions and recommendations to make this dissertation possible.

A special thanks to the students of the Center for Space Exploration Technology Research (cSETR) who have also helped me to conducting my research: Sudipa Sarkar, Sergio Maldonado, Martin de la Torre and Jorge Rosero and Manuel J. Hernandez. A portion of this work was supported by Mike Loya innovation fund.

Abstract

According to US Energy Information Administration coal is predicted to be the dominant source of power production in the United States until 2035. With fifty percent of the electricity generated in the United States originating from coal, the US produces close to 2 billion tons of CO_2 per year from coal-burning power plants. The Integrated Gasification Combined Cycle (IGCC) offers a cleaner way to generate electricity-using coal. IGCC is a process where the feedstock is gasified and converted into to syngas (CO-H_2) which can then be used as a fuel source to power energy-generating gas turbines. Compared to other hydrocarbons, high hydrogen content fuels behave differently because of their much higher specific heat, higher diffusivity, flammability limits and higher laminar flame speed. The design of a fuel injector plays a vital role in terms of mixing which impacts flame stability inside a high-pressure gas turbine combustor (HPTC). The combustor used for experiments in this thesis has the capability to operate at pressures up to 1.5 MPa and temperatures up to 2400 K. A detailed and effective control and ignition system was developed as part of this work to operate with the combustion chamber. The modified ignition system is used to create a pilot flame. A LabVIEW program was introduced to operate the combustor remotely. Stability was of interest for the experiments since when designing combustion devices it is necessary to know the stability regions, this way stable operation can be maintained. For this thesis flame flashback and flame blowout were defined to be outside of the stable operating conditions. The flashback tendency of the flames was determined to be dependent on the flame speed of the hydrogen. It was also observed that due to the boundary layer effect the central injector ports received the maximum flow rates, resulting in premature flashback in the outer injector ports. As the hydrogen concentration was increased, the flame became less susceptible to blowout. The production of NO_x pollutant emission increased for increasing fuel percentage reaching a maximum value at a 40%-60% H_2-CO concentration.

Table of Contents

List of Tables

List of Figures

Chapter 1 : Introduction

In United States the reserve of coal is estimated as one of the largest in the world. According to US Energy Information Administration in 2013 over 92% of the coal consumed in the United States is used for generating electricity. The United States has around 1,400 coal-fired electricity generating units in operation at almost 600 plants across the country. Together, these power plants generate 37% of the total net electricity produced in the United States and consume more than 800 million short tons of coal [1].

Gas turbines have been used for power generation since 1939 and were first explored by the Brown Bovery Company located in Neuchâtel, Switzerland [2]. Gas turbines are internal combustion engines with rotary motion consists of three main parts: compressor, combustor and turbine. In the compressor section air is drawn in and compressed where it is then directed to the combustion chamber where fuel is added, ignited, and burned. The hot gases produced are then routed to the turbine section where energy from the exhaust gas is recovered in the form of shaft power [3]. Current application for gas turbines include the gas and oil industry, emergency power generation facilities, independent power production, and a number of other industrial applications. Generally gas turbines are designed to be fueled with natural gas and coal .Coal is plentiful and fairly cheap relative to the cost of other sources of electricity, but its use produces several types of emissions that adversely affect the environment. Coal emits sulfur dioxide, nitrogen oxide, and heavy metals (such as mercury and arsenic) and acid gases (such as hydrogen chloride), which have been linked to acid rain, smog, and health issues. Coal also emits carbon dioxide, a greenhouse gas. In 2012, coal accounted for 31% of the energy-related carbon dioxide emissions in the United States. On the production-side, coal mining can have a negative impact on ecosystems and water quality, and alter landscapes and scenic views [4].

To solve this challenge associated with coal, Integrated Gasification Combined Cycle (IGCC) is used to produce synthetic gas. Integrated gasification combined cycle (IGCC) is the process to turn carbon based fuels into syngas and redirects any leftover heat to power a second turbine. These kind of Synthetic fuels obtained from the IGCC have the capability to produce lower pollutant emission than traditional coal derived power generation technologies [5]. Based on these issues a future generation modern gas turbine is required which has the capacity to operate with alternative fuels along with different compositions. To extract power from the gas turbine it is necessary to stable the flame inside the combustor. Due to the variation of different parameters related to combustion leads to flashback, blow off and instabilities. To stable a flame inside a next generation gas turbine combustor it is important to have clear understanding of combustion with different fuels.

1.1 Gas Turbine Combustors

Gas turbine combustors technology has developed over last 50 years. Inspite of the continuous advances of gas turbine combustor technology, it is the main challenge to design an ingenuine combustor than even before. In addition the environmental pollutions, energy conservation and higher conversions efficiencies remain on the priority list [6]. Modern technology are still required to operate the combustor at high pressures and temperatures with broader range of fuels. The challenge with the sixties combustor to increase combustor durability and power output. The main concern in the seventies to reduce the gasous pollutants. Combustor durability and design and development process associated with advanced energy was the main issues during eighties. The challenge during ninties was the environmental pollution reduction and energy conversion [7]. Advanced combustion technologies are expected to provide significant advances both in experimental and computational areas. The future genartion gas

turbine combustor should create concerns about energy release rate, turbine inlet temperature, pollutant emissions, fuel variability.

1.2 Combustion

A definition of combustion according to Webstar's Dictionary is as "rapid oxidation generating heat, or both light and heat: also slow oxidation accompanied by little heat and no light". Combustion can occur either flame or non-flame modes. Flame mode can be categorized as premixed and non-premixed (diffusion) flame. In case of premixed flame the mixing of fuel and oxidizer is occurred before any significant combustion reaction. On the other hand a diffusion flame, fuel and oxidizer are initially kept separate and reaction occurs at the interface of fuel and oxidizer [8].

The exact amount of oxidizer which is needed for complete combustion is known as stoichiometric quantity. If the amount of oxidizer is greater than the stoichiometric it is termed as lean combustion. Contrarily if the amount of oxidizer is less than the stoichiometric it is known as rich combustion.

1.3 Pollutant Emissions

One of the major factors to design of a modern combustion system is to control the pollutant emissions. The combustion of most of the fuel can produce gaseous pollutants such as nitrogen oxides (NO_x), sulfur dioxide (SO_2), carbon monoxide (CO), volatile organic compounds (VOCs), particulate matter, and trace species such as mercury and other metals. The amount and type of emissions generated depends on the properties of the fuel as well as the type and operating conditions of the combustor [9].

They pollute the environment and contribute to the acid rain, smog, and respiratory and other

health problems. Hydrocarbons' emissions include a number of toxic substances such as benzene, polycyclic aromatic hydrocarbons (PAHs), butadiene and aldehydes (formaldehyde, acetaldehyde, acrolein). Carbon dioxide is the primary greenhouse gas which may aggravate the global warming [9]. NO_x is a collective term to describe several oxides of nitrogen. The NOx-s participates in a chain reaction removing ozone from the stratosphere allowing more ultraviolet radiation to reach the Earth's surface. The NOx is a major contributor of photochemical smog and ozone in the urban air. Because of this, NOx emission has become one of the most important topics in combustion research. With the steady increase in combustion of hydrocarbon fuels, the products of combustion are distinctly identified as a severe source of environmental damage.

1.4 Alternative Fuels

The need for fuel flexible ultra-low emission gas turbine combustors is imminent to secure future power needs. Distributed combustion technology is demonstrated to provide significant performance improvement of gas turbine combustors including uniform thermal field in the entire combustion chamber (improved pattern factor) at very high combustion intensity, ultra-low emission of NOx and CO, low noise, enhanced stability, higher efficiency and alleviation of combustion instability. Fuel variability greatly changes the flame characteristics like flame speed, flame shape, flame stability.

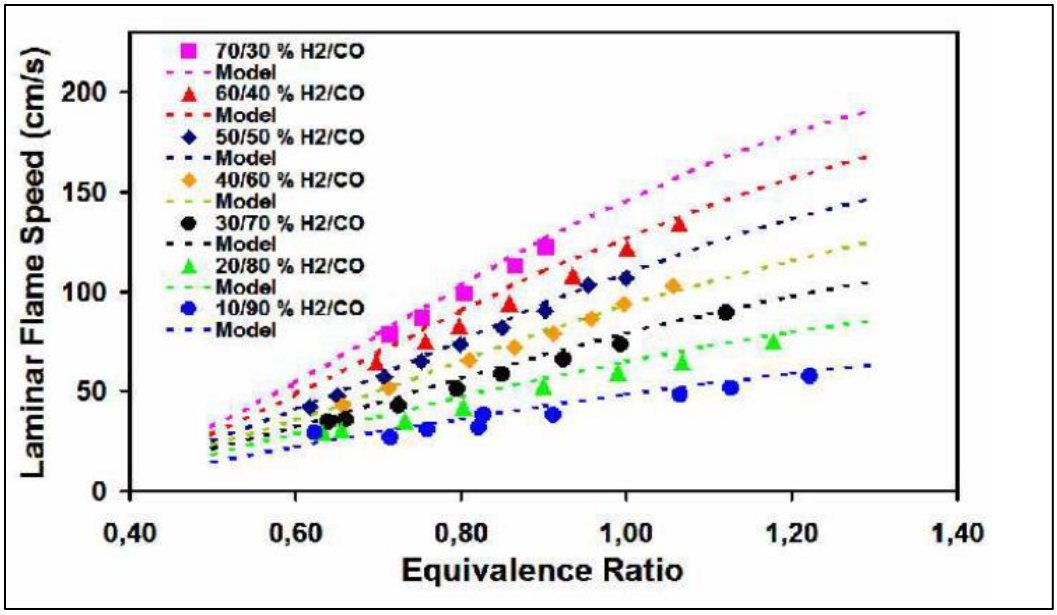

Figure 1.1: Laminar Flame Speeds of Various Syngas Mixtures (Experimental & Computational) Sun et al. [10]

For different fuels, the flame speed changes with equivalence ratio (Figure 1.1). In comparison with other hydrocarbons, hydrogen content fuels behave differently because of its much higher specific heat, higher diffusivity, and flammability limits that mean hydrogen has a wide range of volume concentrations over which it is flammable, and a higher laminar flame speed. These properties induce the flashback in case of high hydrogen content fuel. As the hydrogen content in the fuel is decreased the possibility of blow-out increased.

1.5 Flashback

When the gas velocity is smaller than the flame speed then the flashback occurs (Figure 1.2). It is the tendency of the flame to propagate through the upstream premixing section. Flashback can cause massive hardware damage, detonation, pollutant emissions etc. one of the most important task to stable a flame to avoid flashback. Flashback occurs due to the following:

turbulent flame propagation in the core flow, flame propagation in the boundary layer, combustion instabilities, or combustion induced vortex breakdown (CIVB).

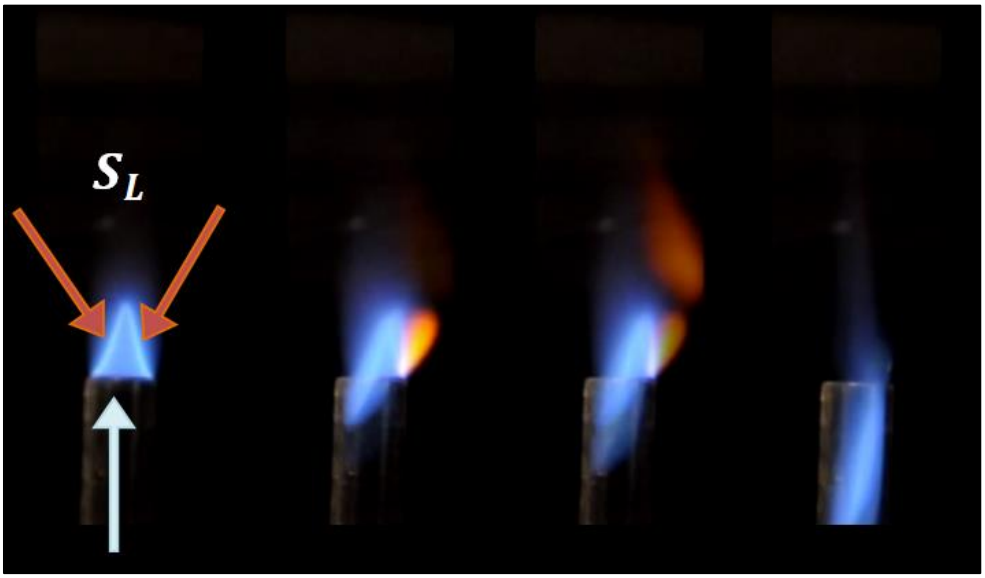

Figure 1.2: Flashback (laminar flame speed S_L>air+fuel speed)

The phenomenon of flashback is related with the matching of local flame speed with local flow velocity. Flashback is normally considered as a transient event, it occurs when the fuel flow is turned off or stopped. The flames will flashback through a burner port that are larger than the quenching distance if the flame speed is greater than the flow velocity. However, syngas has large flashback propensity because of its hydrogen content. Hydrogen has a high Flame speed and low lean flammability which tends to increase the potential for flashback [11].

1.6 Liftoff and Blow out

Another important design criterion for gas turbine combustor is the avoidance of liftoff. It is the condition of the flame when it is not attached with the burner port or tube rather than it is stabilized at a distance from the port. Flame liftoff is undesirable for several reasons such as

most of the time it leads to incomplete combustion due to the escape of unburned gas. It becomes sometime hard to control the lifted flame so that poor heat transfer results. It is also very difficult to achieve ignition above lifting limits. Flame lifting is influenced by the local flame and the flow properties close to the burner or injector port. If the velocity of the gas is increased the cone angle of the flame decreased and the flame is stabilized at a certain distance from the port. As the velocity increases further beyond the liftoff value, results in increasing the liftoff distance until the flame extinguishes. This phenomenon is known as blow out [8]. Liftoff and blow out both are the consequences of radical heat loss to the burner port and the dilution with ambient air increase the flow velocity (Figure 1.3).

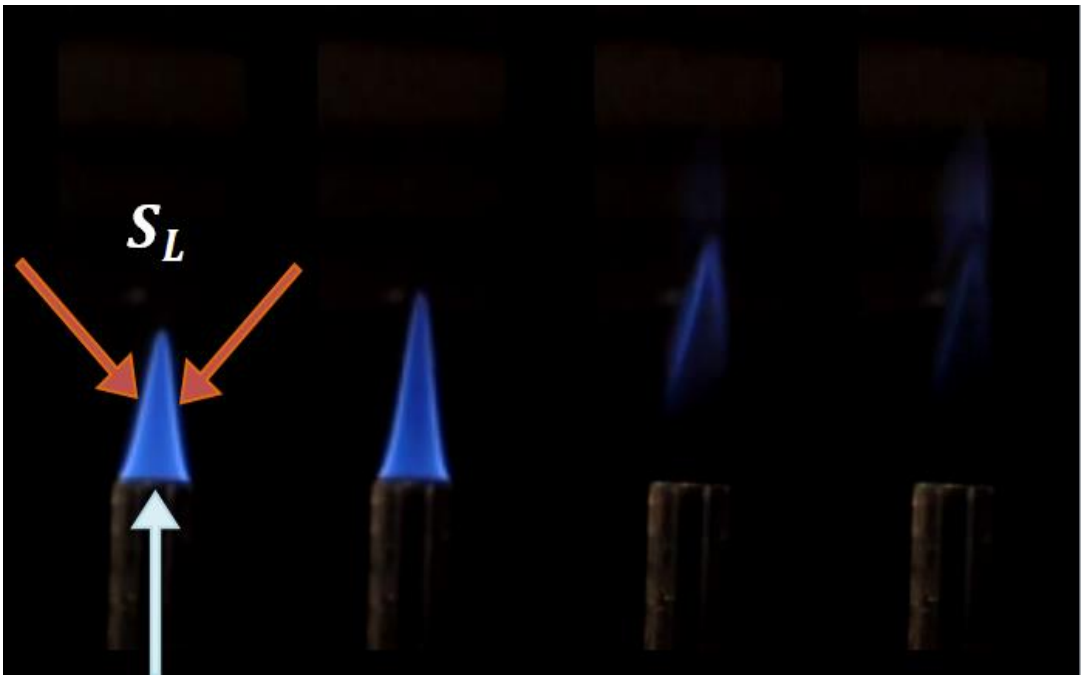

Figure 1.3: Liftoff and Blow Out (laminar flame speed S_L< air + fuel speed)

1.7 Flame Stabilization

Stable a Flame in combustion is the main objective of many theoretical and experimental studies.

Burner design is the most important controlling factor for flame stabilization. Burner design would be greatly facilitated by knowing the effect of the input parameters such as fuel-air ratio, average velocity and its distribution, flame speed and its distribution, and the intensity of swirl, on the stability of the flame [12].

Due to the impossibility of self-propagation of the combustion wave, Bunsen burner could not stabilize turbulent flames with high flow velocity. Several attempts had been made to improve the flame stability in turbulent flames. Turbulent flames may be stabilized by pilot flames, bluff bodies, deflected jets, and swirl jets. Many researchers tried to improve the stability of premixed turbulent flames by creating a recirculation zone. This zone affects the transfer of mass and energy from the burned gases to the unburned ones, which works as a continuous ignition source known as pilot flame. The pilot flame can be used outside or inside the main high velocity flow.

Jensen and Shipman [13] studied the stabilization of flames in high-speed flow using pilot flames. The main flow was propane air mixture, while the pilot stream was hydrogen-air mixture. They found that, the pilot heat would be sufficient to raise the average temperature of 19 mm diameter core of the main stream from its initial temperature 288 K to the required preheat temperature 414 K. The thermal energy generated is sufficient to supply the required preheat to the remainder stream [13].

Bluff-body, reflected jets and swirl jets provide recirculation zone occurs immediately downstream of each of them and works as a pilot. Energy and mass are transferred from the

burned gases of this zone to the unburned portion in the main stream. Failure of flame propagation is due to quenching effect of hot gases due to rapid mixing with the cold unburned combustible main flow. Beltagui and Maccallun [14] studied the effect swirl on the stability of premixed town gas-air flames in a furnace. They used vanes which was placed at 15", 30°, 45" and 60" to jet axis. They found that the central recirculation zone **(**CRZ) is established with swirlers, 45", 60°, but not with either the 15" or 30" swirlers. They also found that in the case of creating the CRZ the spread of the jet is more rapid than in the free case, hence, the flame is more stable.

One advanced concept developed in the nowadays is to apply a "multiple-injection burner (cluster burner)"[15]. This type of burner consists of multiple fuel nozzles and a perforated plate with holes which are coaxially installed. In this burner, air sheathed fuel jets from the injection points join each other and become an annular swirling jet, and fuel is rapidly mixed with air within a short distance because of the turbulence at the entrance and exit of the air passages [16].

Another way to stabilize a turbulent flame is to use bluff body inside a burner. The bluff body provides excellent turbulent mixing characteristics, which improves the flame stability, and ease of combustion control. It decreases the tendency of liftoff and blow out of a flame. A bluff body can be placed inside a single or multi-tube injector to reduce the flow velocity which in turns will be helpful to stabilize the flame on the body. The flame structure produced by bluff-body burners is complex and dominant by time-varying large-scale mixing structures. Axisymmetric bluff body stabilized flames have been studied by several investigators [17][18], improve mixing rates, reduced flame lengths and enhanced burner stability and efficiency. The aerodynamic interaction between the injected fuel (in jet or other form) and the primary

recirculation in bluff body system was conductive to flame stabilization over a wide range of air velocities and fuel injection rates [19].

1.8 Objectives

This study mainly based on the stability of flame inside a gas turbine combustor for high hydrogen content fuel for future power generation purposes. One of the important goals of this work is to reduce the pollutant emissions. In this work an optically accessible high pressure combustor is used inside which the flame stability regime of high hydrogen content fuel along with emission behavior is observed. To accomplish these goals the main objective is to:

1. Development of a LabView controlled remote control system which can deliver fuel oxidizer.
2. Development of a LabView controlled remote ignition system to stabilize a flame.
3. Investigate the effect of multi-tube injector geometry on flame stability
4. Measurement of pollutant emissions of syngas fuel by using the designed high pressure gas turbine combustor

1.9 Practical Relevance

The development of control and ignition systems will help flow the fuel and oxidizer into the combustion chamber and initiate the spark respectively. The experimentation will generate data which will aid to increase the understanding of combustion at high pressure and temperature at gas turbine operating conditions. Flame characteristics such as flame velocity, flame propagation, as well as flashback and blowout propensity can be examined using these systems. This understanding is fundamental for the advancement of gas turbines and the development of the next generation combustors.

1.10 Thesis Organization

Chapter 1 covers brief description about combustion, fuel variability, flashback and blowout and the main objective and practical relevance of this research.

Chapter 2 provides a literature review on current operational combustors operating at comparable conditions, different ignition system, NOx emission and syngas and bluff body flame stabilization used in similar research.

Chapter 3 will cover the detail description of experimental setup and design of the control and ignition system along with the design of multi-tube bluff body injector.

Chapter 4 will cover the results and discussion of the experiment.

Chapter 5 will cover summary of the work and future work needed.

Chapter 2 : Literature Review

Different types of past studies as well as ongoing research related to this work were presented in this chapter. Since the work this thesis is presenting uses a high pressure combustor, it is also important to investigate combustor designs. A background for combustor design is presented in this chapter. Another important part of this work is to establish an effective ignition system; hence a design of an ignition system is also discussed here. This chapter will also review the descriptions of past experiments and work on analyzing different flame stability conditions related to combustion such as flashback, blowout and liftoff. To eradicate these different types of flame characteristics related to combustion, a multi-tube injector was used to stabilize the flame. Some detailed background study was also included in this chapter related to injector design for flame stabilization.

2.1 Previous Combustor Designs

At the UTEP cSTER currently there is an operational optically accessible atmospheric pressure combustor operational, some work performed in this combustor can be found in the reference by Bidhan et. Al [20]. This atmospheric combustor was later used to design the high pressure combustor that is used for the experiments presented in this thesis. The main focus of the atmospheric pressure combustor was to analyze flashback properties in syngas fuels. Different fuel mixtures have been used in the combustor including different synthetic gas mixtures. The combustor rig is shown in Figure 2.1 and is set up using four configurable models: (i) the inlet manifold, (ii) static mixer, (iii) swirler burner with quartz tube, and (iv) the combustion chamber. There are three quartz windows located on the main combustion section allow for high speed imaging of flashback characteristics.

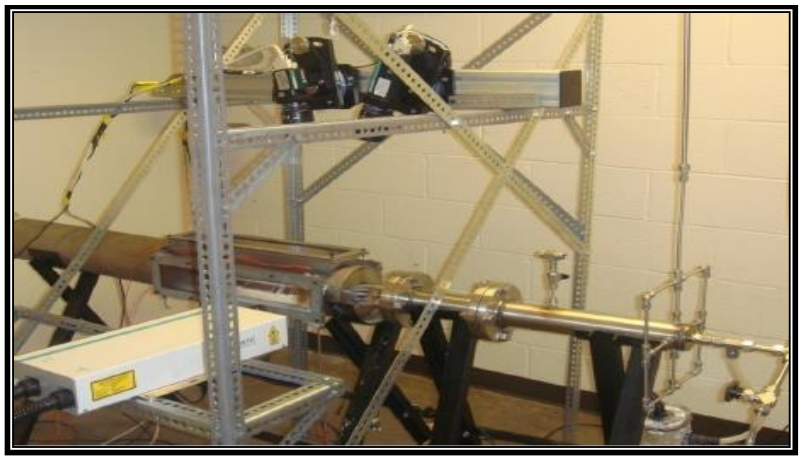

Figure 2.1: Ambient Combustor

Tomezak et al., 2002 [21] also made a combustor that could operate duel phase fuel operation (liquid and gaseous) under 1MPa Pressure. The combustor consists of an alloy steel pressure vessel, designed in modular form, utilizing a lamination valve at the exit to control the pressure in the combustor (figure 2.2). The flame is stabilized using a combination of a swirler device operating with 8 holes for fuel injection as well as recirculation of air. The combustor temperature operating range is 400 to 1200 °C. Pressure transducers are used to measure pressure fluctuation for this combustor.

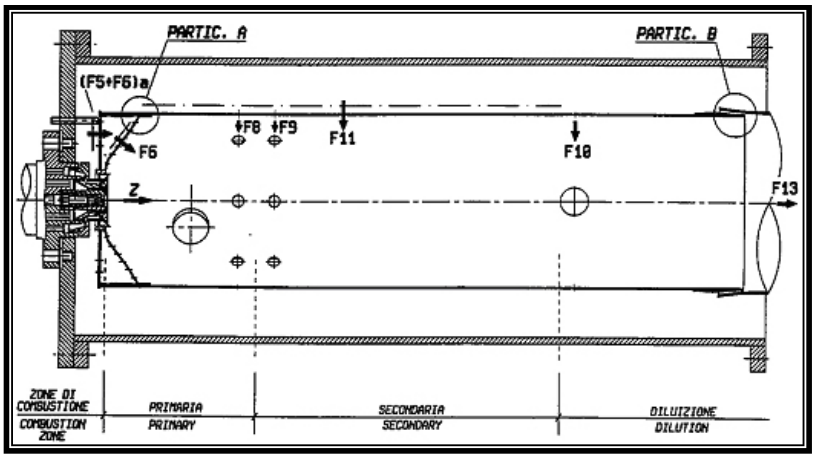

Figure 2.2: Reverse Flow Combustion Chamber

The University of California Irvine Combustion Laboratory (UCICL) [22] has two operational combustors for testing (figure 2.3). One is used for high pressure combustion experiments with optical access. Another one is used for long duration experiments. The flow rate and pressure is up to 1 kg/s and 15 bar respectively.

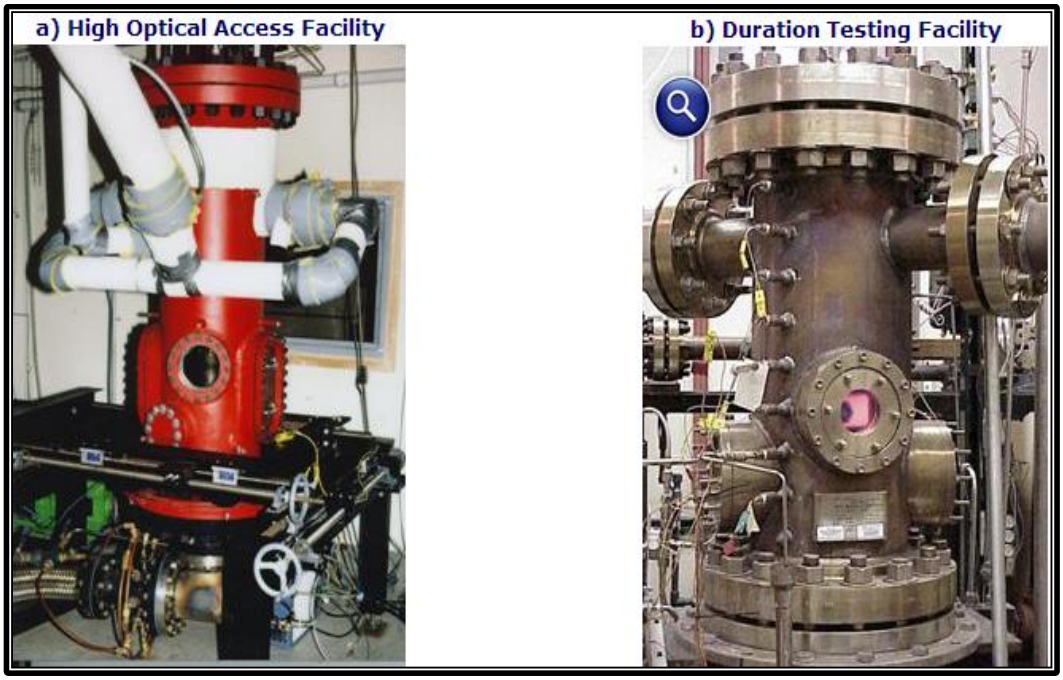

Figure 2.3: Elevated Pressure Facility

The National Energy Technology Laboratory (NETL) [23] has two operational high-pressure combustor facilities. An optically accessible dynamic gas turbine (figure 2.4) with operating pressures of up to 10 bar and air flow at .75 kg/s for both natural gas and liquid fuels. The second combustion facility (figure 2.5) is also optically accessible used for computational fluid dynamic testing and modeling of combustion operates under 22 bar pressure (National Energy Technology Laboratory).

Figure 2.4: Dynamic Gas Turbine Combustion Test Rig

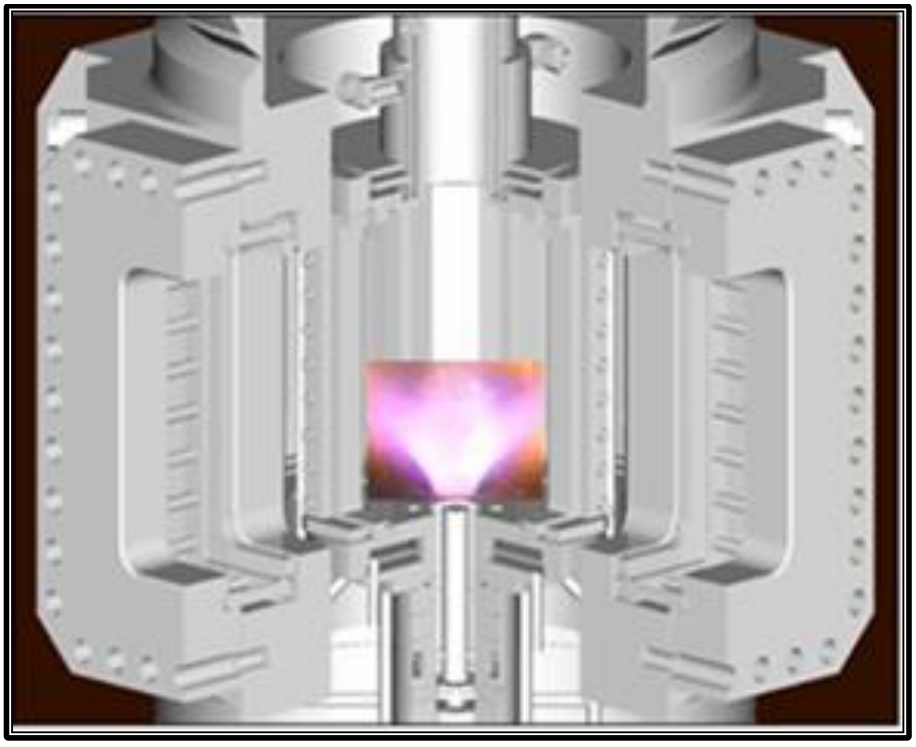

Figure 2.5: Sim Val Test Rig

2.2 Previous Ignition System Designs

An ignition source is needed to stabilize a flame along with fuel and oxidizer. An external ignition source, such as a flame or spark, must have sufficient energy in the form of heat to ignite the mixture. In Poland Ptasinski and Zeglen [24] investigated methane-air mixtures by multiple capacitor discharges. Under continuous flow of the mixture Ignition tests were performed at various compositions. It is consisted of an ignition chamber with stainless steel 19 electrodes of 10 mm in diameter and a separation between 0-10 mm with resolution to 0.01 mm.

Lewis and Von Elbe [25] studied mostly on minimum energies for igniting hydrocarbon gases with various oxygen-nitrogen atmospheres for short durations. The setup consisted of a spark circuit with low capacity high voltage condensers. The charge was transferred from the power unit through a resistor to the spark circuit. Gas is introduced and ignited to a test bomb where electricity was delivered. It was found that the energies shift toward the rich side as the number of carbon atoms is increased.

Usually ignition systems operate with capacitance and inductance components in its electric spark. The spark duration is approximately 0.5 μs. It is operated by changing the values of its resistance and capacitance. Kono et al. [26] used a long duration composite spark. In their experiment they used composite spark of a capacitance spark circuit with dc or ac discharge. The spark electrodes were 0.3 mm diameter tungsten wire with a 30° half angle cone. A 3.0 mm diameter steel rod tipped at 45° half angle cone for a high quenching effect. They experimented that the optimum spark duration varies from 50 to 300 μs. The optimum spark duration depended on the mixture and quenching of the electrodes.

Multi point ignition tests were carried out by Morsy and Chung [27]. Experimentation was done using a single shot laser with two conical cavities to introduce the methane-air mixture.

The combustion chamber was kept at a constant volume. Laser-induced ignition technique is used in which the unfocused laser beam irradiated into the conical cavity in the combustor wall. Multiple reflections of the laser beam along the surface permits ignition through gaseous breakdown.

Weinrotter et al. [28] carried out experiments engine like conditions under high pressure, constant volume chamber (up to 25 MPa) at an initial temperature of 473 K and initial pressures up to 3 MPa. Multi-point laser-induced spark ignition of hydrogen-air mixtures and Laser-induced spark ignition of lean methane-hydrogen-air mixtures were also investigated using Q-switched Nd:YAG laser at 1064nm with a pulse duration of about 5 ns. The two point ignition system reduced the peak pressure almost 50% in comparison to one point ignition. Three point ignitions were done with diffractive lens which separated the laser beam into three focal points with a mutual distance of about 5mm.

For the present study, a laser ignition system was not viable since previous experience in the laboratory and cost restrictions lead to the implementation of a spark ignition in the current combustor.

2.3 Flame Flashback Studies

Flashback is a dangerous issue which can lead to serious hardware damage and increased the pollutant emissions. One of the major tasks was to design an injector to prevent flame flashback from occurring. Laminar flame speed of hydrogen/carbon monoxide fuel mixtures over a large range of fuel compositions was analyzed by Dong et al. [29]. Syngas, a combination of carbon monoxide and hydrogen, was used a fuel in their experiments at various equivalence ratios, from lean to rich conditions. These authors also derived different empirical equations to

calculate laminar flame speeds of hydrogen, carbon monoxide, and hydrogen/carbon monoxide mixtures from their experimental results.

Dam et al. [30] investigated the flashback propensity of H_2–CO mixtures with the effects of N_2 dilution on the critical velocity gradient of H_2–CO mixtures. Additionally, they also analyzed some preliminary flashback propensity data of H_2–CO mixtures in a swirl stabilized combustor.

Blesinger et al. [31] studied the turbulent burning along the vortex axis as well as combustion induced vortex breakdown. Their main focus was on the effect of geometrical scaling of flashback on a cylindrical premixing zone. They also compared two geometrically scaled burners at equal Reynolds number.

To determine flashback limits and operability issues of a modern gas turbine engine Daniele et al. [5] performed experiments at gas turbine like conditions. They also described and discussed the dependence on the combustion parameters such as pressure, inlet temperature, and inlet velocity on characteristic flame behaviors.

Eicheler et al. [32] measured the turbulent flashback limits for atmospheric hydrogen-air mixtures in an unconfined tube burner and compared with literature results. Additionally, flashback limits were measured in a quasi-2D channel flow, which represents the confined situation of a flame already burning inside a duct. The tube burner was modified to allow the flame to enter the tube prior to flashback, which was comparable to the physical situation inside the channel setup.

Laminar burning velocities of hydrogen-air and hydrogen-methane-air mixtures at variable equivalence ratios were studied by Ilbas et al. [33]. Flame speeds were measured using

a high-speed Schlieren photographic technique. Flame propagation was also studied with the optical access for filming.

Fu et al. [34] studied laminar flame speed and flame structure of syngas with different compositions of 20% to 80% of hydrogen from equivalence ratios from 0.5 to 1.2 using OH-PLIF and mass spectrograph. Kinetic simulations were done using CHEMKIN-II. It was determined that the laminar flame speed and flame shape were affected by syngas compositions and a good correlation was achieved between the experimentally measured laminar flame speeds and simulated ones.

Noble et al. [35] experimented that flashback limits upon syngas fuel composition. Syngas fuels are typically composed primarily of H_2, CO and N_2 and may also contain smaller amounts of CH_4, O_2, CO_2 and other higher order hydrocarbons. It was also studied that flame speed appears to be the key parameter describing tendencies.

2.4 Flame Blowout Studies

Zhue et al. [36] experimentally investigated the flow field, reaction zone, and the flame structure properties for a flame near the lean blowout (LBO) limit. Measurements in the flame were made with a 2D-PIV, which is a nonintrusive, laser-based diagnostic technique for velocity measurements. For radical imaging, a laser system was used to excite and cause OH* chemi-luminescence and the information captured using an ICCD camera. This data was then analyzed to generate some key mechanistic conclusions about LBO in methane and hydrogen-enriched flames. The main goal of their study was to expand the knowledge base concerning the fundamental controlling processes associated with LBO in hydrogen-enriched premixed combustion.

Lean blowout limits were measured for premixed methane/hydrogen/air flames with a preheating temperature of 673 K and 773 K and high pressures in a study by Griebel et al. [37]. Fuel mixtures of 0–20% hydrogen by volume in methane were tested. Additionally, LBO was measured also for some hydrogen piloted cases. This stimulated the experimental investigation of lean blowout LBO limits for lean premixed methane/hydrogen/air flames in a generic combustor at conditions relevant to modern, low-emission, and stationary gas turbines. The results showed that premixing of hydrogen can extend the lean stability limit significantly. This extension of the LBO limit is linearly dependent on the hydrogen content of the fuel. Because of a higher OH radical concentration, which leads to a higher global reaction rate and a higher flame speed, the equivalence ratios where LBO is observed were lower with hydrogen enrichment.

Wang et al. [38] studied the effect of hydrogen addition on early flame growth of lean burn natural gas–air mixtures both experimentally and numerically. The authors used a Schlieren photographic technique in order to obtain the propagating photos of premixed combustion and direct-injection combustion. Different hydrogen fractions (from 0% to 40% in volumetric fraction) at overall equivalence ratio of 0.6 and 0.8, respectively were used to get pressure derived initial combustion. The results showed that hydrogen enrichment to natural gas, enhanced both premixed combustion and direct-injection combustion. Hydrogen addition enhanced the initial combustion process significantly for both laminar premixed and direct-injection turbulent combustion at lean mixture condition. The OH and O mole fraction was increased by hydrogen addition and the position of maximum OH and O mole fraction moved closer to the unburned mixture side. Spark ignition enhancement of lean natural gas–air mixtures with hydrogen addition were attributed to the increase of OH and O mole fraction in the flames.

2.5 Flame Studies Emitted from a Tubular Injector

Kushari et al. [39] studied the effect of injector's geometry on the performance of an internally mixed, air-assisted, liquid injector. In this type of injector a small amount of air was injected into a liquid stream within the injector. The interaction of the liquid with the atomizing air inside the injector induced atomization. The results showed that the size of the droplets produced by the investigated injector decreases with a decrease in the air injection area. This is due to the increase in atomizing air injection velocity that accompanied the decrease in the air injection area, which improved atomization.

Dodo et al. [40] applied a "multi-injection burner" as shown in figure 2.6 concept to a preliminary burner for hydrogen-rich syngas simulating that from integrated coal gasification combined cycle (IGCC) with carbon dioxide capture and storage (CCS). In a preliminary experiment, the multi-injection burner worked without any flashback or any blowout under atmospheric pressure. A prototype multi-cluster combustor based on the results of that preliminary study was made to be a dry low NO_x combustor for hydrogen-rich syngas of IGCC with CCS.

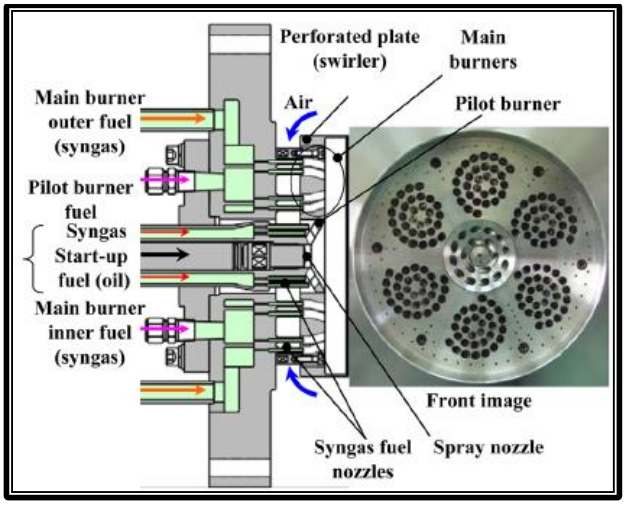

Figure 2.6: Schematic View of Flat Multi-Cluster Injector

Litllejohn et al. [41] conducted experiments to investigate the fuel effects on the turbulent premixed flame produced by a gas turbine low-swirl injector (LSI) (figure 2.7). The lean-blow off limits and flame emissions for seven diluted and undiluted hydrocarbon and hydrogen fuels show that the LSI is capable of supporting stable flames. Velocity statistics shows that the non-reacting and reacting flow fields of the LSI exhibit similarity features. The overall effect of the flame is that of an aerodynamic blockage against the flow supplied through the LSI obtained from the analyses of the non-reacting and reacting flow-fields. The net result is a systematic shift of the divergence flow into the LSI, increases in the divergence rates and increases in the mean axial and radial velocities in the swirl annulus region. These effects are weaker for the flames with lower heat releases.

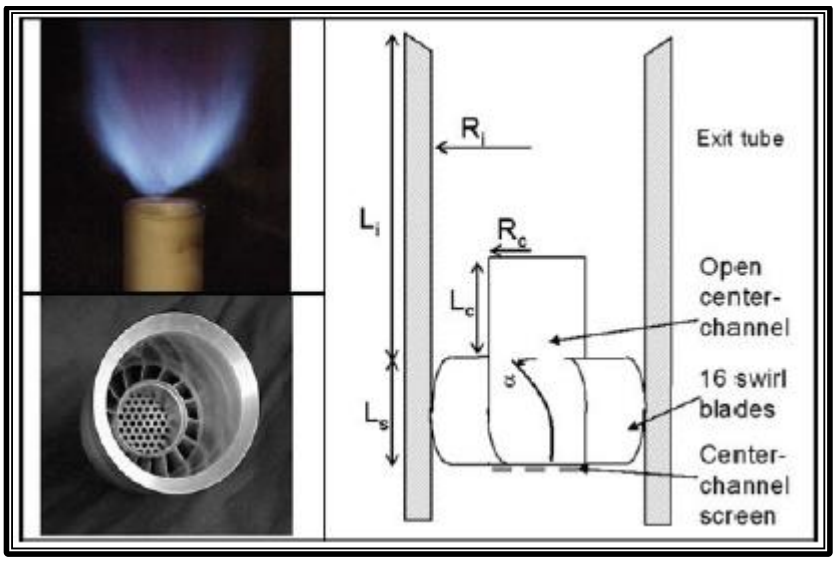

Figure 2.7: Schematic and Photograph of the Injector

York et al. [42] designed a fuel injector as shown in figure 2.8 for low-NO_x combustion of high-hydrogen fuels like carbon-free syngas. The multi-tube mixer utilized jet-in-cross flow mixing of the fuel and air inside of small-diameter tubes at many locations. The multi-tube mixer was tested in a small-scale single nozzle rig where realistic gas turbine conditions were used. The multi-tube mixer concept was employed in full-can combustion system designed for high-

hydrogen fuel based on encouraging single nozzle emissions and operability. The scale up to a multi-nozzle combustor was successful for 100 hrs of operating experience with more than 90% hydrogen in the reactants.

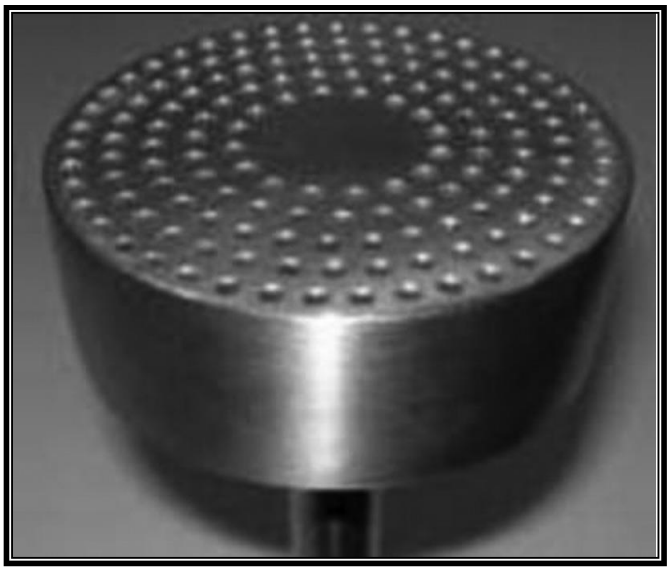

Figure 2.8: Large Scale Multi-tube Mixer with Single Nozzle

2.6 NOx Pollutant Emission Studies

Gobbato et al. [43] studied a CFD steady state analysis on the reverse-low combustor of a medium size heavy duty gas turbine (about 10 MW). The combustor features steam injection to reduce the pollutant emissions. The model of the combustor was conceived for a thermo acoustic analysis requiring unsteady simulations to be performed over an operational period of several seconds. Thus a very coarse mesh and low CPU-usage numerical models were employed in order to reduce the computational effort. This study predicted the overall emissions of the combustor by applying a NO_x post-processing approach on the frozen reactive flow field. The numerical concentrations were compared with the concentrations measured at the discharge of the combustor. The comparison was made against the amount of steam injected when the combustor was fed by natural gas or hydrogen.

Lyra et al. [44] experimented with a premixed methane air jet flows into a cylindrical combustion chamber. The combustion air was preheated. The combustor geometry induced hot recirculation of gases which aids the flame stabilization. On the other hand CFD solutions obtained using a simple global reaction scheme to capture the pollutant emissions. The Equivalent Reactor Network (ERN) approach used gave an accurate reproduction of the flame position and concentrations of CO and NO_x.

Ghenai et al. [45] analyzed a three-dimensional CFD model of syngas fuel combustion in a gas turbine can combustor. Five syngas fuel mixtures with different fuel compositions were tested in this study. The syngas fuels were produced by different gasification processes using different feed stocks (coal, biomass, waste). The k-ε model was used for turbulence modeling, mixture fractions/PDF model for non-premixed gas combustion, and P-1 for radiation modeling. Baseline fuel (methane) combustion: the results of the gas temperature, velocity field, swirling strength and CO_2 and NO_x emissions show that gas turbine can combustor burns the fuel efficiently, reduces the emissions, and, lowered the wall temperature. The predicted maximum temperature of methane fuel combustion compared well with the theoretical adiabatic flame temperature.

Giles et al. [46] used a counter flow configuration to simulate syngas combustion and characterize the effects of diluents on NO_x emission in syngas non-premixed flames. Two representative syngas mixtures, namely 50%H_2/50%CO and 45%H_2/45%CO/10%CH_4 by volume, were selected using data from various syngas power generation facilities around the world. Based on the presence of these diluents during the gasification, refinement, and combustion of syngas, three diluents, namely N_2, H_2O, and CO_2, were selected. The effectiveness of these diluents was characterized in terms of their ability to reduce NO_x

emissions from syngas flames. Syngas non-premixed flames are characterized by relatively high temperatures and high NO concentrations and emission indices. The presence of methane in syngas decreases the adiabatic flame temperature and thus the thermal NO_x, but increases the formation of prompt NO_x significantly.

Fichet et al. [47] studied that the numerical prediction of NO_x emissions from gas turbines generated from the Computational Fluid Dynamics (CFD), a Reactor Network (RN). The NO_x emissions predicted are in good agreement with the measured data (at pressure 15 bar). At last the RN methodology has proved to be the most efficient method to estimate the NO_x emissions with a short response time and small CPU requirements.

Chapter 3 : Experimental Procedure and Design Methodology

3.1 Combustion Chamber

A laboratory scale high-pressure gas turbine combustor (HPTC) was used to study the effects of flame stability as well as emissions produced by syngas at high pressures. The combustion chamber has four configurable modules: (1) Inlet manifold, (2) Front cap, (3) Optically accessible combustion chamber and (4) End cap.

3.1.1 Inlet Manifold

The inlet manifold (Figure 3.1) is composed of three modular sections. The first acts as the fuel/air inlet and mixture section. The second is a removable static mixture section which is composed of honeycomb located inside the chamber that removes irregularities and straightens the flow. This section is then attached to the third section (front cap) which connects the inlet manifold to the main combustor section. Flanges are used as connections between the inlet manifold and three modular sections and the use of 0.635 cm stainless steel bolts connect the inlet manifold to the combustor connecting front cap. There is also a pressure blowout valve located at the third modular section to provide a level of safety in case of malfunction and an increase of pressure. The given dimension of the inlet manifold is 97.79 cm with the three modular section composed of 30.48 cm length of the inlet/initial mixture zone, 30.48 cm length of the static mixture section, and 30.48 cm length of the connecting section. The inner diameter of the piping is 5.08 cm with a 0.635 cm thickness for all three sections. Since improper mixing leads to incomplete combustion causing more CO_2 emission, the combustor developed incorporates a pre-mixing manifold. The fuel-air mixture passes through the static mixture section to eliminate injection induced flow irregularities and insures proper mixing. Also inlet manifold is designed such a way so that it can incorporate different configurations of fuel

injectors. After mixing, the fuel and air pass to the combustion chamber which can accommodate multiple geometrical configurations including a non-swirl stabilized, swirl flow, and center-body stabilized swirl flow flame.

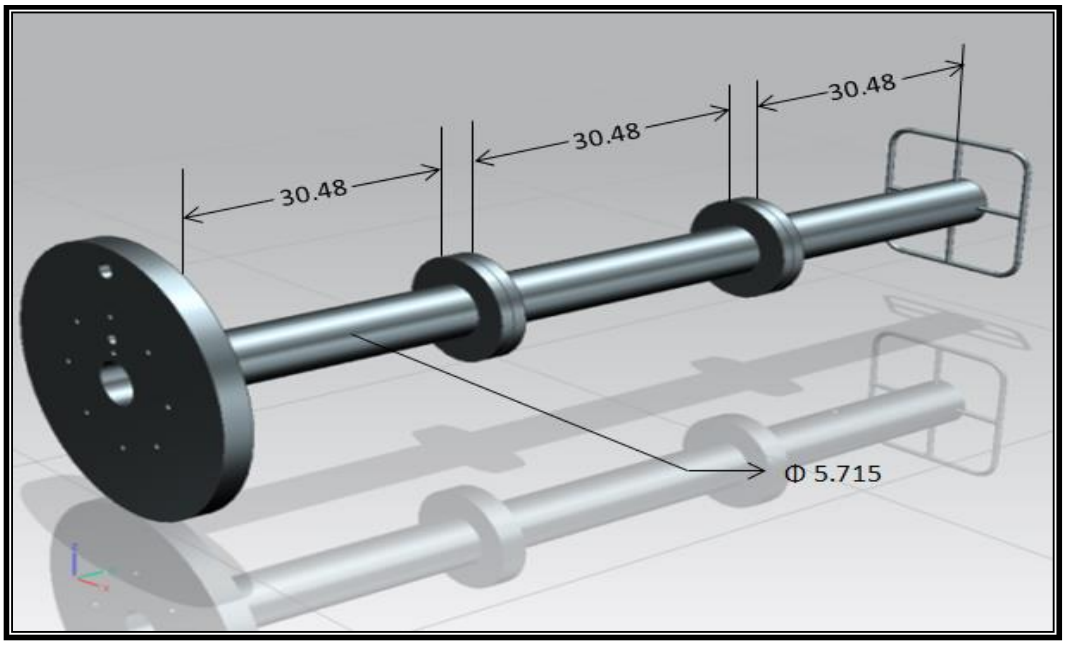

Figure 3.1: Inlet Manifold

3.1.2 Front Cap of Combustor

The purpose of the front cap (Fig. 3.2) is to act as a connection between the inlet manifold and the main combustion chamber. The front cap also houses the removable swirler and an igniter composed of a spark ignition source and a methane tube line that will act as a pilot flame. A 0.635 cm inner hole located in the center of the front cap houses the swirler on other fuel injection unit. The front cap is connected to the main combustion chamber with the use of 21.59 cm stainless steel bolts. The inlet manifold is connected to the front cap through the use of 0.635 cm stainless steel bolts and a half flange configuration in the inlet manifold. The use of an inner circular grove on the front cap is implemented with an inner diameter of 12.96 cm and

outer diameter 23.11 cm to be used to accommodate the quartz tube in future experiments. Two instrumentation ports are also incorporated having a 0.635 cm diameter and will allow the use of pressure transducers, thermocouples, or any other configurable instrumentation device needed. Modifications had to be made on the front cap in order to accommodate an entrance for the ignition system. A 1.91 cm hole was drilled 3.81 cm center to center from the main combustion line to allow a threaded entrance for the ignition system. The entrance port was made at a 10 degree angle in order for the igniter flame to hit the main combustion line.

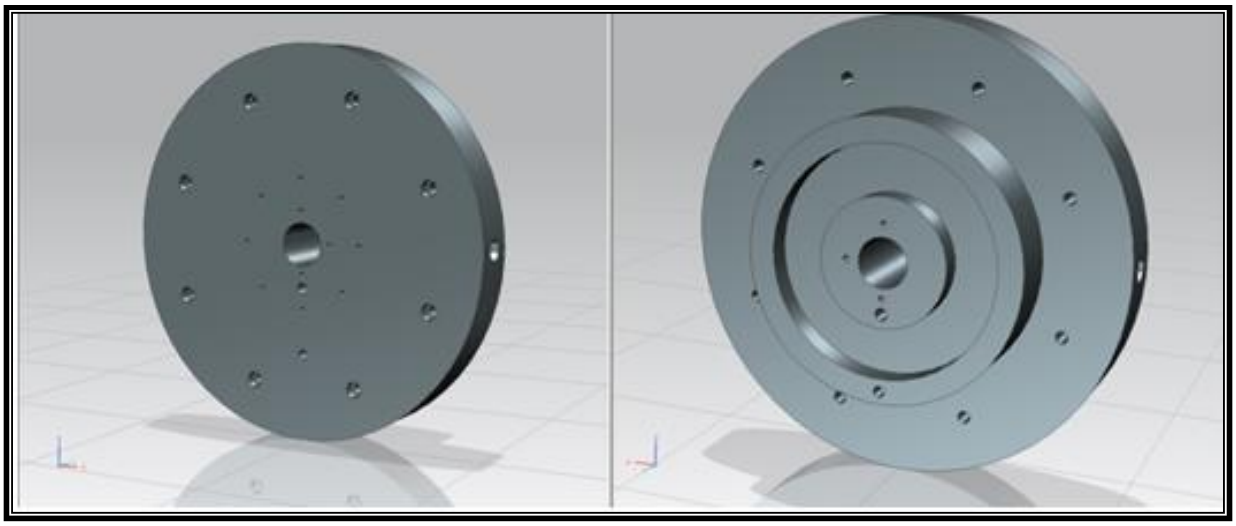

Figure 3.2: Front Cap Outer Side (left) Inner Side (Right)

3.1.3 Optically Accessible Combustion Chamber

The main combustion chamber, Fig. 3.3, houses the combustion of the air and fuel mixture. As mentioned previously the combustor section dimensions were determined based on FEA design calculations. The combustor has an inner diameter of 28.35 cm with an 8.61 cm thickness. The total length of the combustor is 64.77 cm, determined by the expected flame length for the premixed and non-premixed type flames that would be tested. Three window ports

are located on the two sides and top of the combustor evenly spaced by 90 degrees off their center. The three windows span nearly the entire length of the chamber and were selected to allow optical access to flame behaviors, specifically designed for use with OH-PLIF and PIV measurements. This configuration allows for the laser signal to pass through the test section of interest and exit through the opposite facing window. The third window was included to capture flame images using an externally located camera system. The rectangular window slots have dimensions of 31.75 cm by 10.16 cm in length and width with a thickness of 5.08 cm. These dimensions again were based on the FEA calculations and optically accessibility. The rectangular quartz windows fitted into these slots with a tolerance of 3 mm so that expansion of steel and glass did not lead to cracking as temperature increased. Window covers were also designed to accommodate high temperatures; these covers have outer dimensions of 16.51 by 38.1 cm. Three circular ports were also built into the main body of the combustor. These ports having a 5.08 cm diameter allow for instrumentation devices or additional windows to be added at a future date.

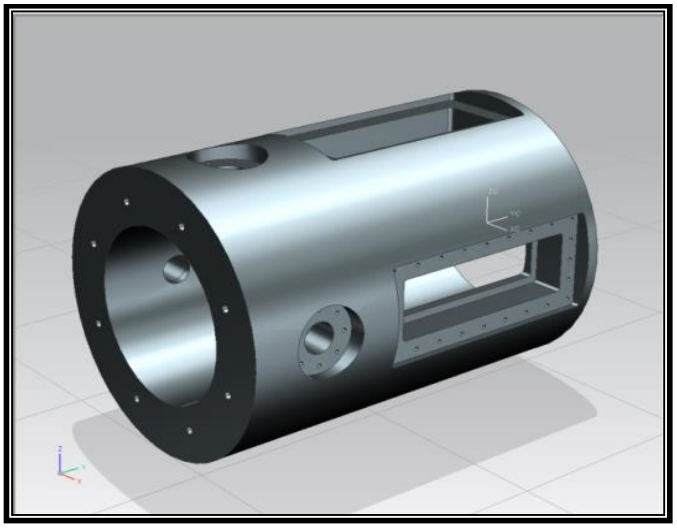

Figure 3.3: Combustion Chamber

3.1.4 End Cap

The end cap shown in Fig. 3.4 was designed into two separate modular sections. These two sections include the converging nozzle and outer cap which connects the end cap to the main combustion chamber. This end cap connects the combustion chamber to the exhaust system. The outer dimensions of the cap system are 45.97 cm and are attached to the main combustor by 21.59 cm stainless steel bolts similar to the front cap. The end cap also has a 5.08 cm diameter port for the converging nozzle exhaust port. The nozzle allows for the control of the pressure drop in the combustor. In order to reach a maximum pressure of 1.5 MPa in the combustor, the throat area was calculated using Eq. (3) and was found to be 161.29 mm^2.

$$A_t = \frac{\dot{m}\sqrt{RT_T}}{P_t\sqrt{\gamma Ma}}\left(1 + \left(\frac{\gamma-1}{2}\right)Ma^2\right)^{\frac{\gamma+1}{2-2\gamma}} \tag{3}$$

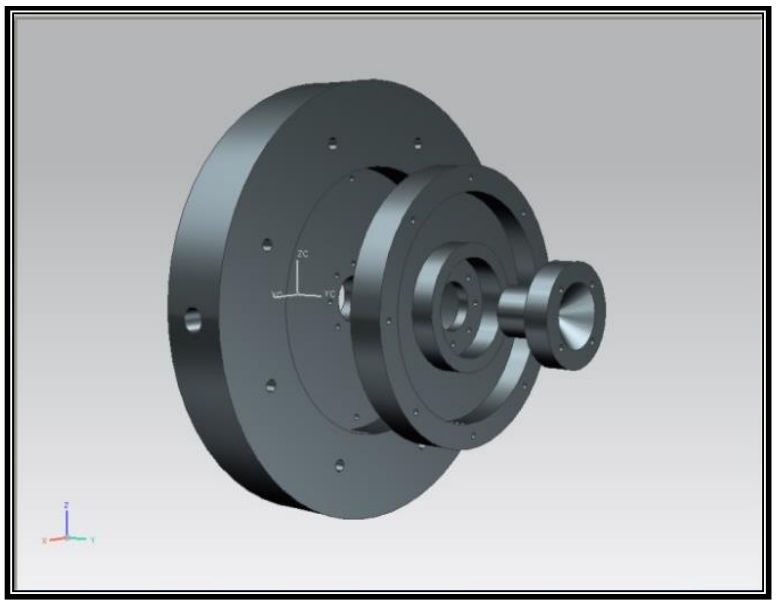

Figure 3.4: End Cap

3.1.5 Swirler

In this work a center body swirler with 12 vanes is used. Its center body is made from stainless steel and the vanes are from anodized aluminum for higher temperature resistance (Fig 3.5). A swirl number of 0.97 is used. Swirl number is defined as the axial flux of swirl momentum divided by the axial flux of axial momentum, times the equivalent nozzle radius using the following equation. The swirl number has a direct effect on the flames size, shape, stability, and combustion intensity as previous studies have proven. In Figure 3.5 it is shown that how the swirler is integrated in the high pressure gas turbine combustor.

$$S = \frac{2}{3}\left[\frac{1-\left(\frac{d_h}{d}\right)^3}{1-\left(\frac{d_h}{d}\right)^2}\right]$$

Where d_h and d are the hub diameter and swirler diameter respectively.

Figure 3.5: Swirler

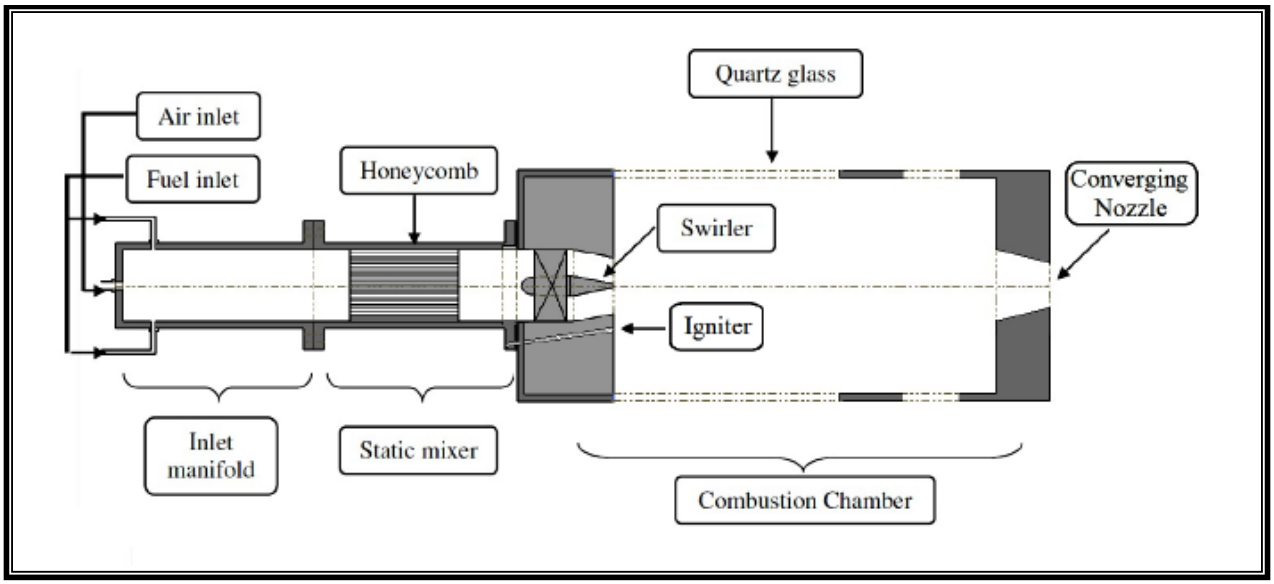

Figure 3.6: Schematic for the High Pressure Gas Turbine Combustor Integrated with Swirler

3.1.6 Injector

Injector consists of three different parts-(1) Injector head. (2) Connecting tube. (3) Base. All the components are made of Stainless Steel 410. Injector head as shown in Fig 3.7 is made out of a converging disc. This disc is converged from diameter 0.05 to 0.03 m.

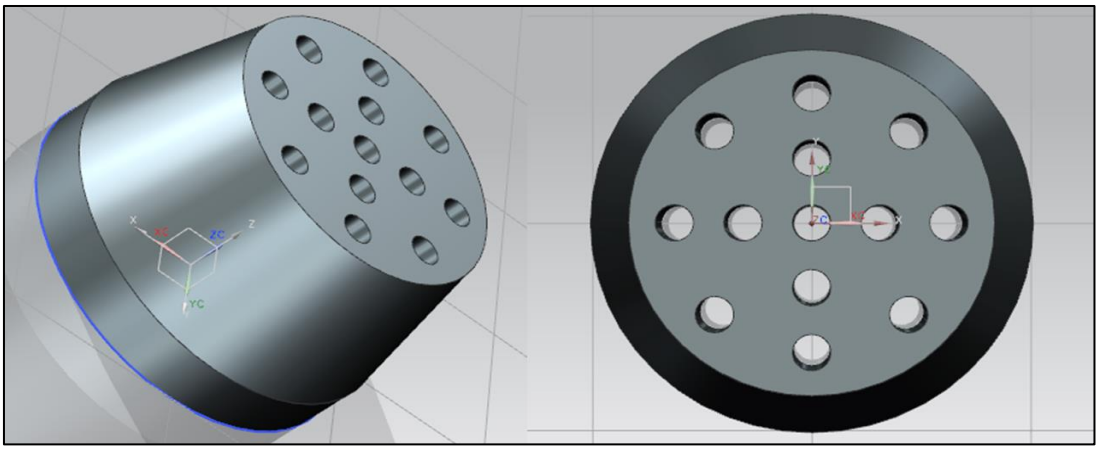

Figure 3.7: Injector Head

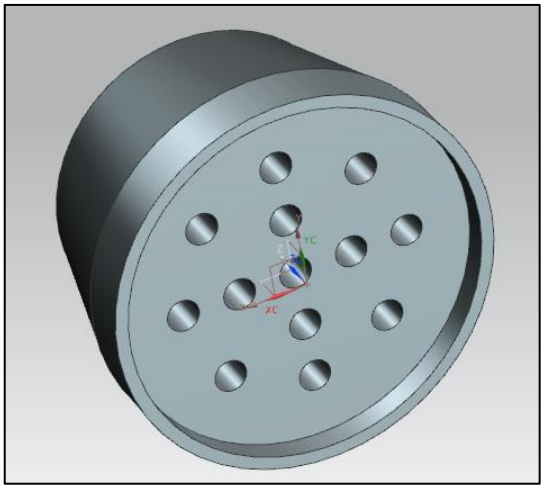

Figure 3.8:: Bottom Surface of Injector Head

It consists of 13 holes having diameter of 0.004 m (Fig 3.8) and depth of 0.02 m, closest orifices are apart by 0. 01 m, while the distant orifices are apart by 0.007 m.

Connecting tube is used to connect the injector head with the injector base. Connecting tube has diameter of 0.03 m and height of 0.1 m. a grouping was made as shown in Fig 3.9 at the bottom side of the injector to wield it with``` the connector.

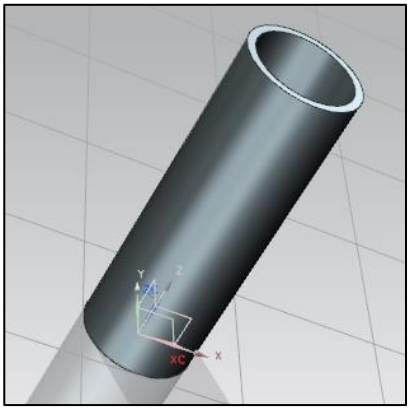

Figure 3.9: Connectiong Tube

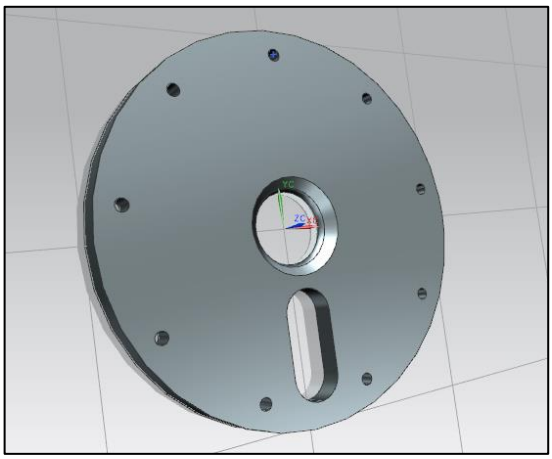

Figure 3.10: Injector Base

Figure 3.10 connects the injector to the front cap of the combustor. The base has the diameter of 0.02 m. Figure 3.11 illustrates how the injector is integrated inside the high pressure combustor.

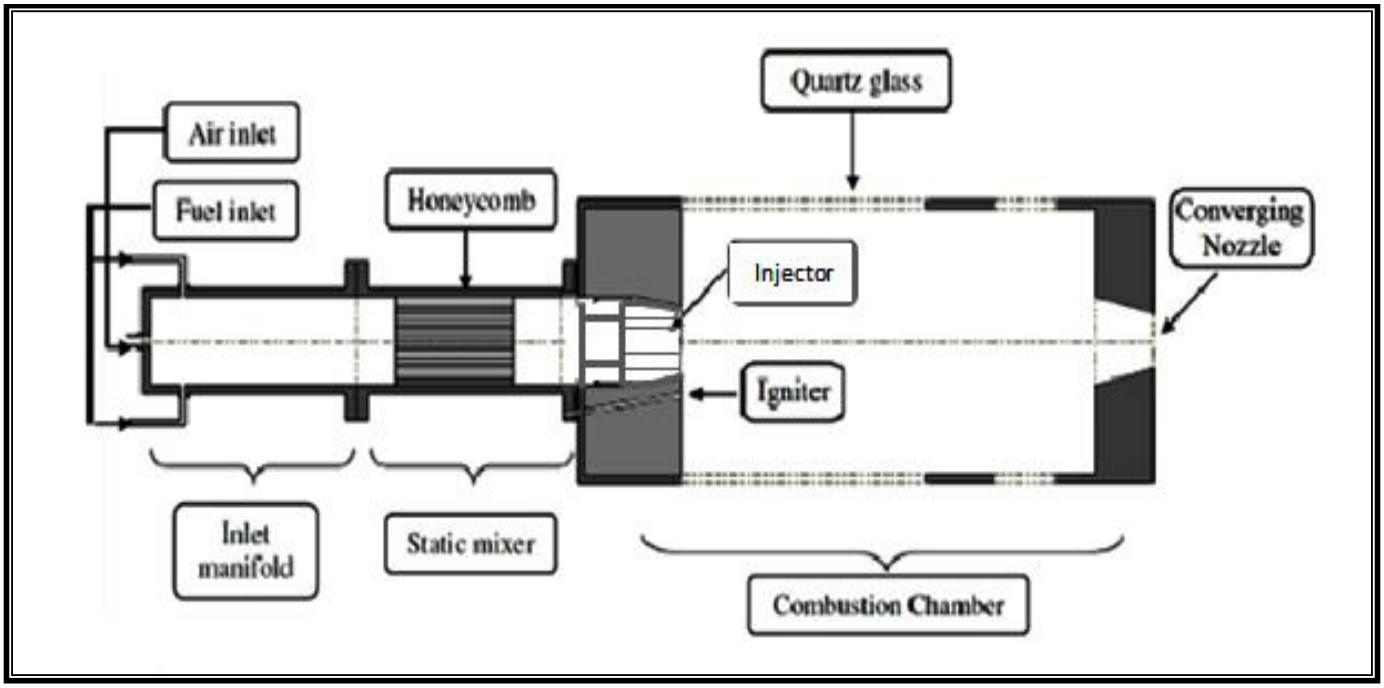

Figure 3.11: Schematic of the High Pressure Gas Turbine integrated with Injector

3.2 Control System

The Control system consists of proportional control valves, solenoid valves, needle valves and flow meters (Fig. 3.12).

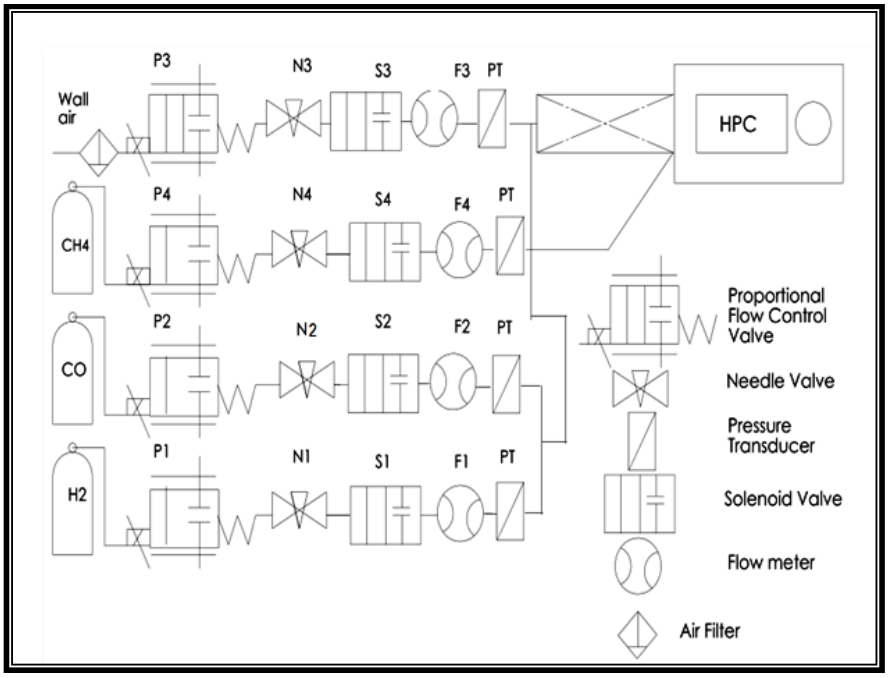

Figure 3.12: Schematic for the Control System

This system is operated remotely using Lab View. Proportional flow control valves are used to regulate the flow using voltage as input. According to the voltage input the valves are opened. Solenoid valves are also known as shut off/on valves. These valves are installed to shut off the lines as per need using LabVIEW. Needle valves are installed in order to regulate the flow precisely. Flow meters are used for recording the flow. A manual emergency shut off button is integrated with the solenoid valves. The emergency button will be used to shut off the solenoid valves all together.

3.2.1 Proportional Flow Control Valves

The Proportional Control Valves (PVC) will control the flow of H_2, CO, Air and the ignition fuel respectively.

Figure 3.13: KZ Valve EH2 Series

The EH2 series PVCs from KZ Valve are powered with 12VDC (Fig. 3.13). These valves are rated at 6895 kPa (approx. 69 bars) and are capable of being regulated with an output of 0-10 V.

3.2.2 Solenoid Valves

The Solenoid Valves (SV) from Jefferson Valves are actuated with 120 VAC (Fig. 3.14). These SVs were selected due to their pressure differential of 1550 kPa (Approx. 15 bars) and a 1.91cm connection that allows high flow rates. They are made of 316 Stainless Steel and normally closed two way valves.

Figure 3.14: Jefferson Valves 1314 Series

3.2.3 Flow Meters

Flow meters are used to measure the gas flow. These flow meters are from Omega and FMA 1843-1845. These flow meters are selected based on their flow measurement capacity as per required for the experiment. Flow meters are connected to the USB 6008 DAQ 1 and to the power supplies. In order to power the flow meters and communicate with the computer, Pins number 2-5 were used as shown in Fig. 3.15. They require an excitation voltage of 12 VDC and current of 0.2 ampere per flow meter.

PIN	FUNCTION
1	Remote LCD display signal
2	0 to 5 VDC output indication
3	0 to 5 VDC common
4	Power supply, positive
5	Power supply, common
6	Remote LCD display reference
7	(unassigned)
8	4 to 20 mA output indication
9	4 to 20 mA common

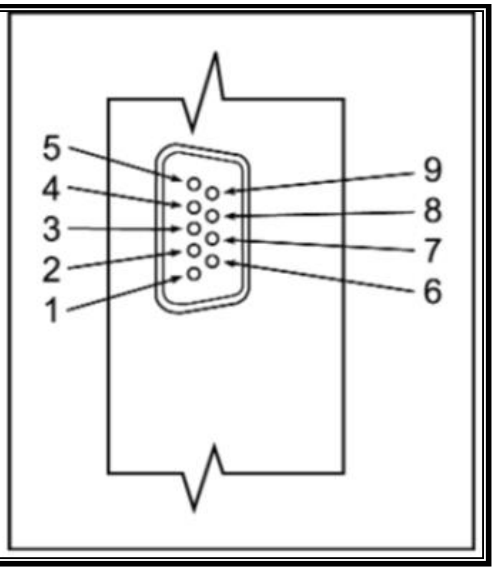

Figure 3.15: Pin out of the Flow Meter

Numeric displays as shown in Fig. 3.16 allow the visual observation of the flow rate that allows comparing the flow rate with the graphical interface.

Figure 3.16: Flow Meter

3.2.4 Pressure Transducer

Pressure transducers are also installed in the system in order to have the line pressure. Omega pressure transducers PX309-300G5V as shown in Fig. 3.17 were integrated into the system. This pressure transducer requires an excitation voltage of 9-30 VDC.

Figure 3.17: Pressure Transducer Omega PX309-300G5V

3.2.5 Needle Valves

A needle valve (Fig 3.18) is a type of valve having a small port and a threaded, needle-shaped plunger. It allows precise regulation of flow, although it is generally only capable of relatively low flow rates.

Figure 3.18: Needle Valves

3.3 Electrical Characteristics of HPC Components

A detailed analysis is done to define requirement for the control of the flow. The requirements for proportional flow control valves, solenoid valves, flow meters and pressure transducers are different. The characteristics of each part of the instrumentation are shown in the Table 3.1.

Table 3-1: Electrical Characteristics of the Components

Purpose	Hardware components	Number	Electrical characteristics
Control	solenoid valves	4	Excitation:120 VAC
	proportional control valves	4	Excitation:12VDC
			Output: 0-10 VDC
Measurement	pressure transducers	3	Excitation: 9-30DC
			Output: 0-5 VDC
	Mass flow meters	4	Excitation: 0-12 VDC
			Output: 0-5 VDC

3.4 Power Supply

Two power supplies are used to meet up the demand for power of the control system. An EXTECH Instrument model number 382270 (Fig. 3.19) is used to deliver power to flow meters and pressure transducers.

Figure 3.19: EXTECH Instrument Model Number 382270

Extech power supply has four outputs: two 0 to 30 V with a maximum of 5 A, one 3 to 6.5 V with a maximum of 3 A and one 8-15 V with a maximum of 1A. MASTECH DC power supply as shown in Figure 3.20 is used to provide power to proportional flow control valves.

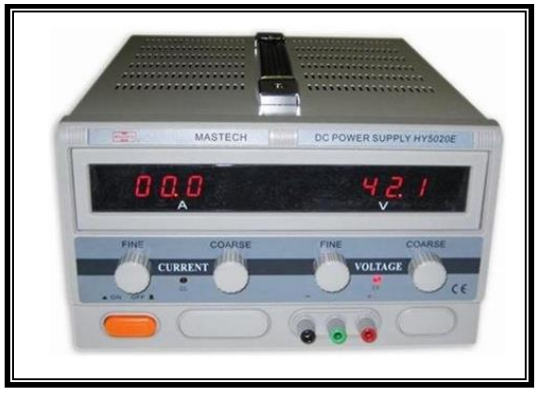

Figure 3.20: MASTECH Instrument

3.5 Hardware Components for Solenoid Valves

This PCI (Fig 3.21) card is used to control the solenoid valves with the mechanical relay outputs via LabVIEW. The NI PCI-6521 has eight mechanical relay outputs (Fig 3.22) and can output 150 Volts AC or DC. The PCI 6521 is solely a relay card which was used to actuate the solenoid shut off valves as well as the igniter coil.

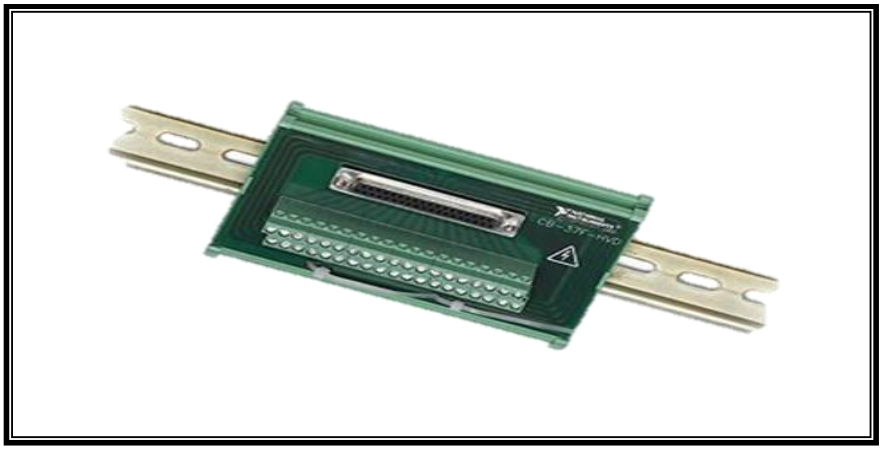

Figure 3.21: PCI 6521 Card

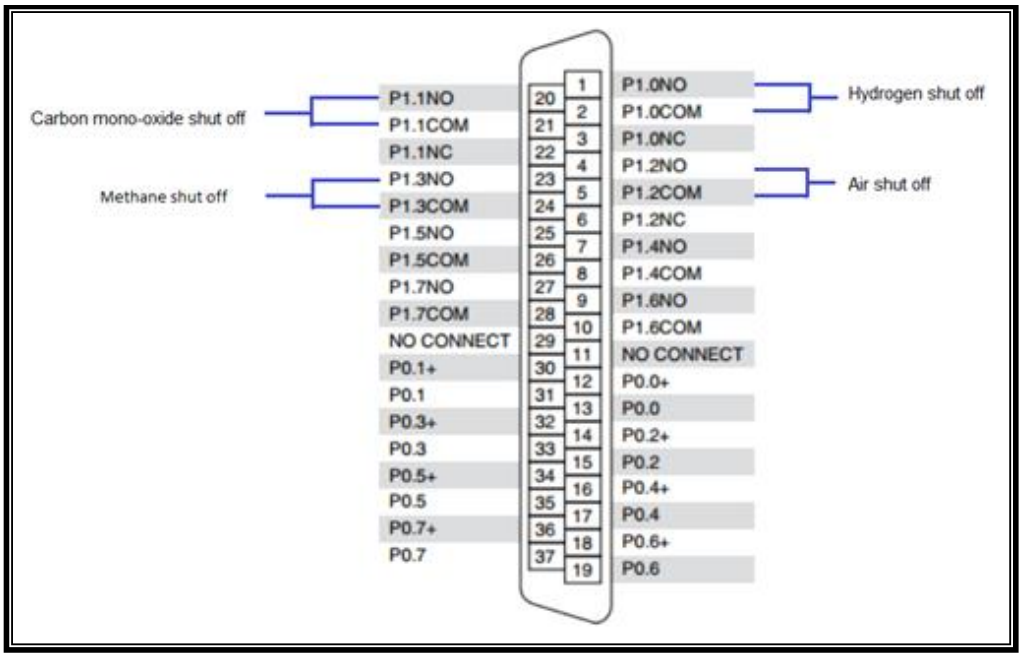

Figure 3.22: PCI Pin Position for Solenoid Valves

3.6 Hardware Components for Proportional Flow Control Valves, Flow meters and Pressure transducers

Two USB-6008s are used in order to control proportional valves, flow meters and pressure transducers. The USB-6008 (Fig 3.23) has eight ±10 V analog inputs and two 0-5 VDC analog outputs. The USB 6008 has both analog outputs and inputs. First DAQ (Fig 3.24) is used for flow meters and two proportional valves and second DAQ (Fig 3.25) is used for pressure transducers and two proportional control valves.

Figure 3.23: USB DAQ-6008

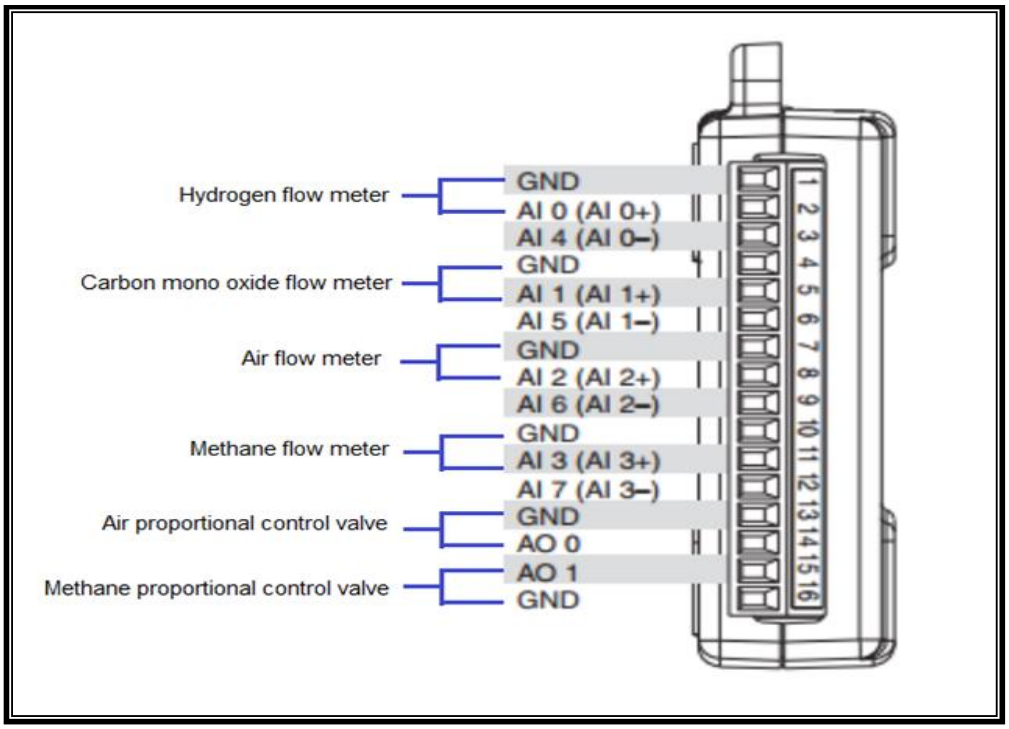

Figure 3.24: USB DAQ-6008 (DAQ-1)

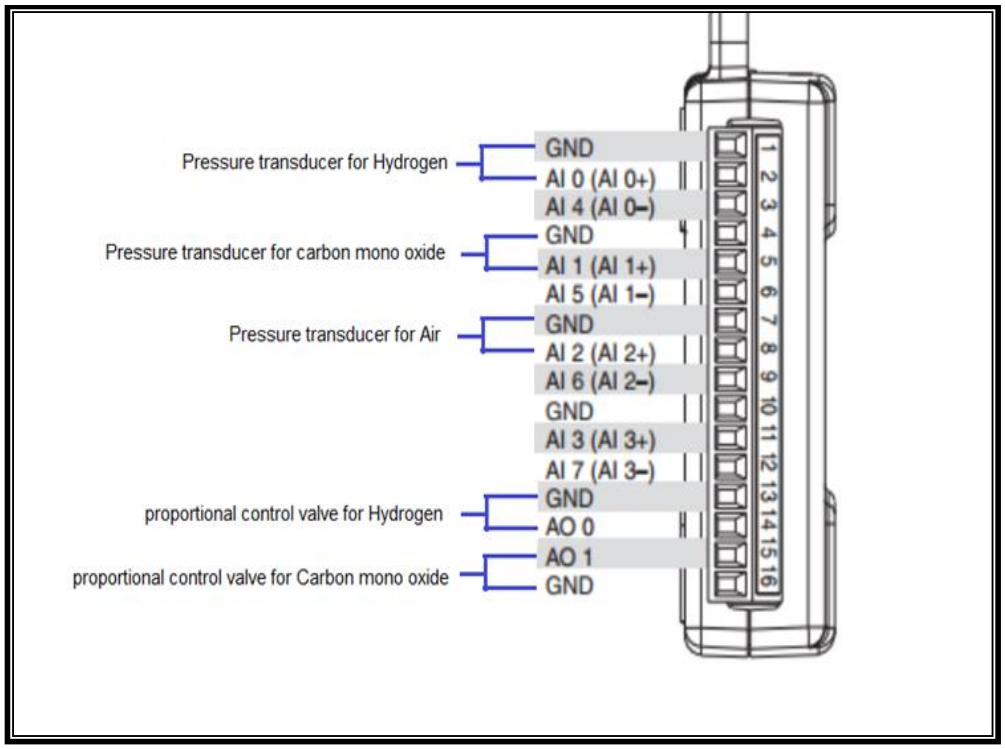

Figure 3.25: USB DAQ-6008 (DAQ-2)

3.7 Ignition System

Ignition system is used to produce spark inside the high pressure gas turbine combustor. This system consists of 12 V battery, ignition coil, signal generator and modified spark plug. The ignition system and its components is discussed below:

3.7.1 Modified Spark Plug

The spark plug is modified and extended in order to meet a length of 45.72 cm. The haynes 230 rod was chosen and it is welded to the spark plug in order to achieve the extension needed and the ground electrode insulator was cut as shown in figure 3.26. Haynes 230 was selected as the central electrode material due to its low resistivity and high melting point.

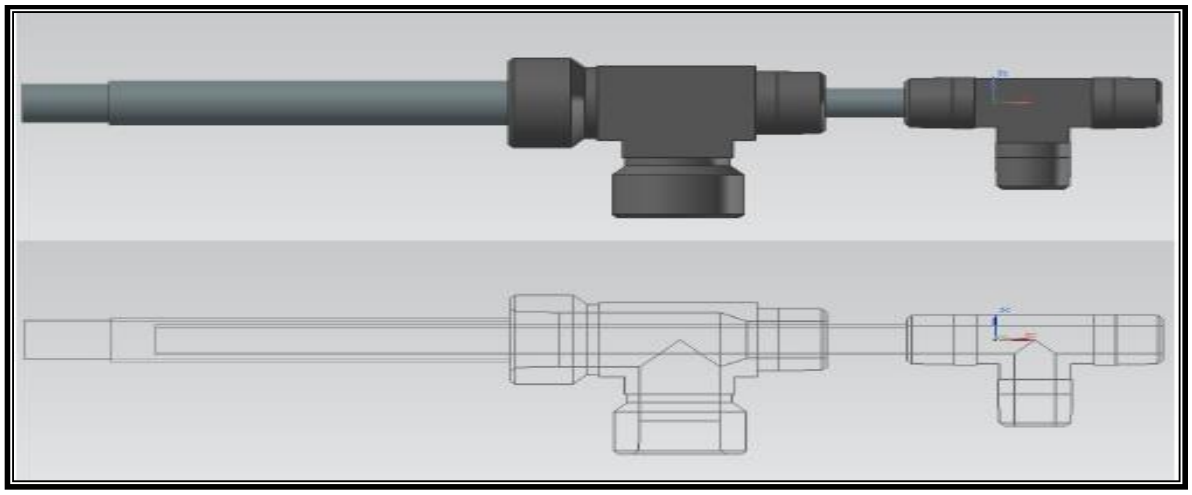

Figure 3.26: Ignitor Design

Ceramic thermocouple insulator from Omega was selected to insulate the electrode due to its high temperature resistance. It is made of mullite type ceramic which can withstand temperatures up to 1650°C. Resbond was also used to attach the insulators to the spark plug. Figure 3.27 shows the components of the spark plug and figure 3.28 demonstrates the complete assembly of the igniter.

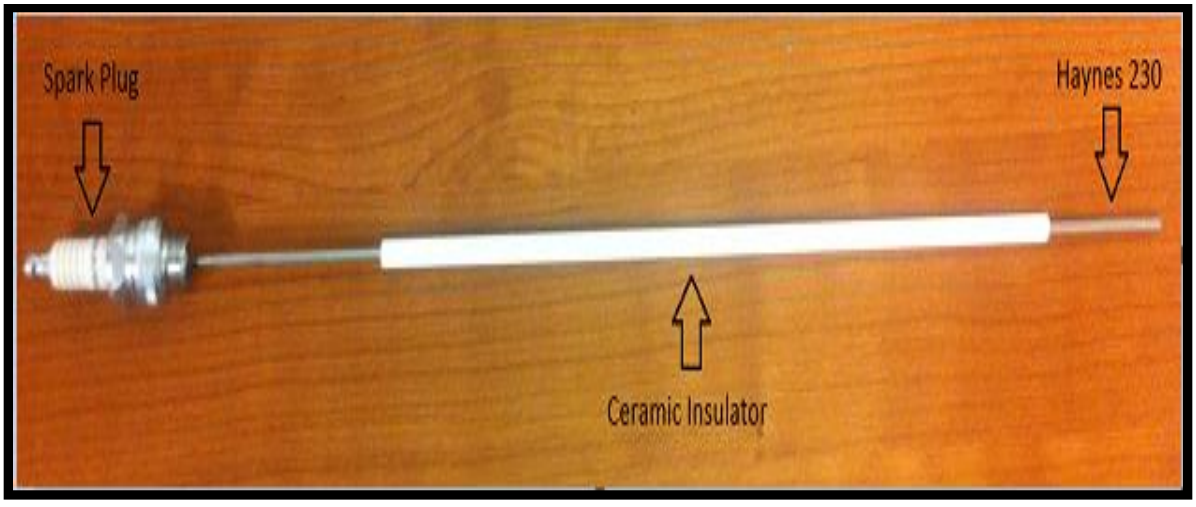

Figure 3.27: Components of the Spark Plug

Figure 3.28: Igniter Assembly

3.7.2 Ignition Coil

MSD 8285 multi-spark coil (Fig 3.29) is chosen to produce the discharge needed for the spark plug. The frequency of 100 Hz and 5V voltage are provided by using a signal generator and a 12 V battery respectively. There are four connector pin (Fig 3.30) inside the ignition coil as shown in the figure. The connections of the connector pin are described as follows:

- 12 V connector pin point to the 12 V battery positive.
- Coil input to PCI 6521 card
- Coil ground to 12 V battery negative

F

Figure 3.29: MSD 8285 Ignition Coil

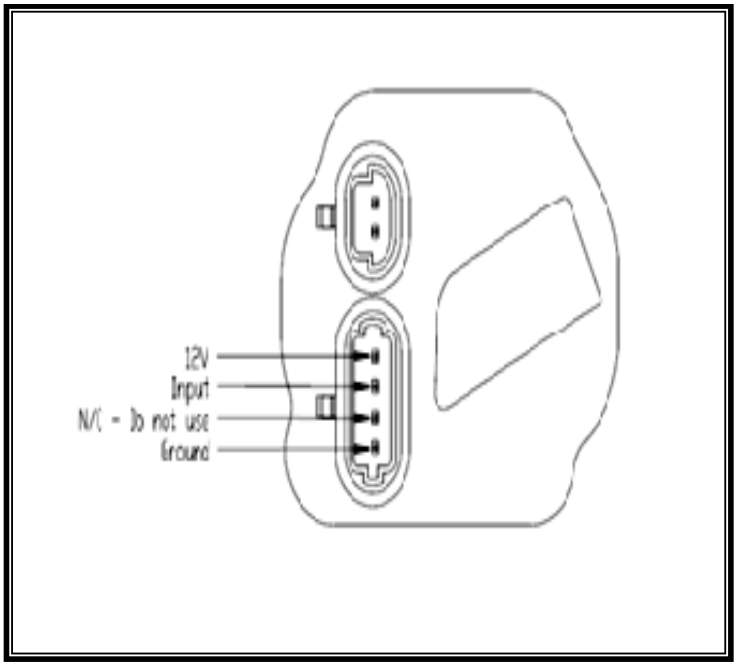

Figure 3.30: Ignition Coil Connection Pin Out

3.7.3 Battery

A 12 V battery (Fig 3.31) is used to supply current for the spark plug. As it is described in the ignition coil section, the positive connection is used as the voltage for the ignition coil. The negative connection of the battery is used as ground for the coil as shown in the figure 3.31. The negative battery connector was also grounded to the power supplies in order to avoid any undesired current. Figure 3.32 demonstrates the battery connector with all its components. The two green cables are used as ground and each one connects to one power supply for safety purposes.

Figure 3.31: 12 V Battery

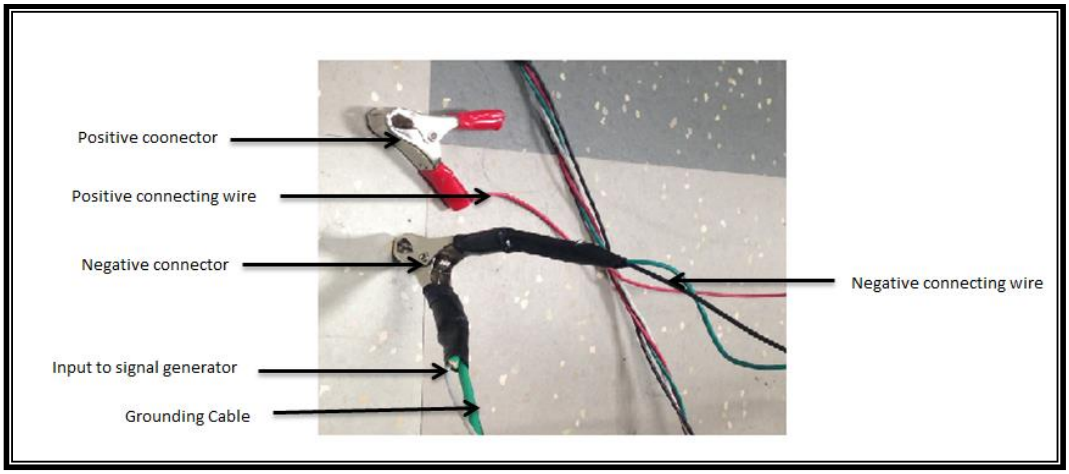

Figure 3.32: Battery Connectors

3.7.4 Signal Generator

A BK Precision 4012A signal generator, Fig 3.33, is selected to produce 100 Hz frequency which is the requirement for the coil. A square signal is sent via a transistor-transistor logic (TTL) channel. It is very important to connect only to the TTL channel because the output channel gives 14 V which can burn the coil. Another reason, the coil will not turn on unless the TTL 5V signal is sent via LabVIEW. The Bayonet Neill-Concelman (BNC) cable was used in order to connect the positive and negative wires.

Figure 3.33: Signal Generator

Figure 3.34 demonstrates the complete assembly of the ignition system with all of its components

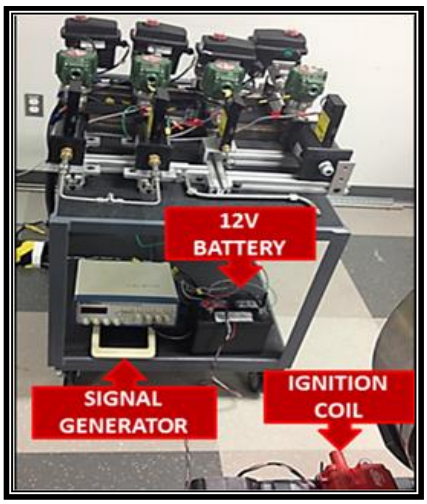

Figure 3.34: Ignition System

3.8 Integration of the Control and Ignition Components

All the hardware equipment is configured with LabVIEW software. LabVIEW has graphical user interface that helps remote operation and controlling. Both USB DAQ and PCI card are configured with this software. Figures 3.35 and 3.36 show the configuration of the flow meters for CO, H_2, CH_4, air and proportional control valves for CO and H_2 with DAQ 1. Figures 3.37 and 3.38 demonstrates the configuration of the pressure transducers for CO, H_2, air and proportional control valves for CH_4 and air with DAQ 2. Figure 3.39 shows PCI card configuration of the solenoid valves for CO, H_2, CH_4 and air.

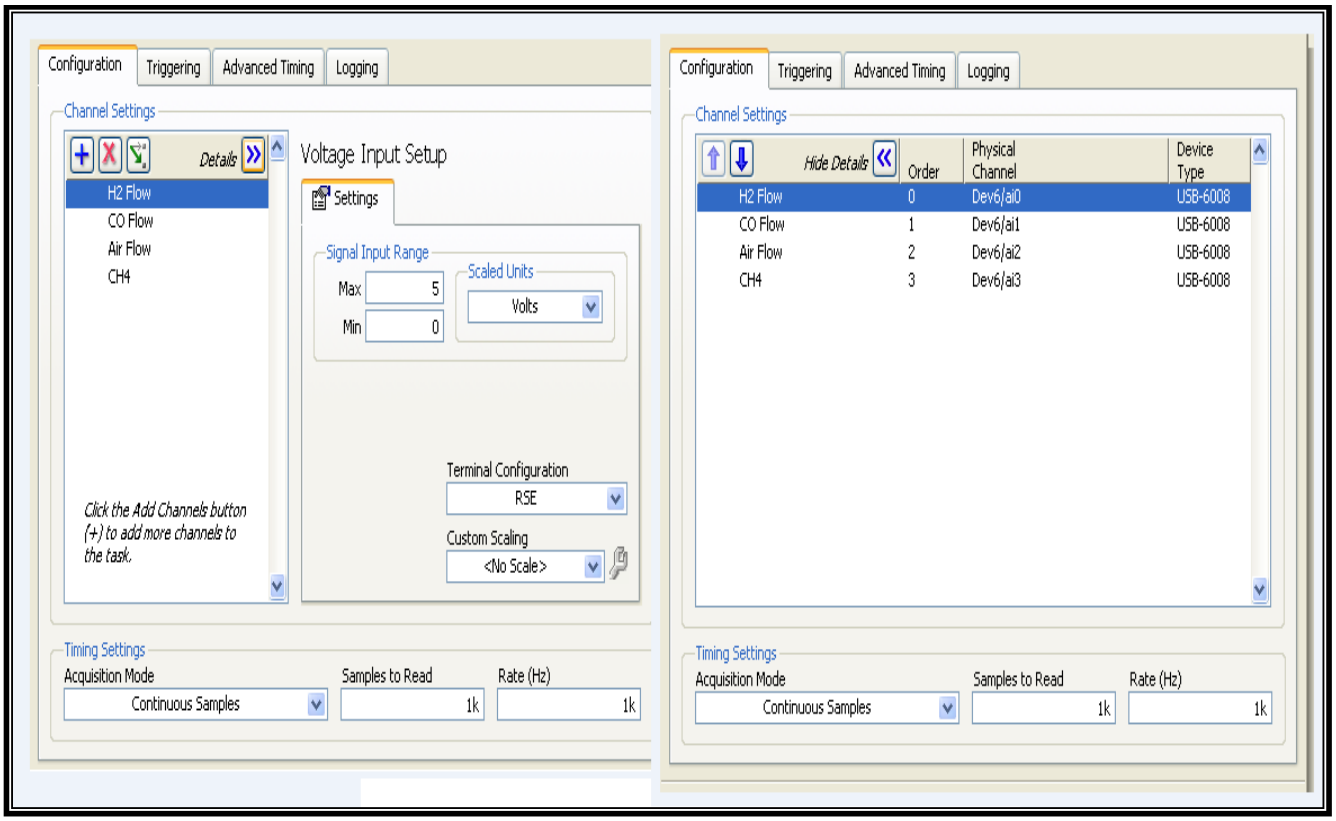

Figure 3.35: USB DAQ 1 Configuration for Flow meters

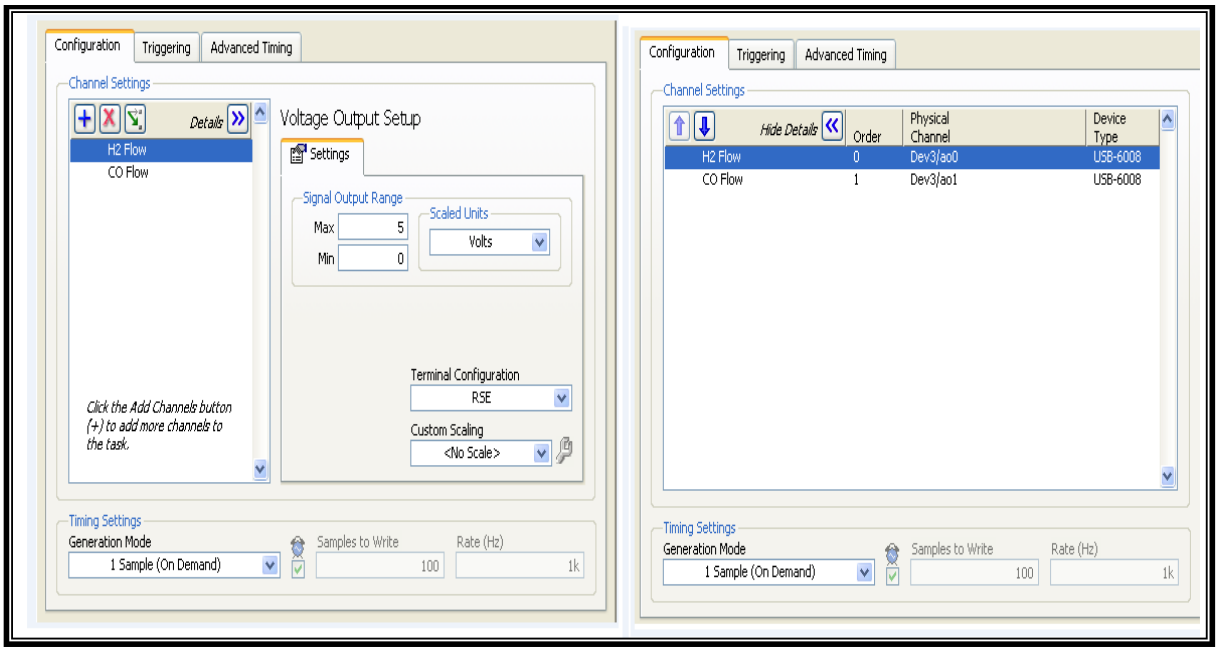

Figure 3.36: USB DAQ 1 Configuration for Proportional Control Valves

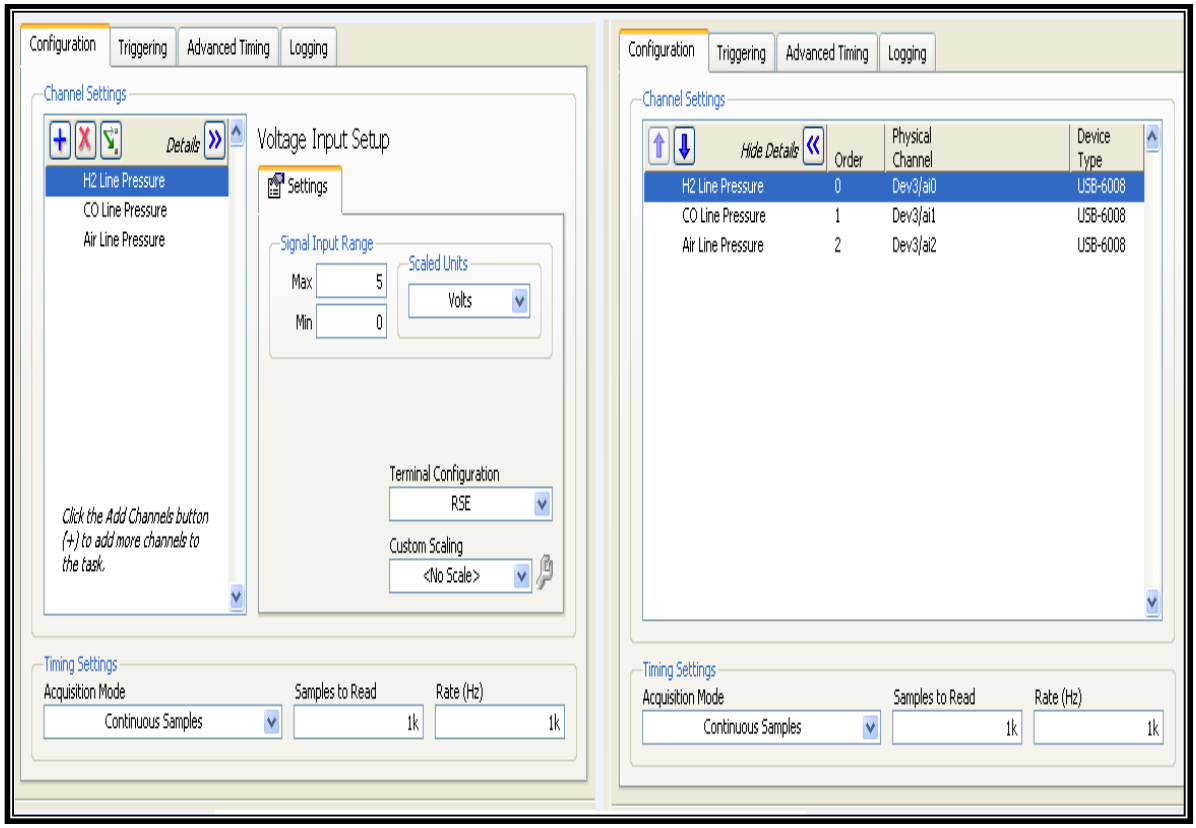

Figure 3.37: USB DAQ 2 Configuration for Pressure Transducers

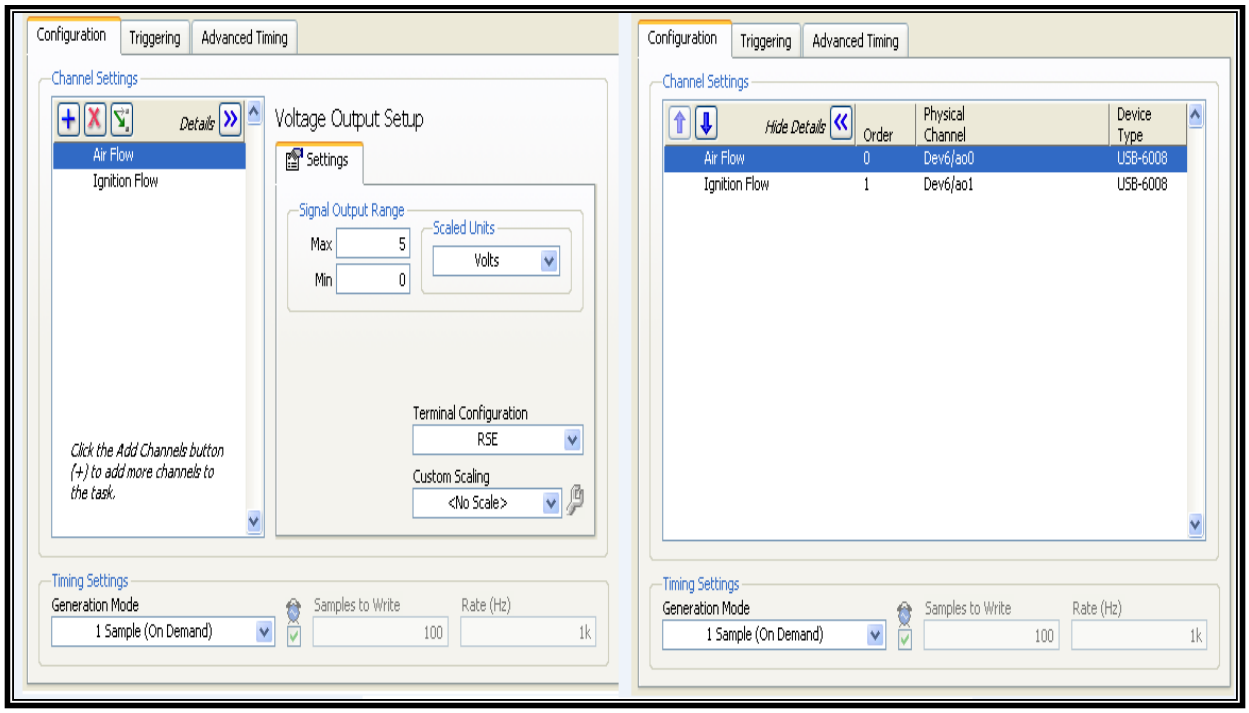

Figure 3.38: USB DAQ 2 Configuration for Proportional Control Valves

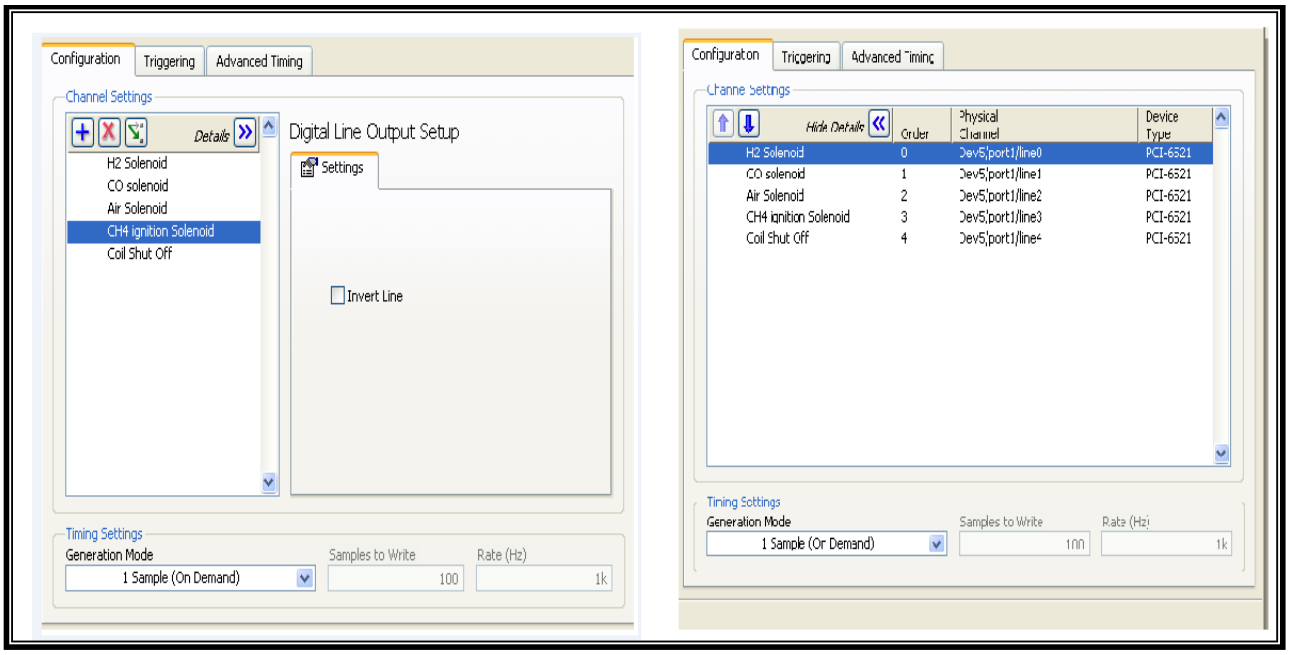

Figure 3.39: PCI Card Configuration

3.8.1 Logic for Solenoid Valves

The relay card diagnostics is programmed after the array as an indicator to visually inspect the channel that is being used. Figure 3.40 demonstrates the logic for the solenoid valve control that the four solenoid valves are getting signals from the relay card.

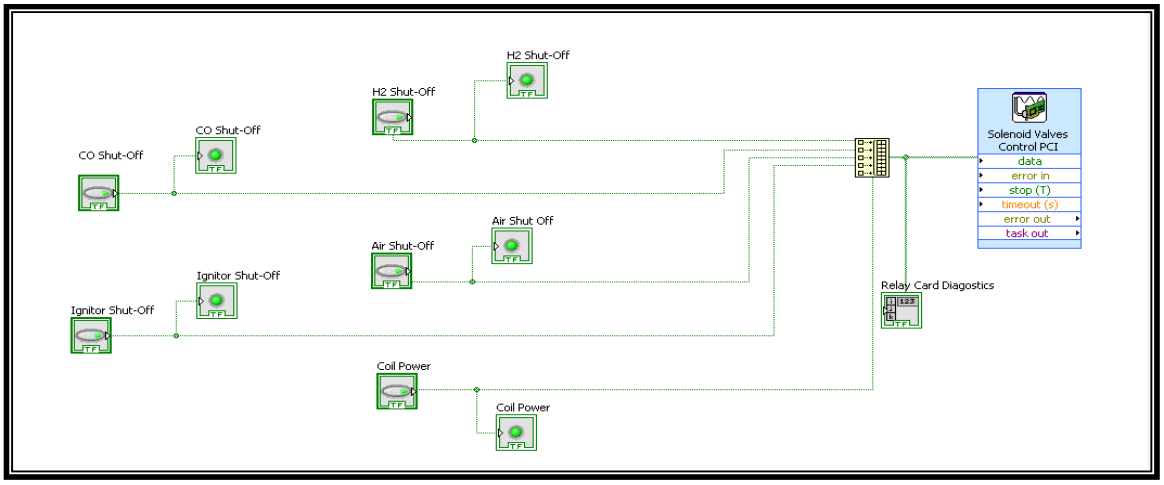

Figure 3.40: Logic for Solenoid Valve Control

3.8.2 Logic for Proportional Valves

A numeric controller controls the proportional valves and then it is converted into dynamic data. Figure 3.41 illustrates the logic for proportional control valves.

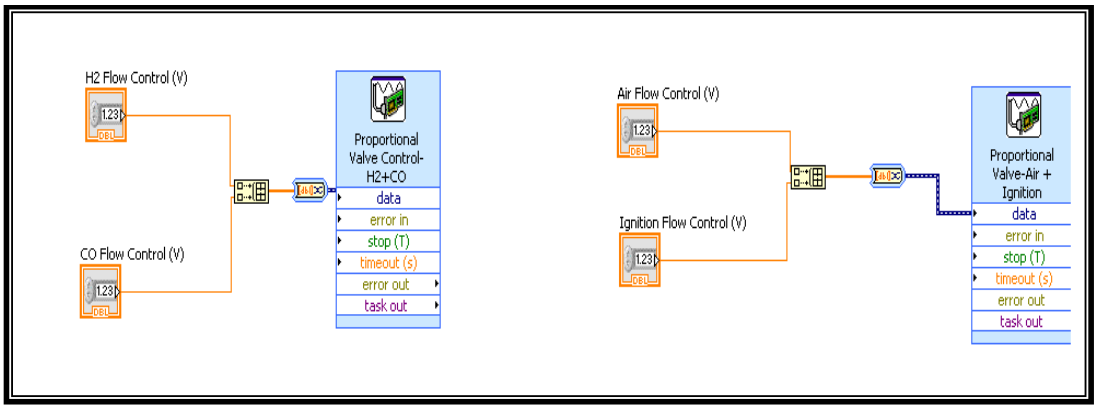

Figure 3.41: Logic for Proportional Valves

3.8.3 Data Acquisition and Recording

In Lab View using the "Write to Measurement File" tool data is recorded and saved in a series of files indicating the date and time of testing which allows further investigation of data. Data is acquired using DAQ 1 for flow meters and DAQ 2 for pressure transducers. The signals come in as voltage for the flow meters and pressure transducers and it is converted to L/min and bar respectively. Figure 3.42 illustrates respectively data acquisition and recording of flow meters and pressure transducers.

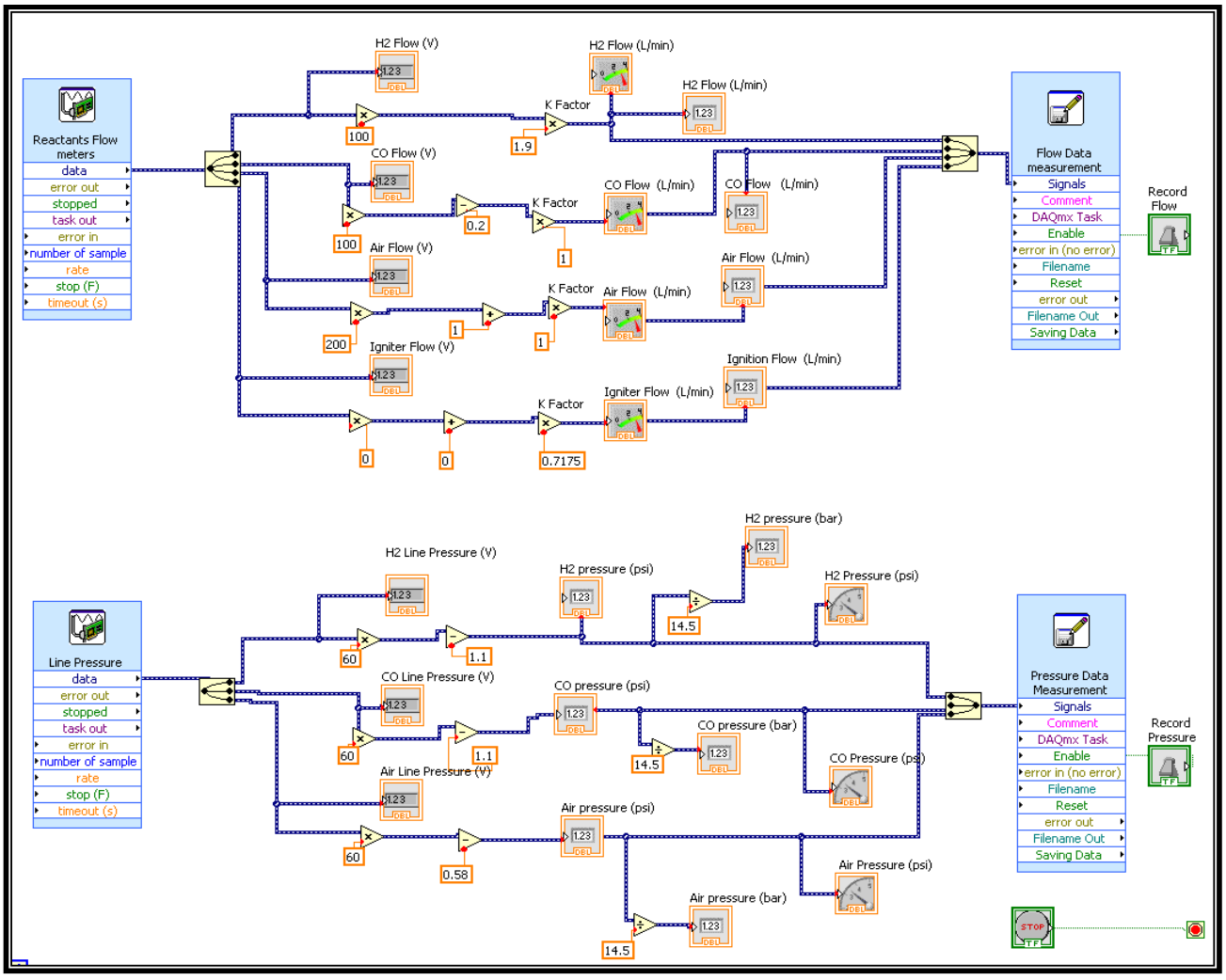

Figure 3.42: Data Acquisition and Recording Logic

3.8.4 Graphical User Interface Configuration

All proportional controls valves, solenoid valves and ignition system are controlled with the GUI window. With the help of this window the data are recorded for flow meters and pressure transducers. By changing the voltage from 0-5 volts, expected flow control can be maintained by proportional control valves. Solenoid valves can be actuated using the control panel. When the valves are open a green light will be tuned on. Under the HPC Flow Diagnostics section all the readings for flow meters and pressure transducers can be seen. Coil power button is used to turn on the spark in the beginning. Figure 3.43 demonstrates the graphic interface panel for the control and ignition system.

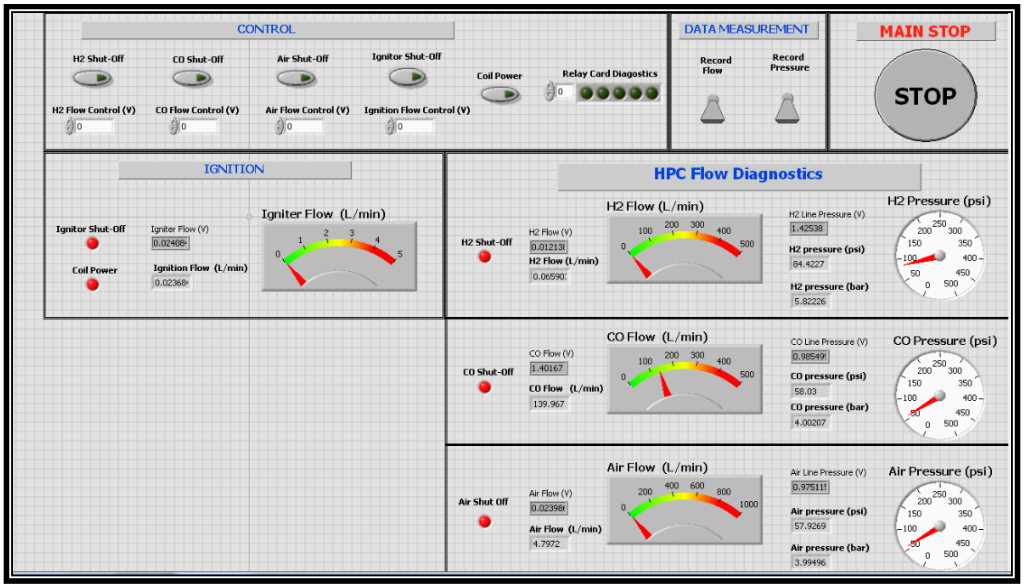

Figure 3.43: Graphic User Interface for LabView

3.8.5 Integration of PCI, USB DAQ and Power Supplies

Figure 3.44 represents the integration of PCI 6521 and two USB 6008 DAQ to the control system, ignition system and also the power supplies. Red cables deliver the 120 V to the positive lines, and black cables deliver the 120 V to the negative lines. Starting from the left, first 16

terminal blocks are used for flow meters, next 16 terminal blocks are used for proportional control valves and last 12 terminal blocks are used for pressure transducer. A movable cart (Fig 3.45) is used to accommodate solenoid valves, proportional control valves, flow meters and needle valves.

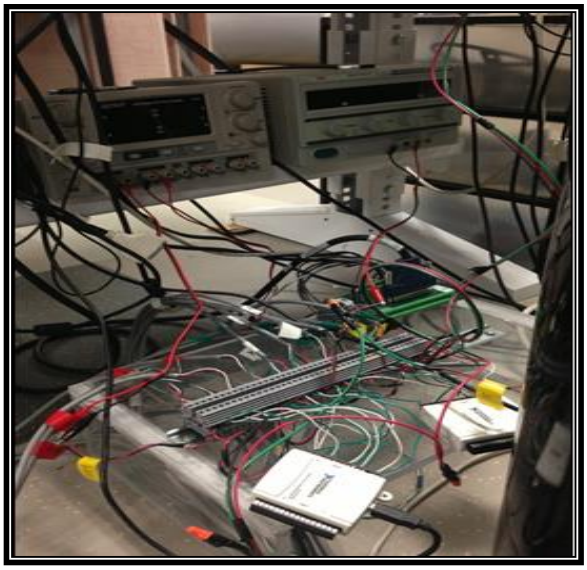

Figure 3.44: PCI, DAQ and Power Supplies

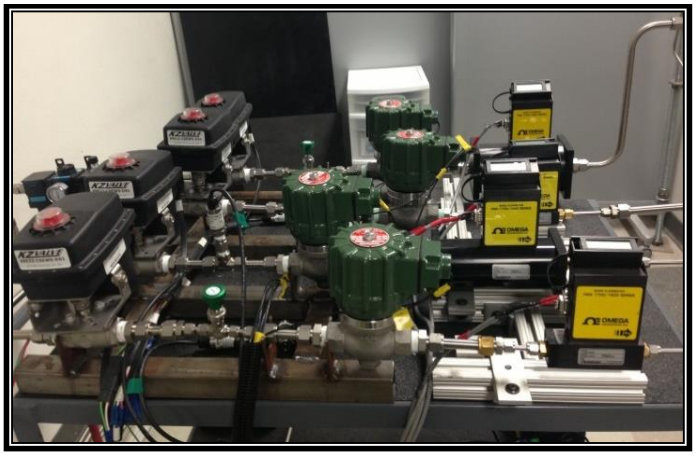

Figure 3.45: Valves in cart

3.9 Description of Gas Analyzers

3.9.1 Principle Operation for NO_x Analyzer

In this experiment to measure NO_x pollutant emission the Model 42i High Level Chemiluminescence NO-NO_2-NOx Analyzer (Fig. 3.46) is used. This instrument combines proven detection technology, easy to use menu-driven software, and advanced diagnostics to offer unsurpassed flexibility and reliability.[48]

Figure 3.46: Model 42i High Level NO-NO_2-NO_x Gas Analyzer

The gas analyzer Model 42i High Level operates on the principle that nitric oxide (NO) and ozone (O_3) react to produce a characteristic luminescence with intensity linearly proportional to the NO concentration. Infrared light emission results when electronically excited NO_2 molecules decay to lower energy states. Specifically, Nitrogen dioxide (NO_2) must first be transformed into NO before it can be measured using the chemiluminescent reaction. NO_2 is converted to NO by a stainless steel NO_2-to-NO converter heated to about 625 °C (the optional molybdenum converter is heated to 325 °C).

The sample flows through a capillary, and then to the mode solenoid valve. The solenoid valve routes the sample either straight to the reaction chamber (NO mode) or through the NO_2-

to-NO converter and then to the reaction chamber (NO_x mode). A flow sensor prior to the reaction chamber measures the sample flow. Dry air enters the Model 42i High Level through the dry air bulkhead, passes through a flow switch, and then through a silent discharge ozonator. The ozonator generates the ozone needed for the chemiluminescent reaction. At the reaction chamber, the ozone reacts with the NO in the sample to produce excited NO_2 molecules.

A photomultiplier tube (PMT) housed in a thermoelectric cooler detects the luminescence generated during this reaction. From the reaction chamber, the exhaust travels through the ozone (O_3) converter to the pump, and is released through the vent.

The NO and NO_x concentrations calculated in the NO and NO_x models are stored in memory. The difference between the concentrations is used to calculate the NO_2 concentration. The Model 42i High Level outputs NO, NO_2, and NO_x concentrations to the front panel display, the analog outputs, and also makes the data available over the serial or Ethernet connection.

3.9.2 Calibration for NO_x Analyzer

Before starting the calibration it is necessary to verify the following parameters:

1. Bench Pressure = 220 – 250 mmHg (HL=35-40mmHg)
2. Sample Flow = 0.7 LPM; 0.35 w/lag volume option
3. Internal Temp~ 30 ^oC
4. Chamber Temp = 50 ^oC
5. PMT Voltage = >-1050 V

After verifying the above parameters the calibration is started. The calibration procedure has six steps mentioned as following:

1. Calibrate Input Board – 3 KHz to 6 KHz

- Zero air is flown to the instrument. As there is a filter inside the instrument so no need to filter the air, ambient air can be used as zero air. A pipe is connected with the sample port and it is kept in the ambient air.
- Turn on >Instrument as well as the Pump
- In the Main Menu Instrument Controls is chosen
- Instrument Controls > Ozonator > turn off ozonator
- Instrument Controls > PMT Supply > turn off PMT
- In the Main Menu, choose Instrument Controls > Service Mode > Turn on Service
- Main Menu > Service > Input Board Calibration > Automatic Input Cal
- Press RUN PB, NO & NO_x should read zero

2. PMT Test

- Main Menu > Instrument Controls > PMT Supply >turn PMT back on
- Any increase in readings is the dark current (noise)
- Increase should not exceed 15 ppm in the single or LO range or 1ppm in the HI range
- If readings are good the PMT is good. Usually the dark current is very high when the PMT fails. In this case the variation is very little so the readings are good to consider.

3. Contamination test – for instrument or zero gas

- Main Menu > Instrument Controls > Ozonator > turn ozonator back on. If the reading goes low, the zero air is contaminated. If the readings stay high, the

reaction chamber is contaminated and needs to be cleaned. Also, replace Perm Dryer and tubing on the input side of the Reaction Chamber.

- The reading from the instruments stays same. So there is no need to change anything in the instruments.

4. Adjust PMT Voltage

- Calibration Factors > NO & NO_x BKG > Set NO & NOx Backgrounds to 0.00
- Calibration Factors > NO, NO2, NO_x Coefficient > Set NO, NO_2, NO_x Coefficients to 1.000.
- Calibration Factors > Reset User Cal Defaults
- Check that PMT supply and Ozonator is ON
- To flow the sample gas inside the analyzer an experimental setup (fig. 3.47) is required.

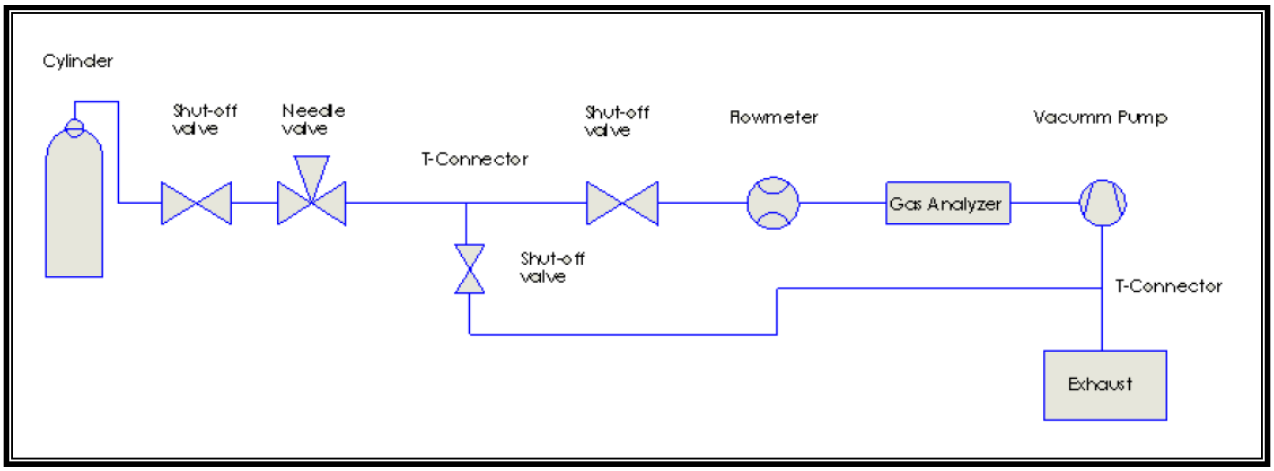

Figure 3.47: Schematic Diagram for the Calibration of the NO_x Analyzer

In this setup there are three shut-off valves, one needle valve, two T-connectors and a flow meter. The shut-off valves are used to turn on or turn off the flow. The needle valve is used to control the flow rate and the flow meter is for recording the flow. From the schematic it can be

also observed that there is a suction line to vent off the excess gas after running the calibration. After setting up the valves the sample gas is flown from the cylinder to the exhaust.

- Full scales NO gas of 70%-90% is flown to the SAMPLE port. Later the instrument needs to stabilize
- PMT Voltage (if DUAL MODE, use HI range) is adjusted until display reads NO concentration +/- 2ppm.
- Service > PMT Voltage Adjustment
- PMT voltage should be >-1050 volts

5. Calibrate NO & NOx Background

- Zero gas is flown to the SAMPLE port
- Instrument is stabilized at the background value
- BKG value is less than 12.5ppm, if higher: noise problem in PMT or Input Board
- Calibration Menu > NO BKG > Set BKG to 0
- NO_x BKG > Set BKG to 0

6. Calibrate NO & NO_x Coefficients

Span Concentration can be calculated

Range > Read NO > Reading *(80-90)%= Span concentration

Range > Read NO_x > Reading * (80-90)%= Span concentration

- NO gas is connected to the SAMPLE port
- The instrument needs to stabilize for NO reading
- From the cylinder of the sample gas is entered inside the analyzer
- ENTER button is pressed to save

3.9.3 Principle Operation for CO_2 Analyzer

The Model 410i (figure 3.48) operates on the principle that carbon dioxide (CO_2) absorbs infrared radiation at a wavelength of 4.6 μm. The sample is drawn into the Model 410i through the sample bulkhead, as shown in. The sample flows through the optical bench. Radiation from an infrared source is chopped and then passed through a rotating optical wheel alternating between sample and reference filters. The radiation then enters the optical bench where absorption by the sample gas occurs. The infrared radiation then exits the optical bench and falls on an infrared detector. The chopped detector signal is modulated by the alternation between the filters with amplitude related to the concentration of CO_2 in the sample cell. Because infrared absorption is a non-linear measurement, it is necessary to transform the basic analyzer signal into a linear output. The Model 410i uses an internally stored calibration curve to accurately linearize the instrument output over any range up to a concentration of either 10000 ppm (Standard) or 25% (High Level). The Model 410i outputs the CO_2 concentration to the front panel display, the analog outputs, and also makes the data available over the serial or Ethernet connection.

Figure 3.48: Model 410i CO_2 Gas Analyzer

3.9.4 Experimental Setup for Multipoint Calibration Test

In this setup figure 3.49 there are three shut-off valves, two needle valves, two flow meters, three T-connectors, sample gas cylinder CO_2 and Nitrogen N_2 gas cylinder for dilution purposes. The shut-off valves are used to turn on or turn off the flow. The needle valve is used to control the flow and flow meters to measure the flow. From the schematic it can be also observed that there is a suction line to vent off the excess gas after running the calibration. After setting up the valves the sample gas is flown from the cylinder to the exhaust.

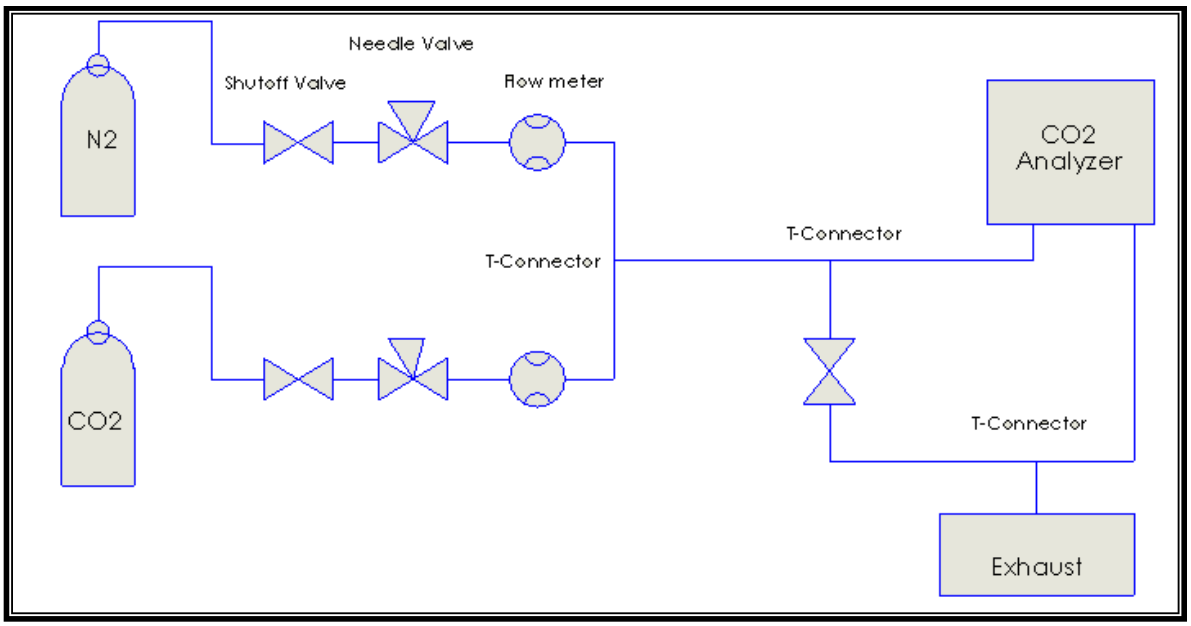

Figure 3.49: Schematic Diagram for Multipoint Calibration of the CO_2 Analyzer

3.9.5 Calibration for CO_2 Analyzer:

Before starting the calibration it is necessary to verify the following parameters:

1. Bench Pressure = 740 mmHg
2. Sample flow = 0.85 – 1.20 LPM
3. Internal Temp = 30° C

4. Bench Temp = 47° C – 49° C

1. Instrument Set-Up

- Zero air is flown to the Sample port (Zero port on Z/S option)
- Range = 2000 ppm (410i-D) or 20% (410i-E) pg. 3-14
- Averaging time = 30 seconds
- BKG to 0.000 & COEF to 1.000
- Main Menu > Calibration Factors > Reset User Cal Defaults
- Pressure Compensation "ON"
- Main Menu > Instrument Controls
- Temperature Compensation "ON"
- Main Menu > Instrument Controls

2. Set the Detector/Pre-amp Board Gain

To Set the Raw Intensity:

- Service Mode is put inside the Main Menu

  Main Menu > Instrument Controls > Service Mode
- The Pre-amp Board Cal screen is accessed

  Main Menu > Service > Preamp Board Cal
- Up/Down PB is pressed to increase or decrease S/R frequencies

  The two numbers should be an average of 150,000Hz – 165,000Hz

To View the AGC frequency:

- Main Menu > Diagnostics > AGC Intensity

- It should be read 195,000Hz to 205,000Hz. In this case the reading is 196000 Hz.

3. **Save the Initial S/R value**
    - Zero air is flown to sample port for 10 to 15 minutes
    - CURRENTLY value to the MEASURED value
    - Main Menu > Service Menu > Initial S/R ratio
    - Initial S/R value should be 0.800 – 1.2

4. **Reset Multipoint Cal Coefficients**
    - Main Menu > Service Menu > Multipoint Cal > Default Coeff
    - Enter PB is pressed to reset the default values

5. **Multi-Point Cal/Linearity Test – requires gases of 80%, 50%, 20% F/S**
    - Full scale 80% gas is flown to the sample port.

      Main Menu > Service Menu > Calibrate Point 1 > Set Cal Gas Pt

      Calibration gas is sent to the analyzer (calculates cal factor 1)

      ENTER is pressed
    - Again the process is repeated for 50% and 20% gas to calculate cal factor 2 and 3.

6. **Calibrate CO_2 background**

    Zero air is flown to the Sample port (Zero on Z/S option)

    Main Menu > Calibration > Cal Background

    If > 2.0 ppm, re-run Initial S/R setting.

7. **Calibrate CO_2 (Span)**

- 70%-90% F/S gas is entered.
- Main Menu > Calibration > Cal Coef
- Cal Gas 1 concentration on cylinder and Enter PB is pressed to store.
- Cal Factor should be 0.90 – 1.10. Cal Factor for present experiments was 0.95.

3.9.6 Principle Operation for CO Analyzer

The Model 48*i* High Level operates on the principle that carbon monoxide (CO) absorbs infrared radiation at a wavelength of 4.6 µm. Because infrared absorption is a non-linear measurement technique, it is necessary to transform the basic analyzer signal into a linear output. The Model 48*i* High Level uses an internally stored calibration curve to accurately linearize the instrument output over any range up to a concentration of 20,000 ppm. The sample is drawn into the Model 48*i* High Level through the sample bulkhead, as shown in figure 3.50.

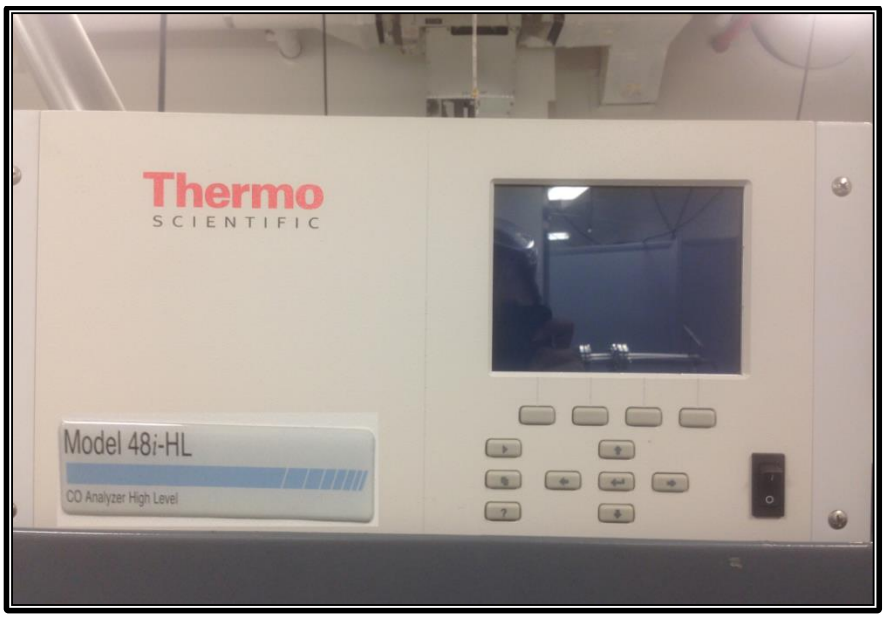

Figure 3.50: Model 48i-HL CO Analyzer High Level

The sample flows through the optical bench. Radiation from an infrared source is chopped and then passed through a gas filter alternating between CO and N_2. The radiation then passes through a narrow bandpass interference filter and enters the optical bench where absorption by the sample gas occurs. The infrared radiation then exits the optical bench and falls on an infrared detector. The CO gas filter acts to produce a reference beam, which cannot be further attenuated by CO in the sample cell. The N_2 side of the filter wheel is transparent to the infrared radiation and therefore produces a measurement beam, which can be absorbed by CO in the cell. The chopped detector signal is modulated by the alternation between the two gas filters with an amplitude related to the concentration of CO in the sample cell. Other gases do not cause modulation of the detector signal since they absorb the reference and measure beams equally. Thus, the GFC system responds specifically to CO. The Model 48*i* High Level outputs the CO concentration to the front panel display, the analog outputs, and also makes the data available over the serial or Ethernet connection. Experimental setup for multipoint calibration test for CO Analyzer is same as the CO_2 analyzer. Only difference is the sample gas will be CO_2 instead of CO gas.

3.9.7 Calibration for CO Analyzer

Before starting the calibration it is necessary to verify the following parameters:

Chapter 4 Bench Pressure = 740 mmHg

Chapter 4 Sample flow = 0.85 – 1.20 LPM

Chapter 4 Internal Temp = 30° C

Chapter 4 Bench Temp = 46° C – 50° C

Instrument Set-Up

- Zero air is flown to the Sample port (Zero port on Z/S option)

- Range = 30 ppm
- Averaging time = 30 seconds
- BKG to 0.000 & COEF to 1.000
- Main Menu > Calibration Factors > Reset User Cal Defaults
- Pressure Compensation “ON”
- Main Menu > Instrument Controls
- Temperature Compensation “ON”
- Main Menu > Instrument Controls

Set the Detector/Pre-amp Board Gain

To Set the Raw Intensity:

- Service Mode is put inside the Main Menu

  Main Menu > Instrument Controls > Service Mode
- The Pre-amp Board Cal screen is accessed

  Main Menu > Service > Preamp Board Cal
- Up/Down PB is pressed to increase or decrease S/R frequencies

  The two numbers should be an average of 150,000Hz – 160,000Hz

To View the AGC frequency:

- Main Menu > Diagnostics > AGC Intensity
- It should be read 195,000Hz to 205,000Hz. In this case the reading is 197,780 Hz.

Save the Initial S/R value

- Zero air is flown to sample port

- CURRENTLY value to the MEASURED value
- Main Menu > Service Menu > Initial S/R ratio
- Initial S/R value should be 1.13 – 1.18

Reset Multipoint Cal Coefficients

- Main Menu > Service Menu > Multipoint Cal > Default Coeff
- Enter PB is pressed to reset the default values

Chapter 4 Multi-Point Cal/Linearity Test – requires gases of 80%, 50%, 20% F/S

- Full scale 80% gas is flown to the sample port.

  Main Menu > Service Menu > Calibrate Point 1 > Set Cal Gas Pt

  Calibration gas is sent to the analyzer (calculates cal factor 1)

  ENTER is pressed
- Again the process is repeated for 50% and 20% gas to calculate cal factor 2 and 3.

Chapter 4 **Calibrate CO background**

Zero air is flown to the Sample port (Zero on Z/S option)

Main Menu > Calibration > Cal Background

If > 2.0 ppm, re-run Initial S/R setting.

Chapter 4 Calibrate CO (Span)

- 70%-90% F/S gas is entered.
- Main Menu > Calibration > Cal Coef.
- Cal Gas 1 concentration on cylinder and PB is pressed to store.
- Cal Factor should be 0.90 – 1.10. Cal Factor was 0.97.

3.10 Emission Measurements

The combustion of syngas produces gaseous pollutants such as nitrogen oxides (NO_X), carbon dioxide (CO_2), carbon monoxide (CO), volatile organic compounds (VOCs), particulate matter, and trace species such as mercury and other metals. The laboratory syngas used in the present experiments is composed of CO and H_2 results in production of primarily CO, CO_2, and NO_x. Additionally, other unburned hydrocarbons that may be produced in larger quantities for rich combustion are only in trace amounts since lean combustion was considered for all test conditions. In this work emissions are measured by collecting gas sample from the exhaust of the combustor using 0.00635 m diameter tube at the top of the condenser (figure 3.51). Inside the condenser the sample gas is condensed with water and is collected inside the gas collector flask. Three gas analyzers are used to measure the emissions for NO_x, CO_2 and CO. A 42i High level analyzer for NO_x, a 410i analyzer for CO_2 and 48i analyzer for CO are used to measure the emission. The emission measurement principle and calibration process for the analyzers are described in the previous sections.

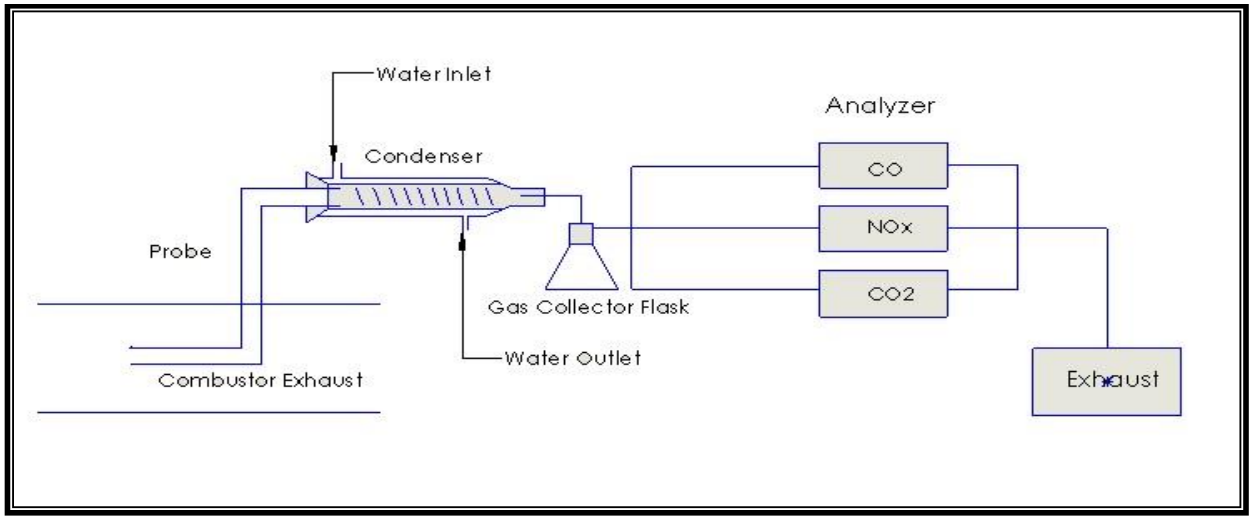

Figure 3.51: Complete Experimental Setup for Emission Measurements

Chapter 4 : Results and Discussions

4.1 Visual Observation of the Flame

Experiments are conducted to visualize the flame at flashback and blowout conditions for 20%, 30%, and 40% H_2 in the syngas mixture. Some flashback images are presented in Fig 4.1. From the images it can be seen that the flame is first attached to the injector face. The flame on the injector tube heats the tube wall and increases the temperature of the upstream fuel-air mixture. The flame then rapidly moves inside the injector to cause a flashback. From the below figure it is visible that the outer flame is not anchored and the inner flame surrounding the inner port is attached to the faceplate. This is because of the boundary layer effect the inner injection ports getting more flow than the outer orifice. As the flow rate is very low, the outer portion does not have a high velocity. The inner flames hold the flame of the produced on the outer section. This process ultimately leads to flame flashback along the inner portion of the injector.

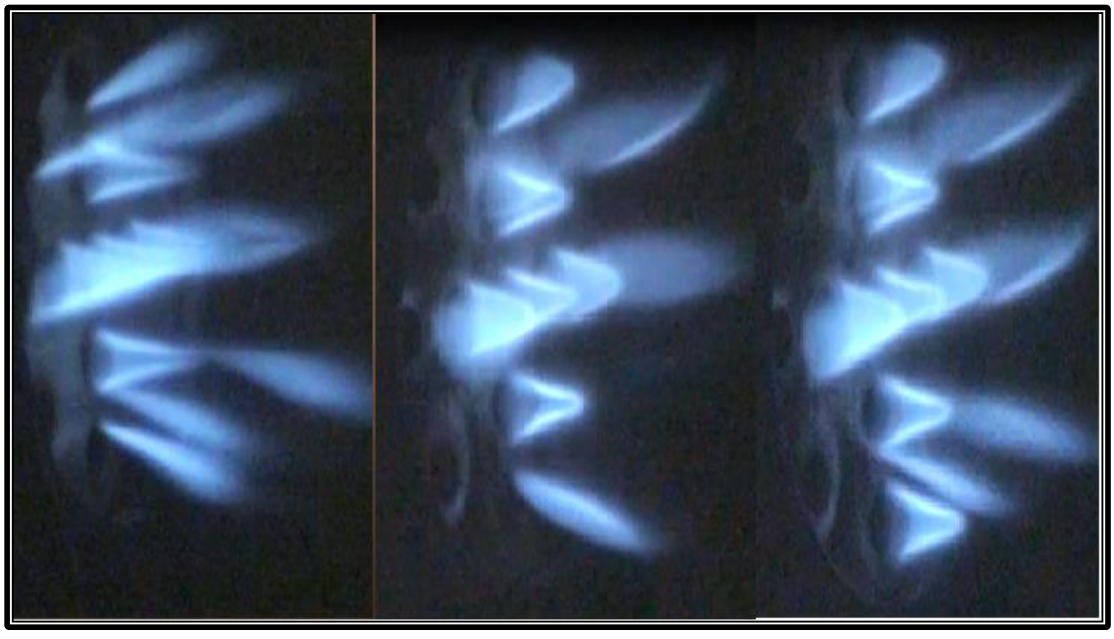

Figure 4.1: Flashback from inner holes of the Injector

Experiments are also conducted to visualize the flame images at a blowout conditions for 20%, 30% and 40% H_2 in the syngas mixture are presented in Fig 4.2. From the images it can be seen that the flame is first attached to the injector face. Heat is then transferred to the injector face causing the flame to quench, ultimately resulting in blowout.

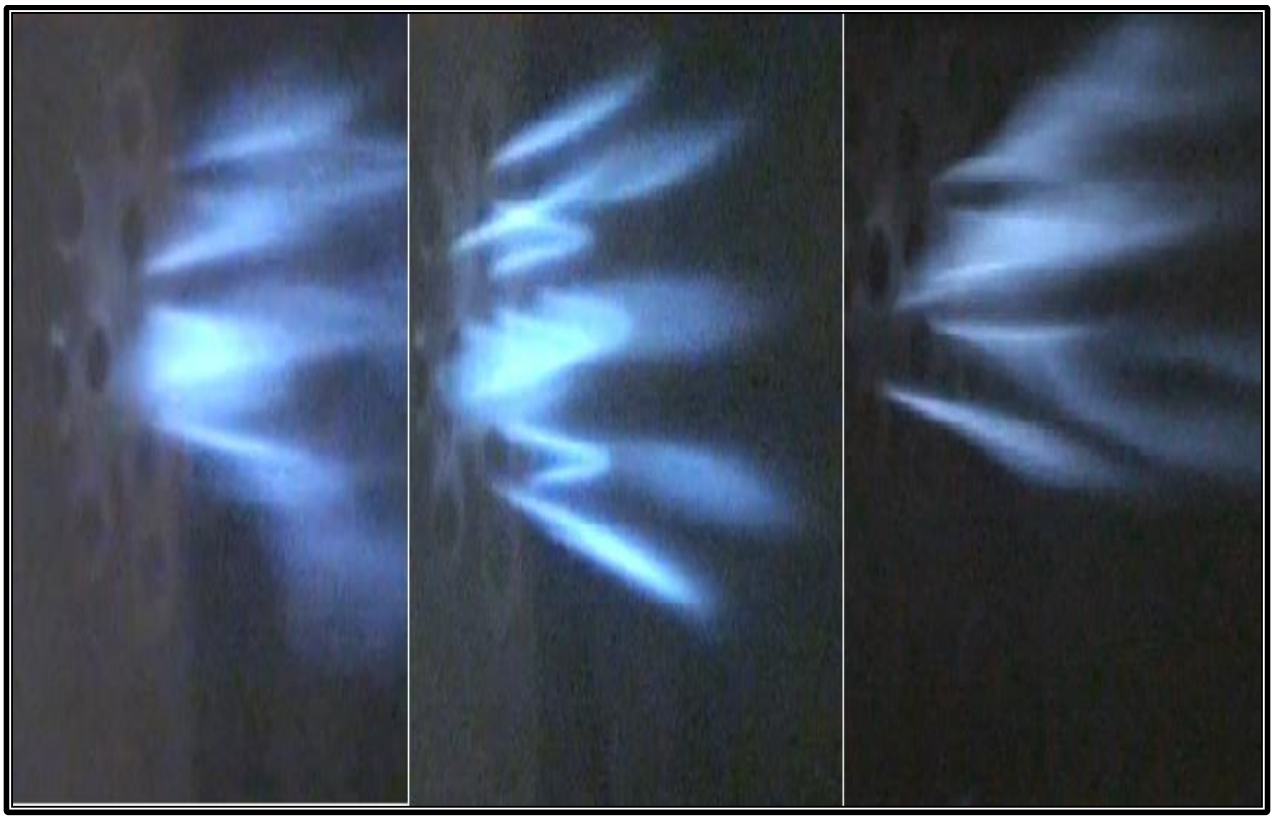

Figure 4.2: Blowout Condition for almost all holes

4.2 Stability Map

Flashback and blowout both are unstable conditions in combustion. Flashback and blowout will lead to more pollutant emissions and possibly cause a catastrophic failure of the system. To mitigate the flashback and blowout condition it is required to obtain stable flames Fig. 4.3.

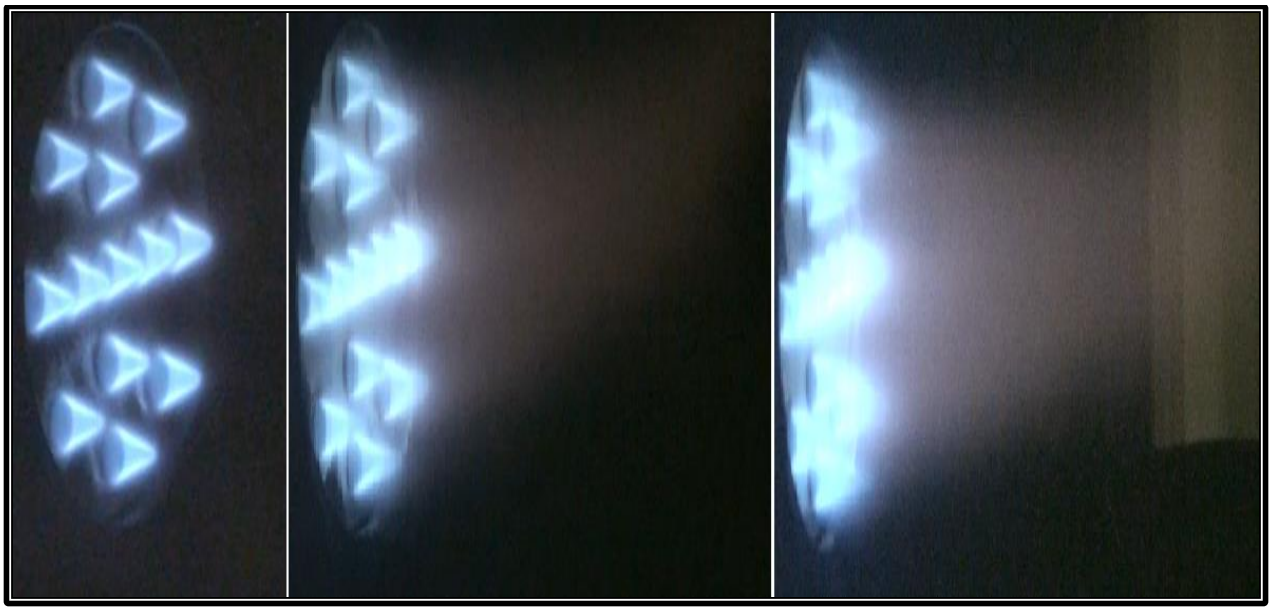

Figure 4.3: Stable Flame

Several experiments are performed in order to obtain the flame stability region. The experimental conditions are changed by changing the flow rates which is dependent on bulk velocity. The stability region of the composition of 20% H_2 and 80% CO for synthesis gas is discussed.

As the combustion chamber can accommodate a wide range of fuel variety, and for the present experiments fuel percentage (% F) varied from 13.3 to 23. To determine the stability map the experiments are conducted at different flow rates shown in Table 4-1. In the Table 4-2 the mass flow rate is increased to change the flow rates. The bulk velocity in this work is calculated based on the flame speed of the outer holes. When the mass flow rate is increased to 0.2 g/s the flame is observed to flashback and when increased to 0.27 g/s this total flow rate causes a blowout condition. This same procedure is followed to determine the stability region for different fuel percentage.

Table 4-1: Test Results for 20% H_2 & 80% CO (Φ=0.6)

	Φ=0.6					
	Bulk Velocity (m/s)	**H_2 Flow(L/min)**	**CO flow (L/min)**	**Air Flow (L/min)**	**Total Mass Flow (g/s)**	**Test Result**
20% H_2 - 80% CO	0.856	0.33	1.34	6.53	0.16	Lifted unstable flame
	1.07	0.42	1.68	8.17	0.20	Stable about flashback
	1.284	0.50	2.01	9.80	0.24	Stable liftoff
	1.498	0.58	2.35	11.43	0.27	Stable about to blowout
	1.925	0.75	3.02	14.70	0.35	Blowout
	2.353	0.92	3.69	17.97	0.43	Blowout
	2.781	1.09	4.36	21.23	0.51	Blowout

Table 4-2: Test Results for 20% H_2 & 80% CO (Φ=0.7)

	Φ=0.7					
	Bulk Velocity (m/s)	**H_2 Flow (L/min)**	**CO flow (L/min)**	**Air Flow (L/min)**	**Total Mass Flow (g/s)**	**Test Result**
20% H_2 - 80% CO	1.165	0.52	2.07	8.66	0.24	Near flashback
	1.332	0.59	2.37	9.89	0.30	Unstable
	1.665	0.74	2.96	12.37	0.37	Stable
	1.998	0.89	3.55	14.84	0.43	Stable
	2.331	1.03	4.14	17.31	0.55	Stable
	2.997	1.33	5.33	22.26	0.67	Stable Almost blowout
	3.663	1.62	6.51	27.21	0.79	Almost Blowout
	4.328	1.92	7.70	32.15	0.91	Blowout

For these experiments at different fuel percentage the flashback and blowout points were detected visually. This stability map developed based on these observations will help to avoid the flashback and blowout condition for the multi-tube injector. From Fig. 4.4 it is visible that stability increases with fuel percentage. It is because as the equivalence ratio increases the bulk velocity which broadens the stability region for the lean combustion.

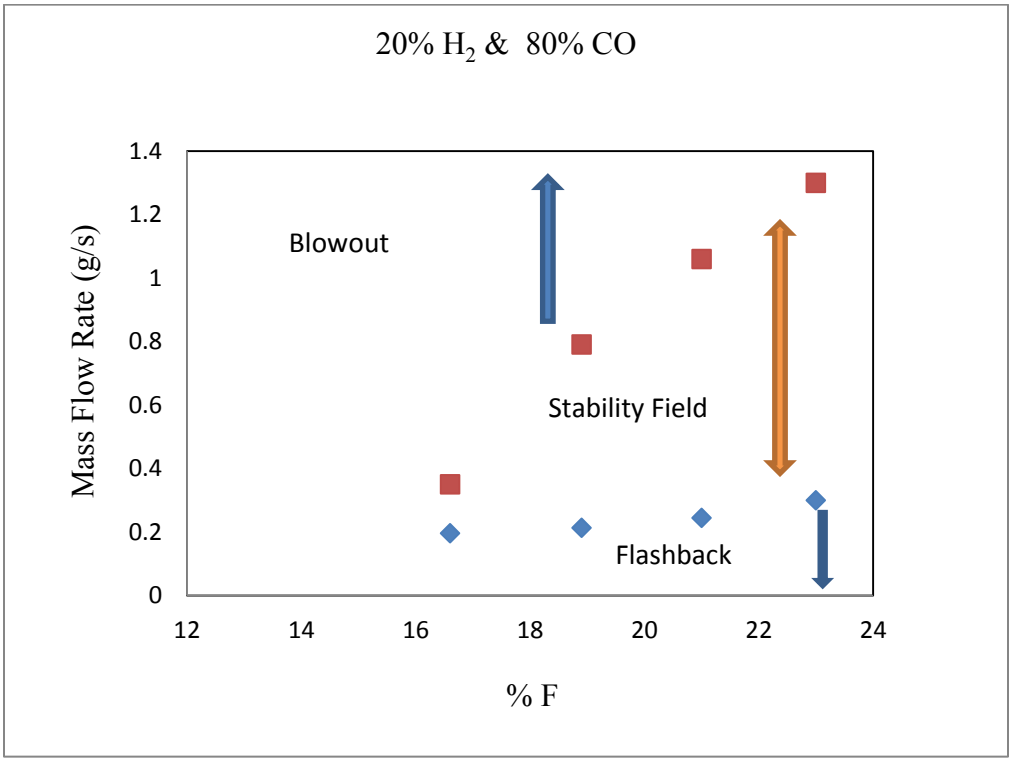

Figure 4.4: Mass Flow Rate vs % F (20% H_2 & 80% CO)

Similarly the stability region for 30% and 40% H_2 is determined and shown in Fig. 4.5 and 4.6. Hydrogen has a higher flame speed thus as hydrogen concentration is increased it is required to increase the velocity to stabilize the flame. That is why the stability range increases with higher hydrogen concentration.

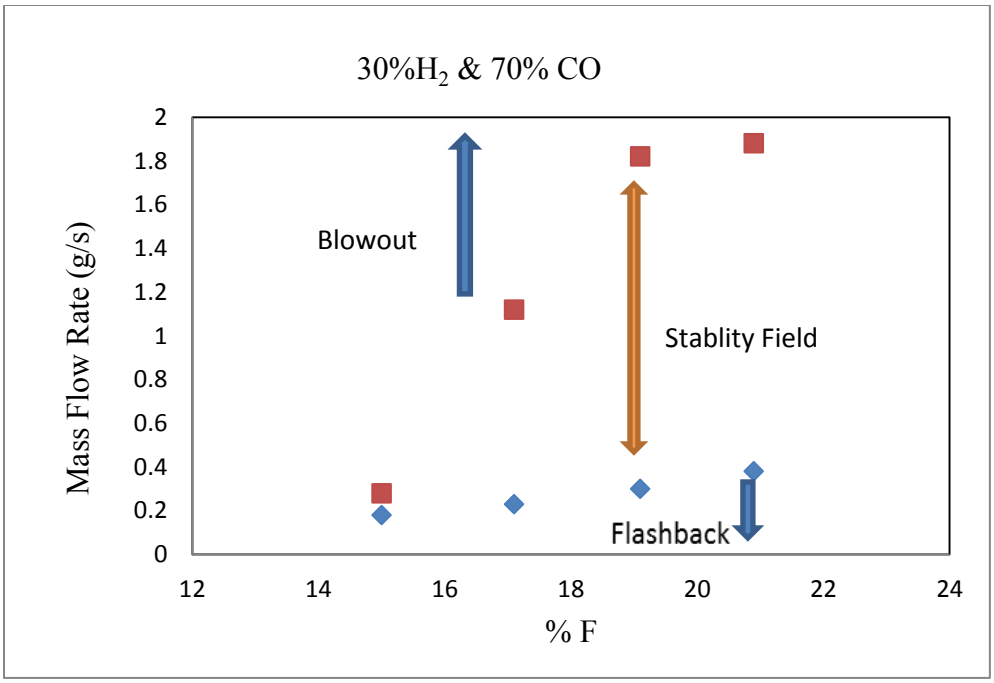

Figure 4.5: Mass Flow Rate vs % F (30% H_2 & 70% CO)

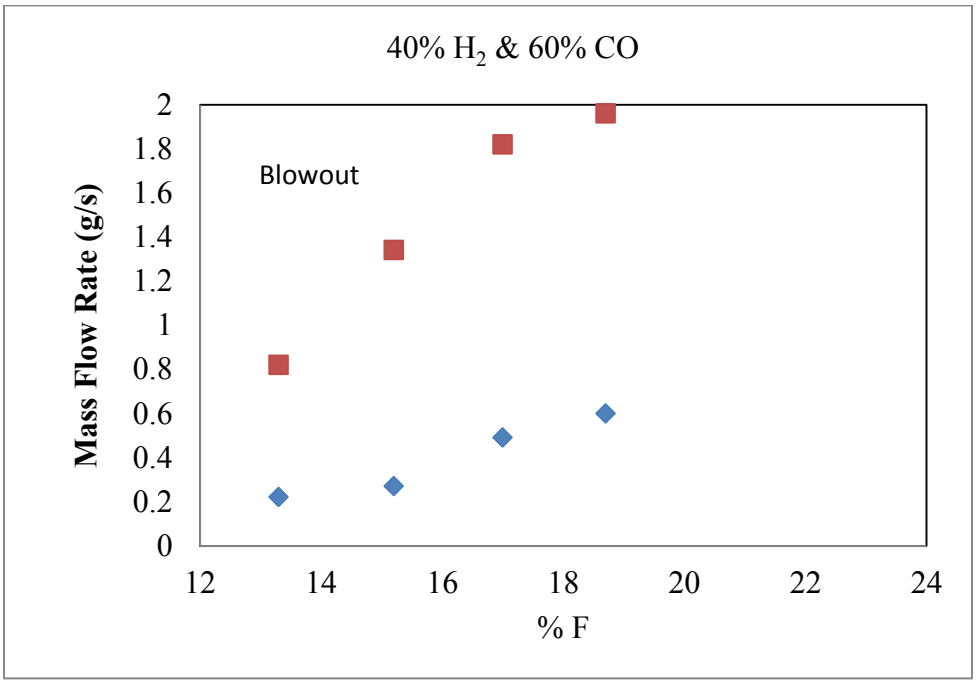

Figure 4.6: Mass Flow Rate vs % F (40% H_2 & 60% CO)

4.3 NO_x Emission Measurements

The primary pollutants that are associated with premixed combustion are the oxides of nitrogen, carbon monoxide, unburned and partially burned hydrocarbons and soot. Sulfur oxides are emitted based on the concentration of sulfur contents in the fuel. As syngas contains very small amounts sulfur it is anticipated that there will be no SO_x emissions. This work is only focused on premixed lean combustion. In lean combustion there will be excess in air. Therefore, it is considered that all carbon monoxide is transferred to CO2 for the following calculations.

4.3.1 NO_x Formation Mechanism:

The expression NO_x represents all the oxides of nitrogen. The most important pollutants are the nitrogen dioxide (NO_2) and nitrogen monoxide (NO). Four types of mechanisms are found to contribute to the formation of nitrogen oxides. (i) thermal NO (ii) prompt NO (iii) fuel NO, and (iv) nitrous oxides N_2O. Nitrous oxide (N_2O) is generally a minor constituent of NO_X except in certain combustion devices that operate at lower temperatures, such as fluidized bed combustors. For this study it is assumed that Nitric oxide (NO) is generally the most commonly emitted NO_X species from combustion process

Thermal NO forms because of the oxidation of molecular nitrogen (N_2) in the combustion air at high temperature. The fundamental steps which are involved in the formation of thermal NO are given by the extended Zeldovich mechanism.

$$O + N_2 \leftrightarrow NO + N$$

$$N + O_2 \leftrightarrow NO + O$$

$$N + OH \leftrightarrow NO + H$$

Extended Zeldovich mechanism reactions involve different radical species (O, N, H, OH). These radical species initially formed through decomposition or abstraction reactions. Due to the inherent stability of the N_2 molecule, considerable energy is required to oxidize N_2, and thus thermal NO is only formed in appreciable quantities at elevated combustion temperatures (>1370°C,2500°F). Thermal NO_x is primarily produced in the flame region that has both high temperature and high concentrations oxygen and OH radical. The temperature distribution in this region is determined by the chemical kinetics and fluid mechanics. When the O and H species are at equilibrium levels, the extended Zeldovich mechanism is also known as the thermal mechanism. Below the temperature of 1800°C the thermal reactions are relatively slow. To reduce the thermal NO_x emission most common approach is to reduce the combustion temperature in combustion process.

Prompt NO forms very quickly in the flame the mechanism is followed by a sequence of reactions converting HCN to NO. NO emission will be dominated by formation through HCN route due to high hydrogen concentrations and absence of hydrocarbon content. In modern gas turbine systems in which syngas are used are now commonly regulated with very low NO_x levels. So it very important to take accounts the prompt mechanism. The prompt mechanism sometimes is known as 'Fenimore-prompt' or only 'Fenimore'.

$$N_2 + CH \leftrightarrow HCN + N$$

$$N_2 + CH_2 \leftrightarrow HCN + NH$$

$$C + N_2 \leftrightarrow CN + N$$

Fuel NO is produced from the oxidation of nitrogen bearing species. These species are basically HCN and NH_3. These species (HCN, NH_3 etc.) are converted to NO in the presence of oxygen at combustion tempertures.

$$Fuel - N \leftrightarrow HCN \leftrightarrow NHI$$

$$N\,HI + O, OH \leftrightarrow NO$$

Nitrogen dioxide (NO_2) emissions are more serious health and environmental risk than NO. NO_2 generally produced from the oxidation of NO. It is a secondary oxidation reaction after the primary oxidation reaction of nitrogen. NO_2 emission is risky because it can produce ozone after further chain reactions.

A 42i NO-NO_2-NO_x analyzer is used measure the NO_x emission in the experiments for stable flame conditions. 20%, 30% and 40% H_2 composition for different % F in lean condition are used to measure the emissions. All the experiments are executed from % F 15.2 to 23 for the stability map. The stability region is very narrow when the percentage of fuel is low. Figures 4.7, 4.8 and 4.9 show NO_x concentrations for 20%, 30% and 40% H_2. It was observed that NO_x emission increases as % F increased. This is due to a high flame temperature, which can be estimated based on the adiabatic flame temperature, and excess oxygen is available for formation of nitrogen with oxygen.

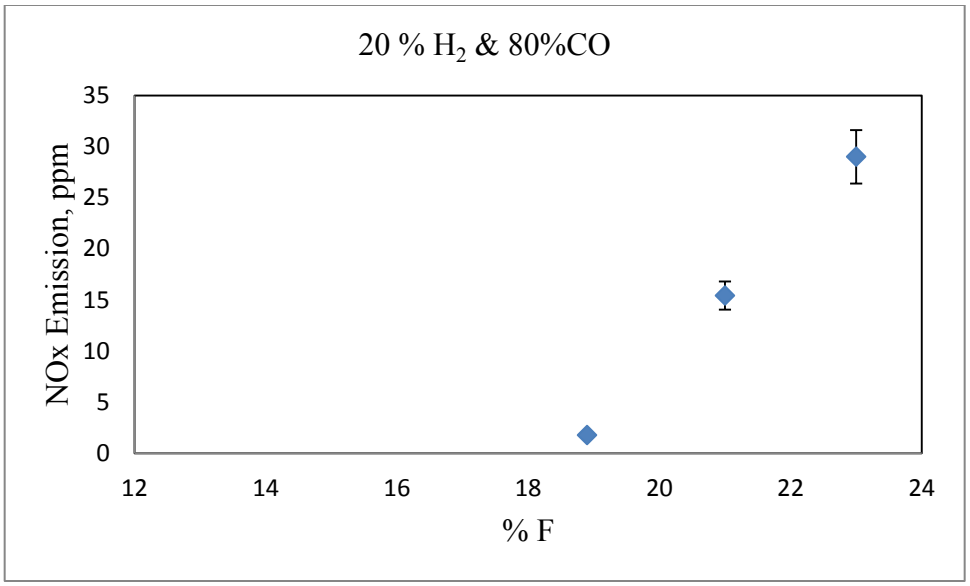

Figure 4.7: NO_x emission for 20% H_2 & 80% CO

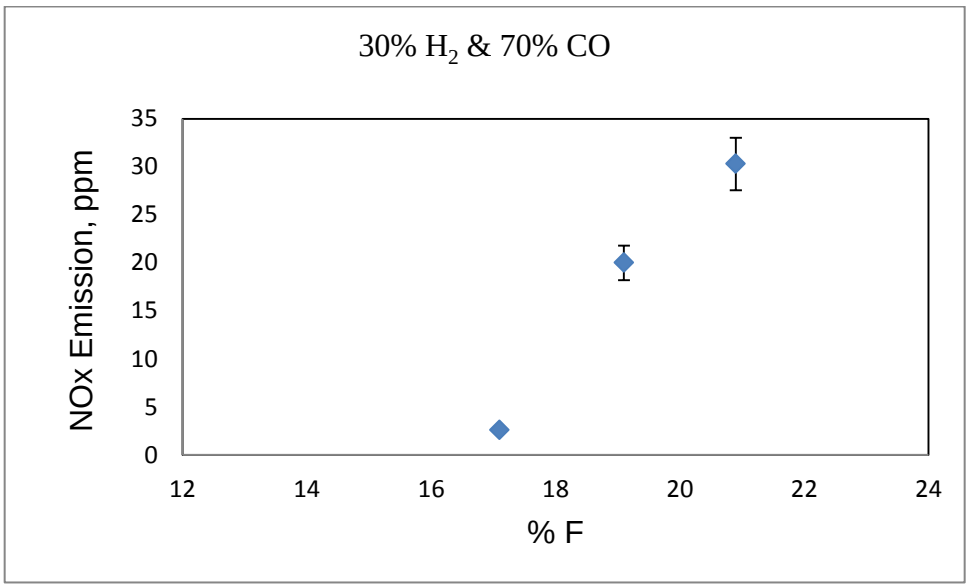

Figure 4.8: NO_x Emission for 30% H_2 & 70% CO

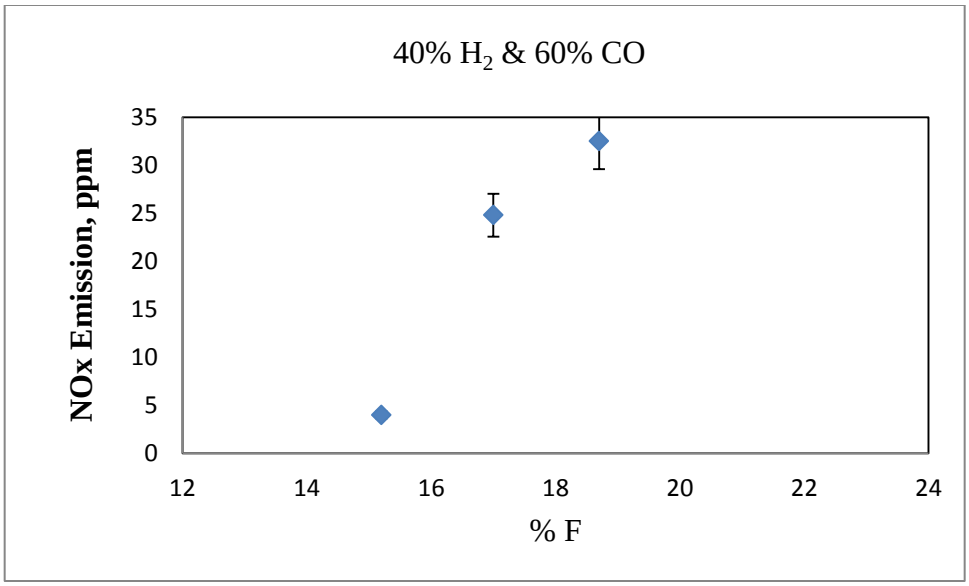

Figure 4.9: NO_x Emission for 40% H_2 & 60% CO

Chapter 5 : Summary and Conclusion

This present work can be summarized by the following points:

(1) The development of the control system to flow the fuel syngas, pilot fuel methane and air for the existing high pressure combustor was developed

(2) The project presented an effective ignition system to initiate spark and pilot flame

(3) The project demonstrated the control and ignition system with combustor

(4) A LabVIEW program was implemented with control and ignition system to perform the experiments remotely

(5) A multi-tube injector was designed and tested, tests included measurements of flame stability of different synthetic gas mixtures at different equivalence ratios

(6) The pollutant emissions were evaluated for flames from the novel multi-tube fuel injector

Overall, flashback and blowout characteristics of syngas mixtures emitted from a novel multi-tube injector have been studied for syngas from 20% to 40% hydrogen concentrations in carbon monoxide (CO).

Three different conditions were tested for these compositions:

- ✓ Equivalence ratio changed from 0.6 to 0.9 in terms of percentage change in fuel
- ✓ Bulk velocity was varied according to the flame speed

Measured parameters for these experiments:

- ✓ Stability map was plotted to show the flashback, blowout and stability field of the synthetic gas fuel
- ✓ NO_x emission was measured to determine the pollutant emissions out of this multi-tube injector.

Results were presented included:

- ✓ The flashback tendency of the flames dependent on the flame speed of the hydrogen. Because of the boundary layer effect the central holes of the injector received the maximum flow rates. The bulk velocity is calculated based on the outer holes. The bulk velocity through the outer holes is kept equal to the flame speed so that it could sustain the flame
- ✓ The degree of blowout tendencies decreased with increasing hydrogen concentration for this multi-tube injector for all three conditions.
- ✓ NO_x emission increases with the increase of equivalence ratio for all three condition of hydrogen concentration.

In future work different hydrogen composition of syngas can be tested in order to characterize the flame stability. Also CO emissions can be determined with the help of CO analyzer. As the NO_x emission depends on the flame stability so that a new injector can also be designed based on the data from this present multi-tube injector.

References

[1] "What is the role of coal in the United States? Retrieved from US,"." [Online]. Available: http://www.eia.gov/energy_in_brief/role_coal_us.cfm.

[2] "The World's First Industrial Gas Turbine Set .' . ASME, 07/1988. Web.,' January 2012."[Online]. Available: <http://www.pdfdownload.org/pdf2html/view_online.php?url=http://files.asme.org/asmeorg/Communities/History/Landmarks/12281.pdf>..

[3] J. Davison, "Performance and costs of power plants with capture and storage of CO2," in *Progress in Energy and Combustion ScienceEnergy*, 2007, pp. 1163–1176.

[4] "Clean Energy. Retrieved from US Environmental Protection Agency," 28 December 2007." [Online]. Available: http://www.epa.gov/cleanenergy/energy-andyou/.

[5] S. Daniele, P. Jansohn, and K. Boulouchos, "Experimental Investigation of Lean Premixed Syngas Combustion at Gas Turbine Relevant Conditions : Lean Blow Out Limits , Emissions and Turbulent Flame Speed," pp. 1–11.

[6] A. H. Lefebvre, "Gas Turbine Combustor Design Problems," in *Hemisphere Publishing Co., Washington D.C.*, 1980, pp. 225–244.

[7] A. K. Gupta, "Gas Turbine Combustion: Prospects and Challenges," *Elsevier Sci. Ltd*, vol. 38, no. 10–13, pp. 1311–1318, 1997.

[8] S. R. Turns, *An Introduction to Combustion*. Mc Graw Hill, 2000.

[9] V. Y. and R. Y. T. Lieuwen, *Synthesis Gas Combustion*. New York: CRC Press, 2010.

[10] S. I. Y. and C. K. L. H. Sun, "No Title," in *Proceedings Combustion Institute 31*, 2007.

[11] C. T. and J. Z. J. Wang, Z. Huang, "Effect of hydrogen addition on early flame growth of lean burn natural gas–air mixtures," *Int. J. Hydrogen Energy*, vol. 35, no. 7246–7252, 2010.

[12] F. E.-M. and S. E.-D. Habik, *Fundamentals and Technology of combustion*. London: Elsevier Science Ltd, 2002.

[13] W. P. S. and C. W. Jensen, "No Title," in *Seventh Symposium on Combustion*, 1959.

[14] S. A. M. and N. R. L. Beltagui, "No Title," in *European Combustion Symposium*, 1973.

[15] N. K. and T. W. T. Saitou, H. Inoue, "Development of Multicluster burner for Fuel Grade DME," in *Proceedings of ASME Turbo Expo*, 2004.

[16] N. K. and S. S. T. Saitou, K. Miura, H. Inoue, "Performance Demonstration of the Full Size Multi Cluster Combustor for DME Under Real Engine Conditions," in *Proceedings of ASME Turbo Expo*, 2005.

[17] B. P. and B. Lenze, "No Title," in *Twenty-Fourth Symposium (International) on Combustion, The Combustion Institute*, 1992.

[18] R. S. B. and C. D. C. A. R. Masri, B. B. Dally, "No Title," in *Twenty-Fifth Symposium (International) on Combustion, The Combustion Institute*, 1994.

[19] M. N. and R. W. S. R. H. Chen, J. F. Driscoll, J. Kelly, "No Title," in *Combustion Science Technology*, 1990.

[20] B. Dam, G. Corona, M. Hayder, and A. Choudhuri, "Effects of syngas composition on combustion induced vortex breakdown (CIVB) flashback in a swirl stabilized combustor," *Fuel*, vol. 90, no. 11, pp. 3274–3284, Nov. 2011.

[21] I. Of, "IFRF Combustion Journal Article Number 200207, December 2002," no. 200207, 2002.

[22] UC Irvine Combustion Laboratory, "No Title." [Online]. Available: http://www.ucicl.uci.edu/2/RESEARCHPROJECTS/CombustionScienceResources/TestCells/Index.aspx.

[23] NETL, "No Title." [Online]. Available: http://www.netl.doe.gov/onsite_research/Facilities/high-pressure.html.

[24] L. Ptasin, "Ignition investigation of methane } air mixtures by multiple capacitor discharges," vol. 52, pp. 395–401, 2001.

[25] M. V. Blanc, P. G. Guest, G. von Elbe, and B. Lewis, "Ignition of explosive gas mixtures by electric sparks," *Symp. Combust. Flame, Explos. Phenom.*, vol. 3, no. 1, pp. 363–367, 1948.

[26] M. Kono, S. Kumagai, and T. Sakai, "The optimum condition for ignition of gases by composite sparks," *Symp. Combust.*, vol. 16, no. 1, pp. 757–766, Jan. 1977.

[27] M. H. Morsy and S. H. Chung, "Laser-induced multi-point ignition with a single-shot laser using two conical cavities for hydrogen/air mixture," *Exp. Therm. Fluid Sci.*, vol. 27, no. 4, pp. 491–497, Apr. 2003.

[28] M. Weinrotter, H. Kopecek, M. Tesch, E. Wintner, M. Lackner, and F. Winter, "Laser ignition of ultra-lean methane/hydrogen/air mixtures at high temperature and pressure," *Exp. Therm. Fluid Sci.*, vol. 29, no. 5, pp. 569–577, Jun. 2005.

[29] C.-W. Chiu, Y.-C. Dong, and S. S. Shy, "High-pressure hydrogen/carbon monoxide syngas turbulent burning velocities measured at constant turbulent Reynolds numbers," *Int. J. Hydrogen Energy*, vol. 37, no. 14, pp. 10935–10946, Jul. 2012.

[30] B. Dam, N. Love, and A. Choudhuri, "Flashback propensity of syngas fuels," *Fuel*, vol. 90, no. 2, pp. 618–625, Feb. 2011.

[31] G. Blesinger, R. Koch, and H.-J. Bauer, "Influence of flow field scaling on flashback of swirl flames," *Exp. Therm. Fluid Sci.*, vol. 34, no. 3, pp. 290–298, Apr. 2010.

[32] C. Eichler, G. Baumgartner, and T. Sattelmayer, "Experimental Investigation of Turbulent Boundary Layer Flashback Limits for Premixed Hydrogen-Air Flames Confined in Ducts," *J. Eng. Gas Turbines Power*, vol. 134, no. 1, p. 011502, 2012.

[33] M. ILBAS, A. CRAYFORD, I. YILMAZ, P. BOWEN, and N. SYRED, "Laminar-burning velocities of hydrogen–air and hydrogen–methane–air mixtures: An experimental study," *Int. J. Hydrogen Energy*, vol. 31, no. 12, pp. 1768–1779, Sep. 2006.

[34] J. Fu, C. Tang, W. Jin, L. D. Thi, Z. Huang, and Y. Zhang, "Study on laminar flame speed and flame structure of syngas with varied compositions using OH-PLIF and spectrograph," *Int. J. Hydrogen Energy*, vol. 38, no. 3, pp. 1636–1643, Feb. 2013.

[35] D. R. Nobble, "Syngas Mixture Composition Effects upon Flashback and Blowout," in *ASME Turbo Expo 2006: Power for Land, Sea and Air*, 2006, pp. 357–368.

[36] S. Zhu and S. Acharya, "An Experimental Study of Lean Blowout With Hydrogen-Enriched Fuels," *J. Eng. Gas Turbines Power*, vol. 134, no. 4, p. 041507, 2012.

[37] P. Griebel, E. Boschek, and P. Jansohn, "Lean Blowout Limits and NO[sub x] Emissions of Turbulent, Lean Premixed, Hydrogen-Enriched Methane/Air Flames at High Pressure," *J. Eng. Gas Turbines Power*, vol. 129, no. 2, p. 404, 2007.

[38] J. Wang, Z. Huang, C. Tang, and J. Zheng, "Effect of hydrogen addition on early flame growth of lean burn natural gas–air mixtures," *Int. J. Hydrogen Energy*, vol. 35, no. 13, pp. 7246–7252, Jul. 2010.

[39] A. Kushari, "Effect of injector geometry on the performance of an internally mixed liquid atomizer," vol. 91, pp. 1650–1654, 2010.

[40] S. Dodo, T. Asai, H. Koizumi, H. Takahashi, S. Yoshida, and H. Inoue, "Performance of a Multiple-Injection Dry Low NO x Combustor With Hydrogen-Rich Syngas Fuels," *J. Eng. Gas Turbines Power*, vol. 135, no. 1, p. 011501, Nov. 2012.

[41] D. Littlejohn and R. K. Cheng, "Fuel effects on a low-swirl injector for lean premixed gas turbines," vol. 31, no. x, pp. 3155–3162, 2007.

[42] W. D. York, W. S. Ziminsky, and E. Yilmaz, “Development and Testing of a Low NO x Hydrogen Combustion System for Heavy-Duty Gas Turbines,” *J. Eng. Gas Turbines Power*, vol. 135, no. 2, p. 022001, Jan. 2013.

[43] P. Gobbato, M. Masi, A. Toffolo, A. Lazzaretto, and G. Tanzini, “Calculation of the fl ow fi eld and NO x emissions of a gas turbine combustor by a coarse computational fl uid dynamics model,” vol. 45, no. x, pp. 445–455, 2012.

[44] “NOx prediction.pdf.” .

[45] C. Ghenai, “Combustion of Syngas Fuel in Gas Turbine Can Combustor,” *Adv. Mech. Eng.*, vol. 2010, pp. 1–13, 2010.

[46] D. Giles, S. Som, and S. Aggarwal, “NOx emission characteristics of counterflow syngas diffusion flames with airstream dilution,” *Fuel*, vol. 85, no. 12–13, pp. 1729–1742, Sep. 2006.

[47] “Fichet.pdf.” .

[48] I. Manual, “High Level,” no. 2.

Glossary

A_t=	Throat Area	m^2	
$\dot{m} =$	Mass Flow Rate	kg/s	
$R =$	Radius of the tube	m	
$T_T =$	Temperature at throat	k	
$\gamma =$	Specific heat ratio		-
$P_t =$	Pressure at throat	MPa	
$Ma =$	Mach Number	-	
$\varphi =$	Equivalence ratio		-
$V_b =$	Bulk Velocity	m/s	

Appendix A

Experimental Procedure

Hardware & Software Requirements

Ensure that the system meets the following criteria:

1. Computer set-up:

Windows	
	Run-Time Engine
Processor	Pentium III/Celeron 866 MHz or equivalent
RAM	256 MB
Screen Resolution	1024 x 768 pixels
Operating System	Windows 8/7/Vista (32-bit and 64-bit) Windows XP SP3 (32-bit) Windows Server 2003 R2 (32-bit) Windows Server 2008 R2 (64-bit)
Disk Space	382 MB

2. Lab View Software- *Installed In PC*

Equipment Requirements

Ensure that the following equipment is installed in the system. Refer to the equipment manual.

Equipment/Instruments	Quantity	X
Power supply- EXTECH Instruments 382270	1	
Power Supply-	1	
USB Ni-6008 Dev3	1	
USB Ni-6008 Dev6	1	
PCI 6521 Relay Card	1	
Ignition Coil- MSD 8287 PN 121-8287 (or equivalent)	1	
12 V Battery / 11 amp	1	
BK Precision 4012A Signal Generator (or equivalent)	1	
KZ Valve EH2 Series (“P”)	4	
Jefferson Valve 1314 Series (“S”)	4	
Omega FMA Series 1700/1800 Flow meters (“FM”) 0-5 lpm	1	
Omega FMA Series 1700/1800 Flow meters (“FM”) 0-30 lpm	1	
Omega FMA Series 1700/1800 Flow meters (“FM”)0-500 lpm	1	
Omega FMA Series 1700/1800 Flow meters (“FM”)0-1000 lpm	1	
Video Camera (with TV connection)	1	

Television (with Video Camera Connection)	1	
120V wall connection		

Nomenclature

Instrument/equipment is identified with the following nomenclature:

Equipment/Instrument	Nomenclature
Proportional Control Valve	P
Solenoid Valve	S
Flow Meters	F
Needle Valve	N
High Pressure Combustor	HPC
Pressure transducer	PT

Assign a testing gas/fuel to a corresponding number. Refer to Set-up Diagram in page 3.

Gas	Number Code
Methane-CH_4	1
Nitrogen- N_2	2
Air	3
Ignition, Methane CH_4	4

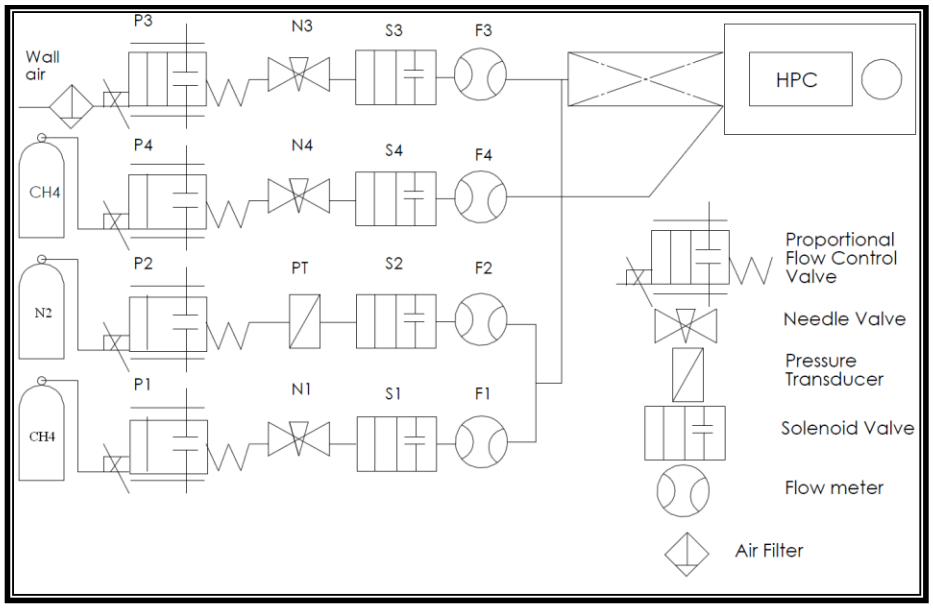

System set-up Diagram

Testing Requirements

Ensure that the following is available before testing. The amount of material/gas depends in the testing needs.

Gas	Quantity	X
Methane-CH_4		
Nitrogen- N_2		
Air	Wall	
Ignition, Methane CH_4		

Set-up Procedure

Follow these tasks in order to set-up the HPC system for testing.

#	TASK	RESULT	IF ADVERSE RESULT	X or N/A
COMPUTER SET-UP				
1	Turn ON Computer	Verity computer is ON	N/A	
2	Open "New_HPC" Lab View File	Lab view program appears in the computer desktop screen	▪ Verify lab view is installed ▪ Verify lab view is running	
EQUIPMENT SET-UP				
1	Connect the following equipment to 120V wall outlet: ▪ Power Supplies ▪ Signal Generator	N/A	N/A	
2	Turn ON Power Supplies	Verify numbers appear in screen	Check Electricity Connection	
3	Verify FM are turned ON	Check for numbers in the display screen	Refer to FM troubleshooting document.	
4	Allow FM to warm-up 10-15 min	Numbers in display screen approximate 0.0 +/- 5% of total volume flow rate of FM after warm-up	Refer to FM troubleshooting document.	
Locate MSD ignition coil				
5	Connect MSD ignition coil to the spark plug located at the HPC front cap if not connected.	N/A	N/A	
6	Connect cables to MSD ignition Coil if not connected. (Refer to Electrical diagram for MSD ignition coil)	N/A	N/A	
Locate 12V battery, Green and Red Alligator Clamps and Signal Generator				
7	Connect Green clamp to the (-) terminal of the 12V battery	N/A	N/A	
8	Connect Red clamp to the (+) terminal of the 12V battery	N/A	N/A	
9	Turn ON the Signal Generator	Check for Number in the screen display	Verify the signal generator is connected to the 120V outlet	
1	Set-up 100HZ frequency in the	"100" should be displayed	Adjust as necessary	

0	signal generator using the knobs under the screen	in the screen		
#	**TASK**	**RESULT**	**IF ADVERSE RESULT**	**X or N/A**
11	Push the "Step Function" button	N/A	N/A	
EQUIPMENT TEST				
12	Run Lab View Program "New_HPC"	N/A	N/A	
The following tasks will be executed using Lab View				
13	Activate S1	Must hear "Click" sound and current should be supplied to the solenoid	Refer to the troubleshoot guide	
14	Deactivate S1	Solenoid will close and current is no being supplied	Refer to the troubleshoot guide	
15	Activate S2	Must hear "Click" sound and current should be supplied to the solenoid	Refer to the troubleshoot guide	
16	Deactivate S2	Solenoid will close and current is no being supplied	Refer to the troubleshoot guide	
17	Activate S3	Must hear "Click" sound and current should be supplied to the solenoid	Refer to the troubleshoot guide	
18	Deactivate S3	Solenoid will close and current is no being supplied	Refer to the troubleshoot guide	
19	Activate S4	Must hear "Click" sound and current should be supplied to the solenoid	Refer to the troubleshoot guide	
20	Deactivate S4	Solenoid will close and current is no being supplied	Refer to the troubleshoot guide	
21	Supply 5V to P1 (enter value in Lab View)	▪ Must hear opening sound for P. ▪ Verify the Red arrow on top of the P is not perpendicular to the line.	Refer to the troubleshoot guide	
22	Enter value 0 volts for P1 in Lab View	▪ Must hear closing sound for P. ▪ Verify the Red arrow on top of the P is	Refer to the troubleshoot guide	

		perpendicular to the line.		
23	Supply 5V to P2 (enter value in Lab View)	▪ Must hear opening sound for P. ▪ Verify the Red arrow on top of the P is not perpendicular to the line.	Refer to the troubleshoot guide	
24	Enter value 0 volts for P2 in Lab View	▪ Must hear closing sound for P. ▪ Verify the Red arrow on top of the P is perpendicular to the line.	Refer to the troubleshoot guide	
#	TASK	RESULT	IF ADVERSE RESULT	X or N/A
25	Supply 5V to P3 (enter value in Lab View)	▪ Must hear opening sound for P. ▪ Verify the Red arrow on top of the P is not perpendicular to the line.	Refer to the troubleshoot guide	
26	Enter value 0 volts for P3 in Lab View	▪ Must hear closing sound for P. ▪ Verify the Red arrow on top of the P is perpendicular to the line.	Refer to the troubleshoot guide	
26	Supply 5V to P4 (enter value in Lab View)	▪ Must hear opening sounds for P. ▪ Verify the Red arrow on top of the P is not perpendicular to the line.	Refer to the troubleshoot guide	
27	Enter value 0 volts for P4 in Lab View	▪ Must hear closing sound for P. ▪ Verify the Red arrow on top of the P is perpendicular to the line.	Refer to the troubleshoot guide	
Once this tasks have been completed, proceed to “Leak Test”				

HPC Leak Test Procedure

Note: The valve names are defined in the LabVIEW program generated by the HPC team. As of 10/24/2013 the file name is "New_HPC". The file can be found in the cSETR lab computer designated to this experimental setup. For additional information refer to the LabVIEW block diagram.

1. Open the exhaust damper and ensure the exhaust system is running
2. Connect the shop airline hose to the main airline regulator (Refer to the plumbing diagram. The air supply should be connected to the line that has the P3, N3, S3 and F3 installed. Set the regulator pressure to 40 psig).

I. Open P3

- Apply snoop leak detection solution to all line joints between the airline hose connection and N3.
- Tighten necessary joints or apply Teflon accordingly until leak has sopped.

II. Open N3

- Apply snoop leak detection solution to all line joints between N3 and S3.
- Tighten necessary joints or apply Teflon accordingly until leak has sopped.

III. Open S3

- Plug the HPC exhaust hole in order to ensure a pressure buildup across the line and combustor
- Apply snoop leak detection solution to all line joints between S3 and inlet manifold.

A through leak test of the combustor can be performed now by applying the leak detection solution to all the combustor joints and window panels. This step is recommended before initial experimentation and is thereafter left to the discretion of the user.

3. Repeat step 2 for all the remaining lines that will be utilized during experimentation

Setting Desired Flow Rates (10/24/2013)

Note: The following procedure should be deemed relevant or not based on the required flow rates needed for experimentation. It is up to the user to determine whether it is necessary or not to control the flow rates using the N3, N4 and N1 valves. The flow should not exceed ±10% of the maximum flow the meter can measure.

1. Connect the shop airline hose to the main airline regulator (Refer to the plumbing diagram. The air supply should be connected to the line that has the P3, N3, S3 and F3 installed. Set the regulator to the desired pressure).
    I. Turn on and allow the flow meters to stabilize.
        - Turn on both power supplies (one for flow meters and another for valves)
        - The flow meters will initially read a value near their maximum. No flow should be allowed to pass through until they have stabilized at a value of 0 L/min.

    II. Open P3 and S3
        - Set N3 so that F3 reads the value dictated by the test matrix
2. Repeat step 1 for all the lines with needle valves installed in them

Test Procedure

Note: The leak test procedure and the flows must be set based off the experimental test matrix before performing the experimental procedure. Two separate methane cylinders are used in the setup, one for the main fuel line and another for the pilot flame. This test procedure is meant for a maximum flow rate of air of 50 L/min and a maximum CH_4 flow rate of 10 L/min at an equivalence ratio of .9.

1. Connect the shop airline hose to the main airline regulator (Refer to the plumbing diagram. The air supply should be connected to the line that has the P3, N3, S3 and F3 installed. Set the regulator to 40 psig).
2. Connect the main CH_4 cylinder tank to the main fuel line
    I. As of 10/24/2013 the main fuel line is the one with P1, N1, S1 and F1 installed (Refer to plumbing diagram)
3. Connect the CH_4 tank to the pilot flame line
    I. As of 10/24/2013 the pilot fuel line is the one with P4, N4, S4 and F4 installed (refer to plumbing diagram)
    II. The flow meter for the pilot flame line should not exceed 5.5 L/min or be less than .5 L/min
4. Connect the N_2 tank to the emergency purging line
    I. As of 10/24/2013 the N_2 purging line is the one with P2, PT, S2 and F2 installed (refer to plumbing diagram)
    II. The N_2 tank could be replaced by standard shop air and it is left up to the user discretion.

5. Ensure the HPC exhaust damper is open and the exhaust system is running and functioning properly
    I. The HPC exhaust damper should be the only one open at the time of experimentation. All other dampers should be closed with the consent of the other students working in the lab
    II. No other experiment should be using the exhaust while HPC experimentations are taking place.
6. Set the camera and ensure a clear image in the remote monitor is visible. The injector face and pilot flame port should be clearly visible
    I. Camera should always be set to recording to keep it from switching to sleep mode
7. Place Kevlar walls around the set up
    I. A total of 4 Kevlar walls should be placed around the HPC
8. Open the CH_4 tanks and N_2 tank and set line pressure to 40 psig
9. Activate the ignition coil
    I. A spark should be heard and seen through the remote monitor
10. Open S4 and P4 (Pilot line)
    I. A diffusion flame should be visible and anchored to the pilot flame port after 3 seconds of opening P4
11. Open S3, then open P3
12. Open S1, then open P1
    I. A flame should be generated at the injector face for evaluation after 5 seconds of opening P1

Appendix B

Statistical Analysis of Experimental Data

For experimental results it is required to identify the specifications for measuring systems. While taking measurement it is observed some randomness into measured data even if the same measurement has taken repeatedly. This randomness mainly caused by uncontrolled variables, less precision of measuring instrument. This randomness can make an effect on drawing a conclusion from measured data table. Thus, before using experimental data it is obvious to make a statistical analysis of those. Table below shows 31 data set of NO_x emission (unit=ppm) for 20% H_2 & 80% CO at 23% fuel condition.

Experimental Data Set of 20% H_2 & 80% CO for 23 % fuel

22.5	25.7	27.6	28.9	29.3
29.8	29.7	33.1	33.1	33
29.4	29.1	28.8	28.8	29
25	23.6	24.5	25.9	27.7
28.4	29.1	28	26	28.9
28.9	28.8	30	23	28.3
28.3				

Thirty second interval were taken before taking each data. Basic statistics of measured data has shown in the following table.

Statistical Description of measured data

Number of Measured Data	Minimum Value	Maximum Value	Mean Value	Median	Standard Deviation
31	22.5	33.1	28.14	28.8	2.63

From statistical analysis it is found that standard deviation is 9.4 Pa. Standard deviations are considered as statistically significant normal random error.

Error Analysis

Mean, ppm	Random Error
28.14	2.63
Errors in %	9.34

On the other hand following figure shows a statistical histogram of NOx emission with bin width range 3 ppm

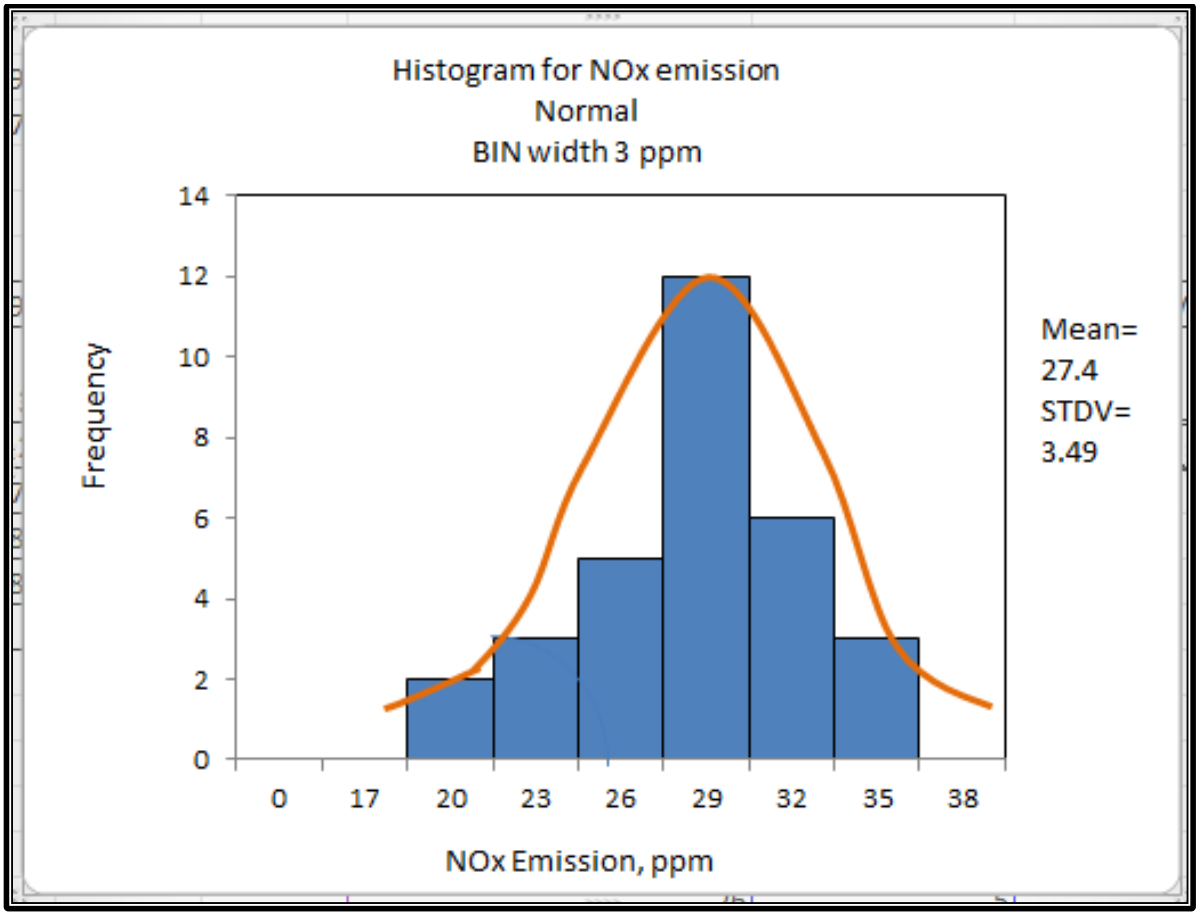

Histogram for NOx Emission

An error was also calculated for measurements using a 95 % Confidence interval by using t-distribution table. Our measured data have 30 degrees of freedom. For a 95% confidence interval and for degree of freedom 30 our required value from t-distribution table is 2.042. Finally, from standard procedure our lower and upper ranges were found. The ranges are 27.17 to 29.1 ppm.

t-distribustion table

ν	$t_{.100}$	$t_{.050}$	$t_{.025}$	$t_{.010}$	$t_{.005}$	$t_{.001}$	$t_{.0005}$
1	3.078	6.314	12.706	31.821	63.657	318.31	636.62
2	1.886	2.920	4.303	6.965	9.925	22.326	31.598
3	1.638	2.353	3.182	4.541	5.841	10.213	12.924
4	1.533	2.132	2.776	3.747	4.604	7.173	8.610
5	1.476	2.015	2.571	3.365	4.032	5.893	6.869
6	1.440	1.943	2.447	3.143	3.707	5.208	5.959
7	1.415	1.895	2.365	2.998	3.499	4.785	5.408
8	1.397	1.860	2.306	2.896	3.355	4.501	5.041
9	1.383	1.833	2.262	2.821	3.250	4.297	4.781
10	1.372	1.812	2.228	2.764	3.169	4.144	4.587
11	1.363	1.796	2.201	2.718	3.106	4.025	4.437
12	1.356	1.782	2.179	2.681	3.055	3.930	4.318
13	1.350	1.771	2.160	2.650	3.012	3.852	4.221
14	1.345	1.761	2.145	2.624	2.977	3.787	4.140
15	1.341	1.753	2.131	2.602	2.947	3.733	4.073
16	1.337	1.746	2.120	2.583	2.921	3.686	4.015
17	1.333	1.740	2.110	2.567	2.898	3.646	3.965
18	1.330	1.734	2.101	2.552	2.878	3.610	3.922
19	1.328	1.729	2.093	2.539	2.861	3.579	3.883
20	1.325	1.725	2.086	2.528	2.845	3.552	3.850
21	1.323	1.721	2.080	2.518	2.831	3.527	3.819
22	1.321	1.717	2.074	2.508	2.819	3.505	3.792
23	1.319	1.714	2.069	2.500	2.807	3.485	3.767
24	1.318	1.711	2.064	2.492	2.797	3.467	3.745
25	1.316	1.708	2.060	2.485	2.787	3.450	3.725
26	1.315	1.706	2.056	2.479	2.779	3.435	3.707
27	1.314	1.703	2.052	2.473	2.771	3.421	3.690
28	1.313	1.701	2.048	2.467	2.763	3.408	3.674
29	1.311	1.699	2.045	2.462	2.756	3.396	3.659
30	1.310	1.697	2.042	2.457	2.750	3.385	3.646
40	1.303	1.684	2.021	2.423	2.704	3.307	3.551
60	1.296	1.671	2.000	2.390	2.660	3.232	3.460
120	1.289	1.658	1.980	2.358	2.617	3.160	3.373
∞	1.282	1.645	1.960	2.326	2.576	3.090	3.291

Source: This table is reproduced with the kind permission of the Trustees of Biometrika from Pearson, E. S., and Hartley, H. O. (eds.) *The Biometrika Tables for Statisticians*, Vol. 1, 3rd ed., *Biometrika*, 1966.

Vita

Sarzina Hossain completed his Bachelor of Science Degree in Mechanical Engineering from the Bangladesh University of Engineering and Technology (BUET) in March, 2012. During her bachelors program she published three conference papers. One in International Conference on Mechanical Engineering, December 2011, Dhaka, Bangladesh and other two papers are published in 5th BSME International Conference on Thermal Engineering, 2012. After finishing her Bachelor's degree she joined in Master's program at the University of Texas at El Paso in January 2013. She also worked as a teaching assistant for the Heat Transfer and Fluid Mechanics class Spring 2013, Mechanics I class for Summer 2013, and Introduction to Thermo-fluid Science class for Fall 2013 and Spring 2014. She also worked as a Graduate Research Assistant in the NASA Center for Space Exploration Technology Research (cSETR) for the last one and half years where she focused on system development of the high pressure gas turbine combustor and investigated the stability field and pollutant emissions of the lean premixed combustion of synthetic gas fuels. Within this period, she published one conference paper and one journal paper. The journal paper is published in Journal of Mechanical Engineering Science, 2014. The conference paper was presented at the AIAA SciTech meeting in 2014 in National Harbor, Maryland. She also presented one article for 3rd Southwest Energy Science and Engineering Symposium and another article for the 4th Southwest Energy Science and Engineering Symposium. Her proposal was awarded for Provost's Summer-2014 Student Research Assistant Program.

Permanent address: Village: Noakati, Post Office: Shahos
Up-zila: Dumuria, District: Khulna

This thesis was typed by Sarzina Hossain.